UNIVERSIDAD **NACIONAL** DE COLOMBIA

Desarrollo de métodos de propagador para el estudio de procesos de ionización molecular empleando la metodología del orbital nuclear molecular y su implementación en el paquete computacional LOWDIN

Jhonathan Romero Fontalvo

Desarrollo de métodos de propagador para el estudio de procesos de ionización molecular empleando la metodología del orbital nuclear molecular y su implementación en el paquete computacional LOWDIN

Jhonathan Romero Fontalvo

Tesis presentada como requerimiento para optar el título de:
Magister en Ciencias Química

Director:
Ph.D. Andrés Reyes Velasco

Área de investigación:
Química Cuántica
Grupo de investigación:
Química cuántica y computacional

Universidad Nacional de Colombia
Chemistry Department
Bogotá, Colombia
2013

Development of propagator methods for studying ionization processes in molecules using the Any Particle Molecular Orbital (APMO) approach and its computational implementation in LOWDIN program

Jhonathan Romero Fontalvo

Universidad Nacional de Colombia
Chemistry Department
Bogotá, Colombia
2013

Development of propagator methods for studying ionization processes in molecules using the Any Particle Molecular Orbital (APMO) approach and its computational implementation in LOWDIN program

Jhonathan Romero Fontalvo

Thesis presented in partial fulfillment of the requirements for the Degree of:
Master in Sciences - Chemistry

Advisor:
Ph.D. Andrés Reyes Velasco

Research Area:
Quantum Chemistry
Research Group:
Quantum and Computational Chemistry Group

Universidad Nacional de Colombia
Chemistry Department
Bogotá, Colombia
2013

La part de l'imagination
dans le travail scientifique
est la même que dans le
travail du peintre ou de
ľ'evrivain. Elle consiste à
découper le réel, et à
recombiner les morceaux
pour créer quelque chose
de neuf.

François Jacob, 1981.

[The part played by the
imagination in scientific
work is the same as in the
work of the painter or the
writer. It consists of cutting
up reality, and recombining
the pieces to create
something new.]

Acknowledgments

Resumen

En este trabajo se propone la teoría de propagadores empleando el método del orbital nuclear molecular para cualquier tipo de partícula (APMO/PT). Esta metodología es una extensión de la teoría del propagador electrónico para estudiar sistemas con más de un tipo de especie cuántica, desarrollada e implementada en su versión diagonal en el programa de química cuántica LOWDIN. La metodología fue aplicada para estudiar efectos cuánticos nucleares en potenciales de ionización electrónicos y energías de enlace de protones en un conjunto de átomos y moléculas de prueba. Los resultados obtenidos demuestran que el nuevo método ofrece una descripción apropiada de los efectos isotópicos en potenciales de ionización electrónicos y predicciones precisas de energías de enlace de protones, afinidades protónicas y energías de solvatación de protones en sistemas moleculares.

Palabras clave: Funciones de Green, propagador, orbital molecular, orbital molecular para cualquier partícula, energía de enlace, autoenergía.

Abstract

In this work we propose a propagator theory using the any particle molecular orbital approach (APMO/PT). This theory is an extension of the electron propagator theory developed to study more than one type of particles (quantum species) that has been implemented in the LOWDIN quantum chemistry software. Our method was applied to study nuclear quantum effects on electron and proton binding energies in a set of atoms and representative molecules. Our results show that this new method can properly describe isotope effects on electronic ionization potentials and predict proton binding energies as well as related properties such as proton affinities and proton solvations energies in molecular systems.

Keywords: Green's function, propagator, molecular orbital, any particle molecular orbital approach, binding energy, self-energy

Contents

1 Introduction

Over the years, quantum chemistry methods have become important tools for predicting and understanding chemical phenomena [1–3]. Several quantum chemical approaches have been developed so far, with a wide range of applicability and efficiency. The success of a specific approach depends on its ability to produce *accurate* predictions of the observable of interest in *plausible* computational times, while keeping a connection with chemical concepts that are common for the entire chemical community. In summary, quantum chemistry methods should be *accurate*, *efficient* and *chemically meaningful*.

Unfortunately, achieving a good performance on any of these aspects usually involves abandoning the other two. Hartree-Fock (HF) calculations, which are the starting point for most of the methods in quantum chemistry, establish the one particle energies as the basis for the definition of reactivity indices and reactivity concepts. However HF lacks of correlation effects and its accuracy is low. Highly correlated methods based on a wavefunction approach, such as Coupled-Cluster (CC) or Configuration Interactions (CI), can achieve high accuracy on energy calculations (>1 kcal/mol), but the one particle properties lose into the multiconfigurational description of the wavefunction. Methods based on Density Functional Theory (DFT), such as Kohn-Sham (KS) are probably the most popular and widely employed by computational chemists and can provide better accuracy than HF. However, one particle properties such as orbitals energies are poorly described by most of the functionals currently available [4, 5].

A third set of methods are those based on propagators (also known as Green's functions or its equivalent formulation of equation of motion). The electron propagator theory (EPT) has proven to be useful to compute electronic binding energies in molecules, offering an excellent compromise between computational efficiency and accuracy, while keeping all the concepts associated to orbitals [6–18]. The major achievement of EPT is to offer an accurate description of one particle functions by introducing an energy dependent potential called the self-energy, which can be sistematically improved. In EPT, equations that contain correlated, one-electron operators resemble the Kohm-Sham equations of DFT and also are related to the extended Koopmans' theorem approach, offering connections with the reactivity indices defined in conceptual DFT.

The success of EPT in the calculation of electron binding energies is a strong indication of the potential of propagator method to predict binding energies for other particles of chemical relevance, such as the H^+, which plays a mayor role determining acidity. Similarly, propagator theory could provide insights into the reactivity of molecular systems containing

positrons and other exotic particles, which has arisen as a new research topic in chemistry [19, 20]. To achieve these new challenges, the EPT developed so far has to be extended to study a system containing more than one type of quantum species.

A natural way to develop an propagator method to treat several quantum species is to employ an Any Particle Molecular Orbital (APMO) wavefunction [21]. In the APMO method, the total wavefunction is expressed as a product of the wavefunctions of each quantum species that are treated on the same footing of electrons in regular electronic structure calculations. The APMO and its equivalent approaches (Nuclear Molecular Orbital and Nuclear Electron Orbital Methods) have been previously employed to simultaneously study electronic and nuclear wavefunctions as well as systems comprising exotic particles [21–33].

In this thesis we develop a generalized propagator method to calculate binding energies for any type of particle in composite molecular systems, using an APMO/HF wavefunction as reference state. Henceforth, we will call our extended propagator method as APMO/PT. The outline of this thesis is: In chapter 2 we present a brief review of propagator methods for many body systems and the EPT. We also introduce the APMO approach. In chapter 3 we present the theoretical development of APMO/PT. In chapter 4 we describe the implementation of APMO/PT in the quantum chemistry program LOWDIN, especially designed to calculate APMO wavefunctions. In chapter 5 we present an assessment of the developed APMO/PT approximations to determine its performace an accuracy stuying: 1) nuclear quantum effects (NQE) in electron detachment processes and 2) proton detachment processes and its related properties, such as proton binding energies (PBE), proton affinities (PA) and proton solvation energies (PSE). In Section 6 we summarize and provide concluding remarks.

2 Theoretical Background

In this chapter we present a brief review of the quantum mechanics and quantum chemistry principles and methods employed in this work. For a detailed description of the following topics, we invite the reader to check references [6, 34].

2.1 Preliminary concepts

2.1.1 Second Quantization

The second quantization is a powerful formalism for quantum mechanics that allow us to introduce the antisymmetry property of the wavefunction onto the algebraic properties of operators. Operators in second quantization are defined in a Fock Space, which is a generalization of the Hilbert that contents the states of the system with all the possible number of quantum particles. The basic operators in second quantization are the annihilation and creation operators, $\bar{a}_i$ and $\bar{a}_i^\dagger$. For a system of fermions whose wavefunction is represented as an Slater determinant (an antisymmetrized product of one particle wavefunctions), the creation operator, $\bar{a}_i^\dagger$ is defined as:

$$\bar{a}_i^\dagger |\chi_k \chi_l .... \chi_N\rangle = |\chi_i \chi_k \chi_l .... \chi_N\rangle \tag{2-1}$$

If the Slater determinant includes the spin-orbital i, the result of applying $\bar{a}_i^\dagger$ is zero:

$$\bar{a}_i^\dagger |\chi_i \chi_k \chi_l .... \chi_N\rangle = 0 \tag{2-2}$$

This results is a consequence of the Pauli exclusion principle, that prevents two fermions to occupy the same spin-orbital. Similarly, the annihilation operator eliminates a spin–orbital from the left, an only from the left, of an Slater determinant:

$$\bar{a}_i |\chi_i \chi_k \chi_l .... \chi_N\rangle = |\chi_k \chi_l .... \chi_N\rangle \tag{2-3}$$

If the spin-orbital is not in the appropriate position to be eliminated, it must be placed in the left part of the Slater determinant by switching spin-orbitals accordingly, for example:

$$\bar{a}_i |\chi_k \chi_l \chi_i .... \chi_N\rangle = -\bar{a}_i |\chi_k \chi_i \chi_l .... \chi_N\rangle = \bar{a}_i |\chi_i \chi_k \chi_l .... \chi_N\rangle = |\chi_k \chi_l .... \chi_N\rangle \tag{2-4}$$

The previous rule introduces the property of antisymmetry of the fermionic wavefunction. Creation and annihilation operators satisfy three anticommutation relations that are consequences of the properties listed above:

$$\bar{a}_i^\dagger \bar{a}_j^\dagger + \bar{a}_j^\dagger \bar{a}_i^\dagger = 0 = [\bar{a}_i^\dagger, \bar{a}_j^\dagger]_+ \tag{2-5}$$

$$\bar{a}_i \bar{a}_j + \bar{a}_j \bar{a}_i = 0 = [\bar{a}_i, \bar{a}_j]_+ \tag{2-6}$$

$$\bar{a}_i \bar{a}_j^\dagger + \bar{a}_j^\dagger \bar{a}_i = \delta_{ij} = [\bar{a}_i, \bar{a}_j^\dagger]_+ \tag{2-7}$$

Finally, we define the vacuum state $|\rangle$, which is a normalized state without particles:

$$\langle|\rangle = 1 \tag{2-8}$$

Using the definition of vacuum state, any Slater determinant can be expressed in terms of creation and annihilation operators. For example:

$$|\chi_i \chi_j \chi_k ... \chi_N\rangle = \bar{a}_i^\dagger \bar{a}_j^\dagger \bar{a}_k^\dagger ... \bar{a}_N^\dagger |\rangle \tag{2-9}$$

The previous equation illustrates the equivalency between an expression written in first quantization an one written in second quantization. For instance, one and two electron operators, O_1 and O_2, employed to describe a system of N interacting electrons, are written in the first quantization formalism as follows:

$$O_1 = \sum_i^N h(i) \quad where \quad h(i) = -\frac{1}{2}\nabla^2 - \sum_1^m \frac{Z_a}{r_i a} \tag{2-10}$$

$$O_2 = \frac{1}{2}\sum_{i,j}^N \frac{1}{r_{ij}} \tag{2-11}$$

where r_i and r_{ij} represents the electron coordinates and interelectron distances, respectively. In the second quantized formalism, definitions 2-10 and 2-11 turn onto:

$$O_1 = \sum_{ij} \langle i|h|j\rangle \bar{a}_i^\dagger \bar{a}_j \tag{2-12}$$

$$O_2 = \frac{1}{2}\sum_{ijkl} \langle ij|kl\rangle \bar{a}_i^\dagger \bar{a}_j^\dagger \bar{a}_l \bar{a}_k \tag{2-13}$$

These definitions can be easily tested applying it to the corresponding Slater determinant wavefunction Ψ^0 of the system. It is important to note that interaction potentials (in this case one and two electron integrals) appear explicitly in the definitions 2-12 and 2-13.

2.1.2 Green's Function

The Green's function method is a procedure usually employed to solve inhomogenious differential equations subject to specific boundary conditions. It is extensively used in many-body theory to gradually improve trial wavefunctions. The Green's Function, $G(x, x')$, of a hermitian linear differential operator, $\hat{L} = \hat{L}(x)$, is defined by the following relation:

$$\hat{L}G(x, x') = \delta(x - x') \tag{2-14}$$

where the $\delta(x - x')$ is the dirac delta funtion. To illustrate how the Green's functions can help to solve inhomogeneous differential equations, we can multiply equation 2-14 by a function $f(x')$ and integrate both sides of the equality in function of x' to obtain:

$$\int \hat{L}G(x, x')f(x')dx' = \int \delta(x - x')f(x')dx = f(x) \tag{2-15}$$

Given that $\hat{L}$ depends only in x, we can write the left side of the equation as the operator acting over a function $u(x)$, defined as follows:

$$\int \hat{L}G(x, x')f(x')dx' = \hat{L}\int G(x, x')f(x')dx' = \hat{L}u(x) \tag{2-16}$$

and finally:

$$\hat{L}u(x) = f(x) \tag{2-17}$$

Then, if we already know $f(x)$ in Eq.2-17 and we want to determine $u(x)$, all we have to do is to calculate the Green's function associated to the operator $\hat{L}$ and determine $u(x)$ as:

$$u(x) = \int dx' G(x, x')f(x') \tag{2-18}$$

Green's function can be easily calculated if operator $\hat{L}$ admits a complete set of eigenvalues λ_n and eigenfunctions Ψ_n. In other words, if eigenvector and eigenfunctions of $\hat{L}$ satisfy the completeness relation:

$$\delta(x - x') = \sum_{n=0}^{\infty} \Psi_n^*(x)\Psi_n(x') \tag{2-19}$$

From equation 2-19 is clear that the Green's function must have the form:

$$G(x, x') = \sum_{n=0}^{\infty} \frac{\Psi_n^*(x)\Psi_n(x')}{\lambda_n} \tag{2-20}$$

Now we consider the following inhomogeneous equation:

$$(E - \mathcal{H}_0)a(x) = b(x) \tag{2-21}$$

where E is a parameter, and $a(x)$ and $b(x)$ are unknown and known function, respectively. The Green's function associated to the operator $(E - \mathcal{H}_0)$ is written in terms of the eigen-functions (ψ_α) and eigenvalues $(E - E_\alpha^{(0)})$ of $(E - \mathcal{H}_0)$:

$$G(x, x', E) = \sum_n^\infty \frac{\psi_\alpha^*(x')\psi_\alpha(x)}{E - E_\alpha^{(0)}} \tag{2-22}$$

and the solution of $a(x)$ is:

$$a(x) = \int dx' \sum_n^\infty \frac{\psi_\alpha(x)\psi_\alpha^*(x')}{E - E_\alpha^{(0)}} b(x') \tag{2-23}$$

Eq.2-21 can be also represented in a matrix form (Heisengerg representation):

$$(E\mathbf{1} - \mathbf{H}_0)\mathbf{a} = \mathbf{b} \tag{2-24}$$

From the previous equation and Eq.2-18 is easy to see that the Green's function will be equivalent to:

$$\mathbf{G}_0(E) = (E\mathbf{1} - \mathbf{H}_0)^{-1} \tag{2-25}$$

If E_α^0 are the eigenvectors of $\mathbf{H}_0$ and c_i^α the coefficients of the eigenfunctions, each element of $\mathbf{G}_0$ can be determined as:

$$(\mathbf{G}_0)_{ij} = \sum_\alpha \frac{c_i^\alpha c_j^{\alpha*}}{E - E_\alpha^0} \tag{2-26}$$

Now, if we wish to solve Eq.2-21 for an operator $\mathbf{H}$, that can be expressed as $\mathbf{H} = \mathbf{H}_0 + \mathbf{V}$, the Green's function, $\mathbf{G}$, will be:

$$\mathbf{G}(E) = (E\mathbf{1} - \mathbf{H}_0 - \mathbf{V})^{-1} \tag{2-27}$$

and is easy to show that $\mathbf{G}$ obeys the equation:

$$\mathbf{G}(E) = \mathbf{G}_0(E) + \mathbf{G}_0(E)\mathbf{V}\mathbf{G}(E) \tag{2-28}$$

The previous equation, called the *equation of motion*, establishes a mathematical procedure to generate approximations for the Green's function of the operator $\mathbf{H}$ given that we know the Green's of $\mathbf{H}_0$. In quantum mechanics, the previous procedure is applied to find approximate solutions of the Schrödinger equation.

2.2 Propagators

2.2.1 Definition

A propagator is a function that "propagates" the wavefunction through time, in other words, that let us to calculate properties of the system at time t from our knowledge of the same

system at a reference time, t'. In order to observe the relation between propagators and Green's function, we are going to follow a deduction proposed in reference [6]. We begin with the expression of the time-dependent Schrödinger equation for a system of N noninterating particles:

$$\mathcal{H}_0\psi(\nu,t) = i\frac{\partial\psi(\nu,t)}{\partial t} \tag{2-29}$$

expanding the wave function in terms of an orthonormal basis:

$$\psi(\nu,t) = \sum_r u_r(\nu)a_r(t) \tag{2-30}$$

and replacing it in equation 2-29 we obtain:

$$i\frac{\partial a_s(t)}{\partial t} - \sum_r h_{sr}a_r(t) = 0 \tag{2-31}$$

where:

$$h_{sr} = \int u_s^*(\nu)\mathcal{H}_0(\nu)u_s(\nu)d\nu \tag{2-32}$$

Now, if we take a unitary transformation of x that diagonalizes the h ($x^\dagger h x = \epsilon$), the solution of the equation 2-31 can be written as:

$$a_s(t) = \sum_k x_{sk}exp[-i\epsilon_k(t-t')]\left(\sum_r x_{kr}^\dagger a_r(t')\right) \tag{2-33}$$

such that $|a_r(t')|=1$, and $|a_s(t')|^2=0$ for $s \neq r$. Then the quantity:

$$|a_s(t)|^2 = |\sum_k x_{sk}exp[-i\epsilon_k(t-t')x_{kr}^\dagger]|^2 \tag{2-34}$$

is the probability of a particle to be "observed" in spin orbital s at time t, when it is known to be in spin orbital r at time t' with unit probability.

Now lets consider the probability of detecting a particle leaving the system from the s spin-orbital in time t provided that a particle enters in spin-orbital r at time t'. An injected electron has access only to unoccupied orbitals, and if it enters at time t', it cannot be observed leaving the system prior to that time, i.e, $t > t'$. Then, the associated probability will be:

$$P_{sr}(t,t') = 0 \quad (t < t') \tag{2-35}$$

$$P_{sr}(t,t') = |\sum_n x_{sk}(1-f_k)exp[-i\epsilon_k(t-t')]x_{rk}^\dagger|^2 \quad (t > t') \tag{2-36}$$

Where f_k is the occupation number (equal to 1 if the spin orbital is occupied or 0 if it is unoccupied). An electron could, of course, be observed leaving the system in spin orbital s at time $t < t'$ provided it is one of the N electrons in the system. This probability is zero for $t > t'$, given that the electron only can be released from an occupied spin-orbital. In this case we have:

$$\hat{P}_{sr}(t, t') = 0 \quad (t > t') \tag{2-37}$$

$$\hat{P}_{sr}(t, t') = |\sum_n x_{sk}(f_k)exp[-i\epsilon_k(t - t')]x_{rk}^\dagger|^2 \quad (t < t') \tag{2-38}$$

Then, the probability amplitude of the total scattering process is equal to:

$$G_{sr}(t, t') = -i\theta(t - t') \sum_n x_{sk}(1 - f_k)exp[-i\epsilon_k(t - t')]x_{rk}^\dagger \tag{2-39}$$

$$+i\theta(t' - t) \sum_n x_{sk}(f_k)exp[-i\epsilon_k(t - t')]x_{rk}^\dagger$$

where $\theta(t)$ is the Heaviside step function. The total probability is given by $|G_{sr}(t, t')|^2$. In this form $G_{sr}(t, t')$ has the information of the probability amplitude of the process in which one particle leaves a spin-orbital s at time t provided a particle enters in the spin-orbital r at time t'. This is the propagator of a system of N noninteracting particles. It is easy to show that the propagator satisfies the following relation:

$$\mathcal{H}_0 G_{sr}(t, t') = \delta_{sr}\delta(t - t') \tag{2-40}$$

According to the definition of Eq.2-15, this allow us to establish that the propagator is the Green's function of the time-dependent Schrödinger equation.

2.2.2 Propagators and second quantization

Evaluating the energy of the wavefunction enunciated in equation 2-29 we obtain the expression:

$$\int \psi^\dagger(\epsilon, t)h\psi(\epsilon, t)d\epsilon = \sum_{s,r} h_{sr}a_s^\dagger(t)a_r(t) \tag{2-41}$$

which is similar to the definition of one electron operator in the second quantization formalism (2-12), suggesting that $a_s(t)$ and its conjugate $(a_s^\dagger(t))$ are related with the annihilation and creation operators. In fact, $a_s(t)$ and $a_s^\dagger(t)$ can be seen as operators rather than functions, and can be shown that it satisfies the anticommutation properties of creation and annihilation (Eqs.2-6 and 2-8). Now we can apply the same transformation used in Equation 2-33 over 2-41, obtaining:

$$\sum_{s,r} h_{sr}a_s^\dagger(t)a_r(t) = \sum_k \left(\sum_s a_s^\dagger(t)x_{sk}\right) \epsilon_k \left(\sum_s x_{kr}^\dagger a_r(t)\right) = \sum_k \epsilon_k \bar{a}_k^\dagger \bar{a}_k. \tag{2-42}$$

The ground state of the electron system (including electron interaction) can be written using the vacuum state as:

$$|0\rangle = \bar{a}_1 \bar{a}_2 ... \bar{a}_N |\rangle \tag{2-43}$$

Now evaluating the following integral, written in bracket notation and using second quantization properties:

$$\sum_k \langle 0| \epsilon_k \bar{a}_k^\dagger \bar{a}_k |0\rangle = \sum_k \epsilon_k \langle 0| \bar{a}_k^\dagger \bar{a}_k |0\rangle = \sum_k f_k \epsilon_k \tag{2-44}$$

That clearly confirms that the Hamiltonian $\mathcal{H}_0$ can be expressed as:

$$\mathcal{H}_0 = \sum_k \epsilon_k \bar{a}_k^\dagger \bar{a}_k = \sum_{s,r} h_{sr} a_s^\dagger(t) a_r(t) \tag{2-45}$$

From this definition and Eq. 2-31 we obtain the value of the commutation between $\mathcal{H}_0$ and $a_s(t)$:

$$[\mathcal{H}_0, a_s(t)]_- = \sum_r h_{sr} a_r(t) \tag{2-46}$$

The Green's function defined in equation 2-39 for a system of N electrons is written in the second quantization notation as:

$$G_{sr}(t,t') \equiv \langle\langle a_s(t); a_r(t') \rangle\rangle = -i\theta(t-t')\langle 0| a_s(t) a_r^\dagger(t') |0\rangle + i\theta(t-t')i\langle 0| a_r^\dagger(t') a_s(t) |0\rangle \tag{2-47}$$

where θ is the Heaviside function. This follows from the expression of $a_s(t)$ in equation 2-33. The double bracket notation was introduced by Zubarev [6] and let us to define the general form of a double time Green's function or propagator as:

$$\langle\langle A(t); B(t') \rangle\rangle = -i\theta(t-t')\langle 0| A(t) B(t') |0\rangle + i\theta(t-t')i\langle 0| B(t') A(t) |0\rangle \tag{2-48}$$

Where A and B are fermion-like dynamical operators, which could, for instances, be formed as sums of products of simple second quantization operators.

2.2.3 Propagator's notation

Equation 2-48 can be transformed to the energy domain by using a Fourier transformation, assuming that **H** has a complete set of eigenvalues and eigenventors ($\mathcal{H}|n\rangle = E|n\rangle$) and using the completeness relation:

$$\langle\langle A; B \rangle\rangle(E) = \lim_{\eta \to \infty} \sum_n \left[\frac{\langle 0|A|n\rangle\langle n|B|0\rangle}{E - (E_n - E_0) + i\eta} \pm \frac{\langle 0|B|n\rangle\langle n|A|0\rangle}{E - (E_n - E_0) + i\eta} \right] \tag{2-49}$$

Tha above equation is called the spectral or Lehmann representation of the propagator. Now, we can rearrange equation 2-49 taking the limit when $\eta \to 0$ and multiplying it by E:

$$E\langle\langle A;B\rangle\rangle(E) = \sum_n \left[E\frac{\langle 0|A|n\rangle\langle n|B|0\rangle}{E - (E_n - E_0)} + E\frac{\langle 0|B|n\rangle\langle n|A|0\rangle}{E - (E_n - E_0)} \right] \tag{2-50}$$

$$= \sum_n \left(1 + \frac{E_0 - E_n}{E - (E_0 - E_n)} \right) \langle 0|A|n\rangle\langle n|B|0\rangle$$

$$+ \sum_n \left(1 + \frac{E_n - E_0}{E - (E_n - E_0)} \right) \langle 0|B|n\rangle\langle n|A|0\rangle \tag{2-51}$$

$$= \sum_n \left[\langle 0|A|n\rangle\langle n|B|0\rangle \pm \langle 0|B|n\rangle\langle n|A|0\rangle \right]$$

$$+ \left[\sum_n \frac{\langle 0|[A,H]_-|n\rangle\langle n|B|0\rangle}{E - (E_n - E_0)} + \sum_n \frac{\langle 0|B|n\rangle\langle n|[A,H]_-|0\rangle}{E - (E_0 - E_n)} \right] \tag{2-52}$$

Notice that the last term in the above equation is the propagator of $[A,H]_-$ and B operators. Then we can rewrite the above expression as:

$$E\langle\langle A;B\rangle\rangle = \langle 0|[A;B]_\pm|0\rangle + \langle\langle [A,H]_-;B\rangle\rangle_E \tag{2-53}$$
$$= \langle 0|[A;B]_\pm|0\rangle + \langle\langle A;[H,B]_-\rangle\rangle_E$$

This corresponds to a form of the *equation of motion.* Now it is possible to expand the above equation following the same procedure, which leads to the expression:

$$\langle\langle A;B\rangle\rangle = E^{-1}\langle 0|[A;B]_\pm|0\rangle + E^{-2}\langle 0|[[A,H],B]_\pm|\rangle \tag{2-54}$$
$$+ E^{-3}\langle 0|[[[A,H],H],B]_\pm|0\rangle - ...$$

In order to obtain a most compact notation we will introduce here the following parenthesis notation:

$$(x|y) = \langle 0|[x^+,y]_\pm|0\rangle \tag{2-55}$$

Now we are going to define the superoperators:

$$\hat{H}y = [H,y]_- \tag{2-56}$$

and

$$\hat{I}y = y \tag{2-57}$$

With these definitions we can rewrite Eq.2-54 as:

$$\langle\langle A;B\rangle\rangle_E = E^{-1}(A|B) + E^{-2}(A|\hat{H}B) + E^{-3}(A|\hat{H}^2 B) + ... \tag{2-58}$$

now using the geometric series expansion:

$$E^{-1}\sum_{n=0}^{\infty}(\hat{H}/E)^n = E^{-1}[\hat{I} - (\hat{H}/E)]^{-1} = (E\hat{I} - \hat{H})^{-1} \tag{2-59}$$

the propagator can be written as

$$G_{A;B}(E) = \langle\langle A, B\rangle\rangle_E = (A|(E\hat{I} - \hat{H})^{-1}B) \tag{2-60}$$

where $(E\hat{I} - \hat{H})^{-1}$ is called the *superoperator resolvent*.

2.3 The Electron Propagator

2.3.1 Definition

The electron propagator is defined in terms of the electron field operators:

$$G_{rs}(E) \equiv \langle\langle a_r^{\dagger}; a_s\rangle\rangle \tag{2-61}$$

$$= \sum_n \frac{\langle 0^N|a_r^{\dagger}|n^{N-1}\rangle\langle n^{N-1}|a_s|0^N\rangle}{E + E_n(N-1) - E_0(N)} + \frac{\langle 0^N|a_s|m^{N+1}\rangle\langle m^{N+1}|a_r^{\dagger}|0^N\rangle}{E + E_m(N+1) - E_0(N)}$$

The poles of the Green's function (values of E for which function is indeterminated) are equal to differences between energies of the N electron and N-1 and N+1 electron states, corresponding to ionization potentials (IE) and electron affinities (EA) of the N electron system. The numerators of the propagator related to the discontinuity of the Green's function are called the Feynman-Dyson amplitudes (FDAs), and are related to the transition probabilities for electron attachment and detachment processes:

$$U_{a,n}^{IE} = \langle n^{N-1}|a_a|0^N\rangle \tag{2-62}$$

$$U_{i,n}^{EA} = \langle n^{N+1}|a_i^{\dagger}|0^N\rangle \tag{2-63}$$

where a and i denoted unoccupied and occupied spin-orbitals. The FDAs can be used to build the Dyson Orbitals (DOs) in terms of spin-orbitals:

$$|g_n\rangle = \sum_{i=1}^{N}|\phi_i\rangle U_{i,n}^{IE} = \sum_{i=1}^{N}|\phi_i\rangle\langle n^{N-1}|a_i|0^N\rangle = \sum_{i=1}^{N}c_{in}\phi_i \tag{2-64}$$

$$|f_n\rangle = \sum_{i=1}^{N}|\phi_i\rangle U_{r,n}^{EA} = \sum_{i=1}^{N}|\phi_i\rangle\langle n^{N+1}|a_r^{\dagger}|0^N\rangle = \sum_{i=1}^{N}c_{rn}\phi_i$$

These orbitals correspond to the overlap between the initial N electron state and the final (N-1 or N+1) electron state. The integral is over the coordinates of all electrons except one (x_1), yielding a one-electron function that can be written as a linear combination of Hartree-Fock (HF) canonical molecular orbitals (ϕ_i) in case that we use the HF approximation as starting point to build the initial wave function $|0^N\rangle$.

2.3.2 Partitioning and inner projection

Using the notation introduced by Eq.2-60 for the propagator matrix, the one electron propagator matrix can be written as:

$$\mathbf{G}(E) = (\mathbf{a}|(E\hat{I} - \hat{H})^{-1}\mathbf{a}) \tag{2-65}$$

where $\mathbf{a}$ is a vector containing all the annihilation operators of the system. $\hat{H}$ is the superoperator corresponding to the exact Hamiltonian operator of the electron system written using second quantization:

$$H = \sum_{p,q} h_{pq} a_p^\dagger a_q + \frac{1}{4} \sum_{p,q,s,t} \langle pq||st \rangle a_p^\dagger a_q^\dagger a_t a_s \tag{2-66}$$

We point out that the superoperator resolvent has a negative exponent that cannot be easily evaluated. To overcome this problem the following inner projection manifold is introduced:

$$\mathbf{h} = \mathbf{a} \cup \mathbf{f}_3 \cup \mathbf{f}_5 \cup \ldots \tag{2-67}$$

$$\mathbf{h} = \{a_i, a_a\} \cup \{a_i^\dagger a_a a_b, a_a^\dagger a_i a_j\} \cup \{a_i^\dagger a_j^\dagger a_a a_b a_c, a_a^\dagger a_b^\dagger a_i a_j a_k\} \cup \ldots \tag{2-68}$$

where indices i, j, k, l stand for occupied orbitals and a, b, c, d for virtual or unoccupied orbitals. Notice that space $\mathbf{h}$ describes processes where the number of quantum particles of the system changes by one. $\mathbf{h}$ also satisfies the completeness relation $(\mathbf{h}|\mathbf{h}) = \mathbf{1}$ that applied to Eq.2-65 yields:

$$\mathbf{G}(E) = (\mathbf{a}|\mathbf{h})(\mathbf{h}|(E\hat{I} - \hat{H})|\mathbf{h})^{-1}(\mathbf{h}|\mathbf{a}) \tag{2-69}$$

where we have avoided the negative exponent of the superoperator resolvent. To proceed with the calculation of $\mathbf{G}(E)$ we separate the space $\mathbf{h}$ into two orthogonal spaces, as follows:

$$\mathbf{h} = \mathbf{a} \cup \mathbf{f} \tag{2-70}$$

$$\mathbf{f} = \mathbf{f}_3 \cup \mathbf{f}_5 \cup \ldots \tag{2-71}$$

And then Eq.2-69 becomes:

$$\mathbf{G}(E) = \begin{bmatrix} \mathbf{1} & \mathbf{0} \end{bmatrix} \begin{bmatrix} E\mathbf{1} - (\mathbf{a}|\hat{H}\mathbf{a}) & -(\mathbf{a}|\hat{H}\mathbf{f}) \\ -(\mathbf{f}|\hat{H}\mathbf{a}) & E\mathbf{1} - (\mathbf{f}|\hat{H}\mathbf{f}) \end{bmatrix}^{-1} \begin{bmatrix} \mathbf{1} \\ \mathbf{0} \end{bmatrix} \tag{2-72}$$

Now using the following property of the inverse 2x2 matrix:

$$\begin{bmatrix} A & B \\ C & D \end{bmatrix}^{-1} = \begin{bmatrix} A - BD^{-1}C & C - DB^{-1}A \\ B - AC^{-1}D & D - CA^{-1}B \end{bmatrix} \tag{2-73}$$

the partitioned form of the inner matrix yields:

$$\mathbf{G}^{-1}(E) = E\mathbf{1} - (\mathbf{a}|\hat{H}\mathbf{a}) - (\mathbf{a}|\hat{H}\mathbf{f})[E\mathbf{1} - (\mathbf{f}|\hat{H}\mathbf{f})]^{-1}(\mathbf{f}|\hat{H}\mathbf{a}) \tag{2-74}$$

Finally, we can separate the exact Hamiltonian H as $H = H_0 + V$ to obtain:

$$\mathbf{G}^{-1}(E) = E\mathbf{1} - (\mathbf{a}|\hat{H}_0\mathbf{a}) - (\mathbf{a}|\hat{V}\mathbf{a}) - (\mathbf{a}|\hat{H}\mathbf{f})[E\mathbf{1} - (\mathbf{f}|\hat{H}\mathbf{f})]^{-1}(\mathbf{f}|\hat{H}\mathbf{a}) \tag{2-75}$$

$$\mathbf{G}^{-1}(E) = \mathbf{G}_0^{-1} - (\mathbf{a}|\hat{V}\mathbf{a}) - (\mathbf{a}|\hat{H}\mathbf{f})[E\mathbf{1} - (\mathbf{f}|\hat{H}\mathbf{f})]^{-1}(\mathbf{f}|\hat{H}\mathbf{a}) \tag{2-76}$$

$$\mathbf{G}^{-1}(E) = \mathbf{G}_0^{-1} - \mathbf{\Sigma}(E) \tag{2-77}$$

Which is the Dyson equation that allow us to find the poles of the exact Green's function by using the Green's function of an already known reference Hamiltonian corrected by a self-energy matrix, $\mathbf{\Sigma}(E)$, which introduces the corrections due to the perturbation V.

An alternative way to find the poles of the Green function is by finding the eigenvalues (ω) of the superoperator Hamiltonian matrix $\mathbf{H}$:

$$\mathbf{U}\omega = \mathbf{H}\mathbf{U} \tag{2-78}$$

$$\omega_n \begin{bmatrix} \mathbf{U}_{a,n} & \mathbf{U}_{f,n} \end{bmatrix} = \begin{bmatrix} (\mathbf{a}|\hat{H}\mathbf{a}) & (\mathbf{a}|\hat{H}\mathbf{f}) \\ (\mathbf{f}|\hat{H}\mathbf{a}) & (\mathbf{f}|\hat{H}\mathbf{f}) \end{bmatrix} \begin{bmatrix} \mathbf{U}_{a,n} \\ \mathbf{U}_{f,n} \end{bmatrix} \tag{2-79}$$

In this formulation, the Dyson Orbital can be written as:

$$|g_n\rangle = \sum_a^{occ} U_a|\phi_i\rangle + \sum_r^{virt} U_r|\phi_i\rangle \tag{2-80}$$

The sum of the squared coefficients of the DO defines the pole strength. Pole strengths above 0.9 indicate that the Koopmans's one-electron description is qualitatively valid. Diagonal approximations (see below) should provide accurate representations of the ionization process if there is a single, dominant term in Equation 2-80. Lower pole strengths (below 0.8) are generally an indication that shake-up states are to be expected, and nondiagonal approximations are recommended to accurately describe the ionization. The electron propagator theory has been developed by introducing Moller-Plesset and Coupled Cluster expansions of the wavefunction in Eqs.2-79 and 2-77. In the theoretical development we will show details of this procedure, not for the case of an electronic system, but for a general system contaning more than one fermionic species. With that aim we need to introduce first an approach to treat several fermionic species using the Hartree-Fock approximation. This approach is the any particle molecular orbital theory.

2.4 Any particle molecular orbital (APMO) theory

The basic idea behind the APMO approach is that the wavefunction of a finite system comprising several type of particles (namely species) can be treated using the Hartree-Fock approximation and applying the same set of methods that has been developed to treat electronic wavefunctions in molecular systems under the Born-Oppenheimer approximation. In this section we briefly review the APMO approach.

2.4.1 APMO/HF theory

The molecular Hamiltonian, H^{TOT}, includes contributions from classical and quantum particles, such that:

$$H^{TOT} = -\sum_i^{N^Q} \frac{1}{2M_i}\nabla_i^2 + \sum_i^{N^Q}\sum_{j>i}^{N^Q} \frac{Q_i Q_j}{r_{ij}} + \sum_i^{N^Q}\sum_j^{N^C} \frac{Q_i Q_j}{r_{ij}} + \sum_i^{N^C}\sum_{j>i}^{N^C} \frac{Q_i Q_j}{r_{ij}} \quad , \quad (2\text{-}81)$$

where Q_i is the charge of the particle i, and N^Q and N^C are the number of quantum and classical particles, respectively [35].

At the APMO/HF level the molecular wavefunction, Ψ_0, is approximated as a product of single-configurational wavefunctions, Φ^α, for different types of quantum species α:

$$\Psi_0 = \prod_\alpha^{N^Q} \Phi^\alpha. \qquad (2\text{-}82)$$

Each Φ^α is represented in terms of molecular orbitals (MO), ψ_i^α. These ψ_i^α are obtained by solving the equations

$$f^\alpha(i)\psi_i^\alpha = \varepsilon_i^\alpha \psi_i^\alpha, \quad \forall i, \alpha, \qquad (2\text{-}83)$$

Each $f^\alpha(\mathrm{i})$ is an effective one-particle Fock operator for the quantum species α written as

$$f^\alpha(i) = h^\alpha(i) + {Q_\alpha}^2 \sum_{j\in\alpha}[J_j^\alpha \mp K_j^\alpha] + \sum_{\beta\neq\alpha}^{N^Q} Q_\alpha \sum_{j\in\beta} Q_\beta J_j^\beta. \qquad (2\text{-}84)$$

In the above equation $h^\alpha(i)$ is the one–particle core Hamiltonian,

$$h^\alpha(i) = -\frac{\nabla_i^2}{2M_\alpha} + \sum_j^{N^C} \frac{Q_j^C Q_\alpha}{r_{ij}} \qquad (2\text{-}85)$$

and J^α and K^α are Coulomb and exchange operators defined as,

$$J_j^\alpha(1)\psi_i^\alpha(1) = \left[\int d\mathbf{r}_2 \psi_j^{\alpha*}(2)\frac{1}{r_{12}}\psi_j^\alpha(2)\right]\psi_i^\alpha(1), \qquad (2\text{-}86)$$

$$K_j^\alpha(1)\psi_i^\alpha(1) = \left[\int d\mathbf{r}_2 \psi_j^{\alpha*}(2)\frac{1}{r_{12}}\psi_i^\alpha(2)\right]\psi_j^\alpha(1). \qquad (2\text{-}87)$$

The sign preceding the exchange operator in Eq. 2-84 is chosen depending on the bosonic (positive) or fermionic (negative) nature of the α particles. In previous studies it has been observed that the exchange integrals between individual nuclei are always negligible and as a result they are neglected in our numerical treatment [25, 35].

2.4.2 Second quantization in APMO theory

As shown in the preliminar sections, extending the propagator theory to multiple particles requires to work in a second quantization approach. We introduce the elementary creation and annihilation operators for the fermionic species α $\{a_p, a_p^\dagger\}$ that act on the pth orbital of the single–configuration wave function Φ^α and satisfy the following relations [6, 34]:

$$\left[a_p^{\alpha\dagger}, a_q^\alpha\right]_+ = a_p^{\alpha\dagger} a_q^\alpha + a_q^\alpha a_p^{\alpha\dagger} = \delta_{qp} \tag{2-88}$$

$$\left[a_p^{\alpha\dagger}, a_q^{\alpha\dagger}\right]_+ = \left[a_p^\alpha, a_q^\alpha\right]_+ = 0 \tag{2-89}$$

Similarly for species β we will have the operators: $\{a_P, a_P^\dagger\}$. The following rule defines the relation between operators of different species [25, 36]:

$$\left[a_p^\dagger, a_P^\dagger\right]_- = \left[a_p, a_P\right]_- = \left[a_p^\dagger, a_P\right]_- = 0 \tag{2-90}$$

Employing the above notation, Eq. (2-81) can be written as [25, 37]:

$$H^{TOT} = \sum_\alpha^{N^Q} H_0^\alpha + V_1^\alpha + V_2^\alpha \tag{2-91}$$

with

$$H_0^\alpha = \sum_{p\in\alpha} (\lambda^\alpha)^2 \varepsilon_p^\alpha a_p^\dagger a_p \tag{2-92}$$

$$V_1^\alpha = \sum_{p,q,r,s\in\alpha} (\lambda^\alpha)^2 \langle pq||rs\rangle \left[\frac{1}{4} a_p^\dagger a_q^\dagger a_s a_r - \delta_{qs}\langle n_q\rangle a_p^\dagger a_r\right] \tag{2-93}$$

$$V_2^\alpha = \sum_{\beta\neq\alpha}^{N^Q} \sum_{\substack{p,q\in\alpha \\ P,Q\in\beta}} \lambda^\alpha \lambda^\beta \langle pP|qQ\rangle \left[\frac{1}{2} a_p^\dagger a_P^\dagger a_Q a_q - \delta_{PQ}\langle n_P\rangle a_p^\dagger a_q\right] \tag{2-94}$$

Here, ε_p^α is the pth orbital energy for species α and λ^α and λ^β include the effects of signs and charges of species α and β.

2.4.3 Many body perturbation expansion (MBPT) of the APMO wavefunction

Taking the APMO/HF wavefunction, $|\Psi_0\rangle$, as reference state, the exact APMO wavefunction, $|\Psi\rangle$, can be expanded as a perturbational series expressed as follows:

$$|\Psi\rangle = (1 + \hat{T})|\Psi_0\rangle \tag{2-95}$$

$$|\Psi\rangle = (1 + \hat{T}_1 + \hat{T}_2 + \ldots)|\Psi_0\rangle \tag{2-96}$$

$$|\Psi\rangle = \mathcal{N}^{-1/2} \left[1 + \sum_\alpha^{N^Q} \sum_{i,a\in\alpha} \kappa_i^a a_a^\dagger a_i + \sum_\alpha^{N^Q} \sum_{\beta>\alpha}^{N^Q} \sum_{\substack{i,a \\ I,A}} \kappa_{iI}^{aA} a_a^\dagger a_A^\dagger a_I a_i + \ldots\right]|\Psi_0\rangle \tag{2-97}$$

where $\mathcal{N}$ is a normalization constant and $|\Psi_0\rangle$ is the APMO/HF wavefunction, as defined in Eq. (2-82); $i, j, \ldots$ $(a, b, \ldots)$ stand for occupied (virtual) orbitals of α particles and $I, J, \ldots$ $(A, B, \ldots)$ stand for occupied (virtual) orbitals of β particles and so on. The correlation coefficients, κ, are obtained from Rayleigh–Schrödinger perturbation theory [27, 32, 38, 39]. For instance:

$$\kappa_i^a = \frac{1}{2}\left[\sum_{jbc}\frac{\langle bc||aj\rangle}{\epsilon_i - \epsilon_a}\kappa_{ij}^{bc} - \sum_{jkb}\frac{\langle ib||jk\rangle}{\epsilon_i - \epsilon_a}\kappa_{jk}^{ab}\right] + \sum_{\beta\neq\alpha}^{N^Q}\left[\sum_{IbA}\frac{\langle iI|bA\rangle}{\epsilon_i - \epsilon_a}\kappa_{iI}^{bA} - \sum_{IjA}\frac{\langle jI|aA\rangle}{\epsilon_i - \epsilon_a}\kappa_{jI}^{aA}\right] \quad (2\text{-}98)$$

$$\kappa_{iI}^{aA} = \frac{\langle iI|aA\rangle}{\epsilon_i + \epsilon_I - \epsilon_a - \epsilon_A}; \quad \kappa_{ij}^{ab} = \frac{\langle ij||ab\rangle}{\epsilon_i + \epsilon_j - \epsilon_a - \epsilon_b} \quad (2\text{-}99)$$

2.4.4 Treatment of rotations and translations within the APMO scheme

The APMO wavefunction for a molecular system where all the particles are considered quantum mechanically should included the description of the translational and rotational motions. The treatment of these motions is of special importance because the localized gaussian basis sets employed in the APMO method are not a suitable basis set to construct the rotational and translational wavefunctions. To avoid the problem of describing rotations and translations we can remove them from the total Hamiltonian. In this section we summarizes the scheme proposed by Nakai et al [37, 40, 41] to do so.

Translational and rotational free treatment

The complete nuclear-electron Hamiltonian, called translational-rotational contaminated (TRC) is expressed as:

$$\hat{H_{TRC}} = \hat{T}^e + \hat{T}^n + \hat{V}^{ee} + \hat{V}^{nn} + \hat{V}^{en} \quad (2\text{-}100)$$

$$\hat{T}^e = -\sum_p \frac{1}{2}\nabla(\boldsymbol{x}_q)^2 \equiv \sum_p \hat{t}^e(\boldsymbol{x}_p) \quad (2\text{-}101)$$

$$\hat{T}^n = -\sum_P \frac{1}{2m_P}\nabla(\boldsymbol{x}_P)^2 \equiv \sum_P \hat{t}^n(\boldsymbol{x}_P) \quad (2\text{-}102)$$

$$\hat{V}^{ee} = \sum_{p<q}\frac{1}{r_{pq}} \equiv \sum_{p<q}v^{ee}(\boldsymbol{x}_{pq}); \; \hat{V}^{en} = \sum_{p,P}\frac{Z_P}{r_{pP}} \equiv \sum_{p<q}v^{en}(\boldsymbol{x}_{pP}); \quad (2\text{-}103)$$

$$\hat{V}^{ee} = \sum_{P<Q}\frac{Z_P Z_Q}{r_{PQ}} \equiv \sum_{p<q}v^{nn}(\boldsymbol{x}_{PQ}) \quad (2\text{-}104)$$

The total wavefunction can be approximated as:

$$\Psi = \Psi^n \Psi^e \tag{2-105}$$

$$\Psi^n = \phi_1^n \phi_2^n ... \phi_N^n \tag{2-106}$$

$$\Psi^e = |\phi_1^e \phi_2^e ... \phi_n^e\rangle \tag{2-107}$$

The Hartree-Fock equations can be written for the TRC as:

$$\hat{f}_p^e \phi_p^e = \epsilon_p^e \phi_p^e; \quad \hat{f}_{P_1}^n \phi^n = \epsilon_{P_1}^n \phi^n \tag{2-108}$$

where the Fock operator is expressed as:

$$\hat{f}_p^e = \hat{h}_p^e + \sum_i^n (\hat{J}_i^{ee} - \hat{K}_i^{ee}) + \sum_I^N \hat{J}_{P_I}^{en}; \quad \hat{f}_{P_I}^n = \hat{h}_{P_I}^n + \sum_{J \neq I}^N \hat{J}_{P_J}^{nn} + \sum_i^n \hat{J}_i^{en} \tag{2-109}$$

where

$$\hat{J}_i^{ee} = \int \phi_i(r_1) \hat{V}^{ne}(r_1, r_2) \phi_i(r_1) dr_1 \quad \hat{K}_i^{ee} = \int \phi_i(r_1) \ \hat{V}^{ne}(r_1, r_2) \phi_j(r_1) \phi_i(r_2) dr_1 dr_2 \tag{2-110}$$

$$\hat{J}_{P_J}^{nn} = \int \phi_I(r_1) \hat{V}^{nn}(r_1, r_2) \phi_I(r_1) dr_1 \quad \hat{J}_{P_I}^{en} = \int \phi_I(r_1) \hat{V}^{ne}(r_1, r_2) \phi_I(r_1) dr_1 \tag{2-111}$$

$$\hat{J}_i^{en} = \int \phi_i(r_1) \hat{V}^{ne}(r_1, r_2) \phi_i(r_1) dr_1 \tag{2-112}$$

To remove translational and rotational corrections, the translational and rotational Hamiltonian are subtracted from $\hat{H}_{TRC}$:

$$\hat{H}_{TF} = \hat{H}_{TRC} - \frac{1}{2M_{TOT}} \sum_\mu \nabla(x_\mu) - \frac{1}{M_{TOT}} \sum_{\mu > \nu} \nabla(x_\mu) \cdot \nabla(x_\nu) \tag{2-113}$$

$$\hat{H}_{TRF} = \hat{H}_{TF} - \sum_\alpha^{x,y,z} \frac{1}{2\hat{I}_\alpha} \left(\sum_\mu L_{\alpha,\mu} + 2 \sum_{\mu > \nu} L_{\alpha,\mu} \cdot L_{\alpha,\nu} \right) \tag{2-114}$$

Then the following procedure is performed [37, 40]: 1) Coordinates of the system are transformed to the those centered on the mass center (r) ; 2) r_μ is expanded in a Taylor series $r_\mu = r_\mu^0 + \Delta r_\mu$ as well as the L operator: $\hat{L}_{\alpha,\mu} = \hat{L}_{\alpha,\mu}^0 + \Delta \hat{L}_{\alpha,\mu}$ where $\hat{L}_{\alpha,\mu}^0$ corresponds to the zero-order rotational Hamiltonian (rigid rotor), where the position of nuclei are fixed to the center of the basis set functions. 3) The translational and rotational Hamiltonians are approximated to the nuclear translational and rotational Hamiltonians. By doing this, the $\hat{t}^n$ and $\hat{v}^{nn}$ operators are modified as:

$$\hat{t}_{TF}^n = -\frac{1}{2} \left(\frac{1}{m_P} - \frac{1}{M_{TOT}} \right) \nabla^2(r_P); \quad \hat{t}_{TRF}^n = \hat{t}_{TF}^n - \sum_\alpha^{x,y,z} \frac{1}{2\hat{I}_\alpha} \hat{L}_{\alpha,P}^0{}^2 \tag{2-115}$$

$$\hat{v}_{TF}^{nn} = \frac{Z_P Z_Q}{r_{PQ}} + \frac{1}{M_{TOT}} \nabla(r_P) \cdot \nabla(r_P); \quad \hat{v}_{TRF}^{nn} = \hat{t}_{TF}^n - \sum_\alpha^{x,y,z} \frac{1}{\hat{I}_\alpha} \hat{L}_{\alpha,P}^0 \cdot \hat{L}_{\alpha,Q}^0 \tag{2-116}$$

3 Theoretical development

3.1 Extension of super-operator formulation for APMO

For a system comprising N^Q fermionic species $\{\alpha, \beta, ...\}$ the spectral representation of a pq element of one–α–particle Green function is given by:

$$G_{pq}^{\alpha}(\omega^{\alpha}) = \sum_m \frac{\langle \Psi(N^{\alpha}, N^{\beta}, ...)|a_p|\Psi^m(N^{\alpha}+1, N^{\beta}, ...)\rangle\langle\Psi^m(N^{\alpha}+1, N^{\beta}, ...)|a_q^{\dagger}|\Psi(N_{\alpha}, N_{\beta}, ...)\rangle}{\omega^{\alpha} - E_m(N_{\alpha}+1, N_{\beta}, ...) + E_0(N_{\alpha}, N_{\beta}, ...)}$$

$$(3\text{-}1)$$

$$+ \sum_n \frac{\langle\Psi(N^{\alpha}, N^{\beta}, ...)|a_q^{\dagger}|\Psi^n(N^{\alpha}-1, N^{\beta}, ...)\rangle\langle\Psi^n(N^{\alpha}-1, N^{\beta}, ...)|a_p|\Psi(N_{\alpha}, N_{\beta}, ...)\rangle}{\omega^{\alpha} - E_n(N_{\alpha}-1, N_{\beta}, ...) + E_0(N_{\alpha}, N_{\beta}, ...)}$$

here $|\Psi^n(N^{\alpha}-1, N^{\beta}, ...)\rangle$ ($|\Psi^n\rangle$ in the rest of the text) stands for the exact wavefunction for a state n containing $N_{\alpha}-1$, N_{β},... particles of each species and $E_n(N_{\alpha}-1, N^{\beta}, ...)$ is its corresponding energy. On the other hand $|\Psi^m(N^{\alpha}+1, N^{\beta}, ...)\rangle$ ($|\Psi^m\rangle$ in the rest of the text) stands for the exact wavefunction for a state m containing $N_{\alpha}+1$, N_{β},... particles of each species and $E_m(N_{\alpha}+1, N^{\beta}, ...)$ is its corresponding energy. The parameter ω^{α} has energy units. It can be inferred that the poles of Eq. (3-1) correspond to exact binding energies for particles of the species α.

Following Pickup and Goscinski[8] now we introduce the superoperator metric, defined as

$$(A|B) = \langle\Psi|[A^{\dagger}, B]_+|\Psi\rangle, \tag{3-2}$$

where A and B are two arbitrary operators (i.e. linear combinations of products of fermion–like creation or annihilation operators). The identity and Hamiltonian superoperators, $\hat{I}$ and $\hat{H}$, can be defined as:

$$\hat{I}A = A \tag{3-3}$$

$$\hat{H}A = [A, H^{TOT}]_- = A\,H^{TOT} - H^{TOT}\,A \tag{3-4}$$

where the Hamiltonian, H^{TOT}, is the APMO Hamiltonian in its second quantized form Eq (2-91). Employing the above definitions, it is possible to write the α propagator matrix as:

$$\mathbf{G}^{\alpha}(\omega^{\alpha}) = (\mathbf{a}^{\alpha}|(\omega^{\alpha}\hat{I} - \hat{H})^{-1}\mathbf{a}^{\alpha}) \tag{3-5}$$

where $\mathbf{a}^\alpha$ contains all the single annihilation operators, $\{a_i^\alpha, a_a^\alpha\}$.

By applying Löwdin's inner projection technique [42] with an appropiate superoperator space $\mathbf{h}^\alpha$ [35], the inversion of the super-operator resolvent in Eq. (3-5) is avoided and only one matrix inversion is needed:

$$\mathbf{G}^\alpha(\omega^\alpha) = (\mathbf{a}^\alpha|\mathbf{h}^\alpha)(\mathbf{h}^\alpha|(\omega^\alpha\hat{I} - \hat{H})\mathbf{h}^\alpha)^{-1}(\mathbf{h}^\alpha|\mathbf{a}^\alpha) \tag{3-6}$$

The elements of the super-operator space, $\mathbf{h}^\alpha$ are defined in such a way that they changes the number of α particles by one, while conserving the number of particles of the other species:

$$\mathbf{h}^\alpha = \{\mathbf{a}^\alpha\} \cup \{\mathbf{f}_3^\alpha\} \cup \{\mathbf{f}_5^\alpha\} \cup \ldots \tag{3-7}$$
$$\mathbf{h}^\alpha = \{\mathbf{a}^\alpha\} \cup \{\mathbf{f}_3^{\alpha\alpha\alpha}, \mathbf{f}_3^{\beta\alpha\beta}, \mathbf{f}_3^{\gamma\alpha\gamma} \ldots\} \cup \{\mathbf{f}_5^\alpha\} \cup \ldots$$
$$\mathbf{h}^\alpha = \{a_a, a_i\} \cup \{a_i^\dagger a_a a_b, a_a^\dagger a_i a_j, a_I^\dagger a_a a_A, a_A^\dagger a_i a_I, a_\Gamma^\dagger a_i a_\Lambda, a_\Lambda^\dagger a_a a_\Gamma, \ldots\} \cup \{\mathbf{f}_5^\alpha\} \cup \ldots$$

The projection space, $\mathbf{h}^\alpha$, can be partitioned for convenience into two orthogonal spaces: the primary space, $\mathbf{a}^{\alpha\dagger} = \{a_a^{\alpha\dagger}, a_i^{\alpha\dagger}\}$ and the complementary space, $\mathbf{f}^\alpha$. The latter space contains operators associated to ionizations of an α particle coupled to excitations of any type of particle in the system. Using this partition, the propagator matrix can be rearranged as:

$$\mathbf{G}^\alpha(\omega^\alpha) = \begin{bmatrix} \mathbf{1} & \mathbf{0} \end{bmatrix} \begin{bmatrix} \omega^\alpha\mathbf{1} - (\mathbf{a}^\alpha|\hat{H}\mathbf{a}^\alpha) & -(\mathbf{a}^\alpha|\hat{H}\mathbf{f}^\alpha) \\ -(\mathbf{f}^\alpha|\hat{H}\mathbf{a}^\alpha) & \omega^\alpha\mathbf{1} - (\mathbf{f}^\alpha|\hat{H}\mathbf{f}^\alpha) \end{bmatrix}^{-1} \begin{bmatrix} \mathbf{1} \\ \mathbf{0} \end{bmatrix} \tag{3-8}$$

After some transformations, the above expression becomes:

$$\mathbf{G}^{\alpha^{-1}}(\omega^\alpha) = (\mathbf{a}^\alpha|(\omega^\alpha\hat{I} - \hat{H})|\mathbf{a}^\alpha) - (\mathbf{a}^\alpha|\hat{H}|\mathbf{f}^\alpha)\left[\omega^\alpha\hat{I} - (\mathbf{f}^\alpha|\hat{H}|\mathbf{f}^\alpha)\right]^{-1}(\mathbf{f}^\alpha|\hat{H}|\mathbf{a}^\alpha) \tag{3-9}$$

which can also be presented as a Dyson-like equation [6]

$$\mathbf{G}^{\alpha^{-1}}(\omega^\alpha) = \mathbf{G_0}^{\alpha^{-1}}(\omega^\alpha) - \Sigma^\alpha(\omega^\alpha) \tag{3-10}$$

with

$$\mathbf{G_0}^\alpha(\omega^\alpha)_{pq} = \frac{\delta_{pq}}{\omega^\alpha - \epsilon_p^\alpha}. \tag{3-11}$$

The self-energy matrix for the α–type particle, $\Sigma^\alpha(\omega^\alpha)$, is defined by Eq. (3-10). The self-energy corresponds to a non-local and energy dependent potential that accounts for the correlation and relaxation effects missing in the zero order solution of the Schrödinger equation. Note that if an untruncated manifold is included in $\mathbf{f}^\alpha$, the poles of the propagator correspond to the exact one–particle binding energies. In order to arrive at a definite approximation for the self-energy, the perturbative expansion (Eq. (2-95)) and the operator space (Eq. (3-7)) must be truncated.

3.2 Self-energy approximations in APMO

3.2.1 Evaluation of inner products

To get working equations for the self-energy we must expand the inner products appearing in Eqs. 3-9 and 3-10 by introducing the perturbational series of Eq.2-95. Terms $(\mathbf{a}^\alpha|\hat{H}\mathbf{a}^\alpha)$, $(\mathbf{f}^\alpha|\hat{H}\mathbf{a}^\alpha)$ and $(\mathbf{f}^\alpha|\hat{H}\mathbf{f}^\alpha)$ can be expanded by following the rule:

$$
\begin{aligned}
(Y|Z) =& \langle\Psi_0|(1+\hat{T}^\dagger)[Y^\dagger,Z]_-(1+\hat{T})|\Psi_0\rangle \\
=& (Y|Z)_0 + (Y|Z)_1 + (Y|Z)_2 + (Y|Z)_3 + \ldots
\end{aligned}
\tag{3-12}
$$

For instance:

$$
(\mathbf{a}^\alpha|\hat{H}\mathbf{a}^\alpha) = (\mathbf{a}^\alpha|\hat{H}\mathbf{a}^\alpha)_0 + (\mathbf{a}^\alpha|\hat{H}\mathbf{a}^\alpha)_1 + (\mathbf{a}^\alpha|\hat{H}\mathbf{a}^\alpha)_2 + \ldots
\tag{3-13}
$$

An inner product evaluated up to order n correspond to:

$$
(Y|Z)^{(n)} = \sum_{i=0}^{n} (Y|Z)_i
\tag{3-14}
$$

Inner products appearing in Eq(3-9) can be categorized into 3 groups:

- Inner products between elements of the primary space, $(\mathbf{a}^\alpha|\hat{H}\mathbf{a}^\alpha)$.

- Inner products between elements of the primary and complementary spaces, $(\mathbf{a}^\alpha|\hat{H}\mathbf{f}^\alpha)$.

- Inner products between elements of the complementary spaces, $(\mathbf{f}^\alpha|\hat{H}\mathbf{f}^\alpha)$.

An order by order construction of the self-energy is achieved by keeping a balance between the truncation of the perturbational series and the truncation of the operator space-manifold (Eq. (3-7)). Up to third order, calculations require the computation of inner products comprising up to three quantum species (α, β, γ) and involving only the elements of the $\mathbf{f}_3^\alpha$ complementary space. With the aim of facilitating the evaluation of the inner products, we follow the algebraic diagrammatic construction (ADC) procedure proposed by Cederbaum et al [9, 10, 13, 36, 36, 43]. For treating several fermionic species we used the modification of the diagrammatic method independently proposed by Cederbaum [36] and Nakai [25], which is summarized in Table **3-1**.

At first we define three type of vertices to represent species α, β and γ. Arrows leaving vertices represents creation operators while annihilation operators correspond to arrows directed towards vertices. In the particle-hole formalism, upward and downward arrows represent "particle" and "hole" lines, respectively. In the following, we show the explicit expressions for the inner products required to compute the full third order self-energy, as obtained by the ADC procedure. We use the notation shown in table **3-2** for the spin-orbitals indices.

Table **3-1**: Elements employed to build diagramms for several fermionic species
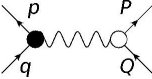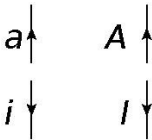
Element	Representation
α, β and γ vertices	
Creation operators: $a_p^\dagger$, $a_P^\dagger$	
Annihilation operators: a_p, a_P	
Intra-species interaction $(pq\|\|rs)$	
Inter-species interaction $(pq\|PQ)$	
Particles: $a_a^\dagger, a_A^\dagger,...$ Holes: $a_i, a_I,...$	

Table **3-2**: Orbital indices for α, β and γ species

Species	Occupied	Virtual	Either
α	i, j, ...	a, b, ...	p, q
β	I, J, ...	A, B, ...	P, Q
γ	Γ, Δ, ...	Λ, Ξ, ...	Υ, Ω

Figure **3-1**: Diagramatic representation of $\mathbf{f}_3^\alpha$ operators: 2ph (left) and 2hp (right)

$$a_i^\dagger a_a a_b \qquad a_I^\dagger a_a a_A \qquad a_a^\dagger a_i a_j \qquad a_A^\dagger a_i a_I$$
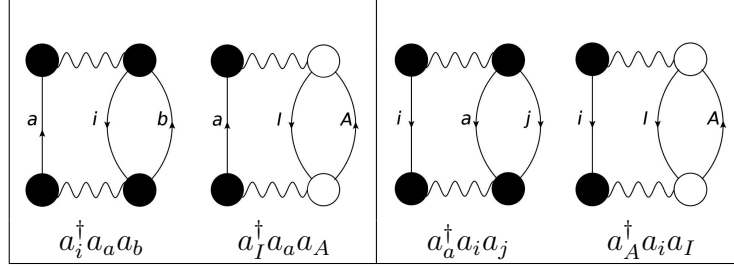
Primary-Primary spaces

Since the vector $\mathbf{a}^\alpha$ contents holes and particle operators, the matrix $(\mathbf{a}^\alpha | \hat{H} \mathbf{a}^\alpha)$ can be further divided into 4 blocks that we will call, $\mathbf{H}_{\mathbf{h,h}}^{\alpha,\alpha}$, $\mathbf{H}_{\mathbf{p,p}}^{\alpha,\alpha}$ and $\mathbf{H}_{\mathbf{h,p}}^{\alpha,\alpha}$, $\mathbf{H}_{\mathbf{p,h}}^{\alpha,\alpha}$, corresponding to products between two holes (hh), two particles (pp) or one hole and one particle (hp and ph). Contributions to an element (p,q) of the matrix $(\mathbf{a}^\alpha | \hat{H} \mathbf{a}^\alpha)$ are shown below, evaluated through third order:

$$(a_p | \hat{H} a_q)_0 = (a_p | \hat{H}_0 a_q)_0 = \delta_{pq} \epsilon_p \tag{3-15}$$

$$(a_p | \hat{H} a_q)_1 = (a_p | \hat{H} a_q)_2 = 0 \tag{3-16}$$

$$(a_p | \hat{H} a_q)_3 = \sum_{rs} (pq||rs) \rho_{rs}^{(2)} + \sum_{\beta \neq \alpha}^{N^Q} \sum_{P,Q} (pq|PQ) \rho_{PQ}^{(2)} \tag{3-17}$$

Where the elements $\rho_{rs}^{(2)}$ for one species can be calculated as:

$$\rho_{ij}^{(2)} = -\frac{1}{2} \sum_{k,a,b} \kappa_{ik}^{ab} \kappa_{jk}^{*ab} + \sum_{\beta \neq \alpha}^{N^Q} \sum_{a,I,A} \kappa_{iI}^{aA} \kappa_{jI}^{*aA}; \quad \rho_{ab}^{(2)} = \frac{1}{2} \sum_{i,j,c} \kappa_{ij}^{ac} \kappa_{jk}^{*ab} + \sum_{\beta \neq \alpha}^{N^Q} \sum_{i,I,A} \kappa_{iI}^{aA} \kappa_{iI}^{*bA} \tag{3-18}$$

$$\rho_{ia}^{(2)} = \frac{1}{\epsilon_i - \epsilon_a} \left[-\sum_{j,k,b} (ji||kb) \kappa_{jk}^{ab} + \sum_{j,b,c} (ab||jc) \kappa_{ij}^{bc} \right] \tag{3-19}$$

$$+ \sum_{\beta \neq \alpha}^{N^Q} \frac{1}{\epsilon_I - \epsilon_A} \left[-\sum_{j,A,I} (ij|AI) \kappa_{jI}^{aA} + \sum_{b,A,I} (ia|AI) \kappa_{iI}^{bA} \right]$$

where κ are the correlation coefficients defined in Eqs. (2-98) and (2-99).

Primary-Complementary spaces

Operators belonging to the $\mathbf{f}_3^\alpha$ space can be classified into 2 holes 1 particle and 2 particle operators, as shown in table **3-1**. Consequently, the matrix $(\mathbf{a}^\alpha | \hat{H} \mathbf{f}^\alpha)$ can be divided into 8 blocks: $\mathbf{H}_{\mathbf{h,2hp}}^{\alpha,\alpha\alpha\alpha}$, $\mathbf{H}_{\mathbf{p,2hp}}^{\alpha,\alpha\alpha\alpha}$, $\mathbf{H}_{\mathbf{h,2hp}}^{\alpha,\beta\alpha\beta}$, $\mathbf{H}_{\mathbf{p,2hp}}^{\alpha,\beta\alpha\beta}$, $\mathbf{H}_{\mathbf{h,2ph}}^{\alpha,\alpha\alpha\alpha}$, $\mathbf{H}_{\mathbf{p,2ph}}^{\alpha,\alpha\alpha\alpha}$, $\mathbf{H}_{\mathbf{h,2hp}}^{\alpha,\beta\alpha\beta}$ and $\mathbf{H}_{\mathbf{p,2hp}}^{\alpha,\beta\alpha\beta}$. To build the third order self-energy, inner products in this blocks needs to be computed up second order. For an element (p,q), we have:

$$(a_p|\hat{H}a_i^\dagger a_a a_b)_0 = (a_p|\hat{H}a_a^\dagger a_i a_j)_0 = (a_p|\hat{H}a_A^\dagger a_i a_I)_0 = (a_p|\hat{H}a_I^\dagger a_a a_A)_0 = 0 \tag{3-20}$$

$$(a_p|\hat{H}a_i^\dagger a_a a_b)_1 = \langle pi||ab\rangle \quad (a_p|\hat{H}a_a^\dagger a_i a_j)_1 = \langle pa||ij\rangle \tag{3-21}$$

$$(a_p|\hat{H}a_I^\dagger a_a a_A)_1 = \langle pI|aA\rangle \quad (a_p|\hat{H}a_A^\dagger a_i a_I)_1 = \langle pA|iI\rangle \tag{3-22}$$

$$(a_p|\hat{H}a_a^\dagger a_i a_j)_2 = \frac{1}{2}\sum_{b,c}\langle pa||bc\rangle\kappa_{ij}^{bc} + (1-P_{ij})\left[\sum_{b,k}\langle pk||bi\rangle\kappa_{jk}^{ba} + \sum_\beta^{N^Q}\sum_{A,I}\langle pA|iI\rangle\kappa_{jI}^{aA}\right] \tag{3-23}$$

$$(a_p|\hat{H}a_i^\dagger a_a a_b)_2 = \frac{1}{2}\sum_{j,k}\langle pi||jk\rangle\kappa_{jk}^{ab} + (1-P_{ab})\left[\sum_{j,c}\langle pc||ja\rangle\kappa_{ji}^{bc} + \sum_\beta^{N^Q}\sum_{A,I}\langle pA|aI\rangle\kappa_{iI}^{bA}\right] \tag{3-24}$$

$$(a_p|\hat{H}a_A^\dagger a_i a_I)_2 = \sum_{a,B}\langle pA|aB\rangle\kappa_{iI}^{aB} - \sum_{a,J}\langle aJ|pI\rangle\kappa_{iJ}^{aA} - \sum_{a,j}\langle pj||ai\rangle\kappa_{jI}^{aA} + \sum_{J,B}\langle pJ|iB\rangle\kappa_{IB}^{AJ}$$
$$\tag{3-25}$$

$$(a_p|\hat{H}a_I^\dagger a_a a_A)_2 = \sum_{i,J}\langle pI|iJ\rangle\kappa_{iJ}^{aA} - \sum_{i,B}\langle pB|iA\rangle\kappa_{iI}^{aB} - \sum_{b,i}\langle pb||ia\rangle\kappa_{iI}^{bA} + \sum_{J,B}\langle pB|aJ\rangle\kappa_{IJ}^{AB}$$
$$\tag{3-26}$$

Complementary-complementary spaces inner products

For third order calculations, the elements of these inner products needs to be evaluated up to first order. The matrix elements between 2ph and 2hp type-operators vanish through first order. For operators of only one species we have:

$$(a_a^\dagger a_i a_j|\hat{H}a_b^\dagger a_k a_l)_0 = \delta_{ab}\delta_{ik}\delta_{jl}\left[\epsilon_i + \epsilon_j - \epsilon_a\right] \tag{3-27}$$

$$(a_i^\dagger a_a a_b|\hat{H}a_j^\dagger a_c a_d)_0 = \delta_{ij}\delta_{ac}\delta_{bd}\left[\epsilon_a + \epsilon_b - \epsilon_i\right] \tag{3-28}$$

$$(a_a^\dagger a_i a_j|\hat{H}a_b^\dagger a_k a_l)_1 = -\delta_{ab}\langle ij||kl\rangle + (1-P_{ij})(1-P_{kl})\delta_{ik}\langle bj||al\rangle \tag{3-29}$$

$$(a_i^\dagger a_a a_b|\hat{H}a_j^\dagger a_c a_d)_1 = \delta_{ij}\langle ab||cd\rangle - (1-P_{ab})(1-P_{cd})\delta_{ac}\langle jb||id\rangle \tag{3-30}$$

For $i < j$ $k < l$ and $a < b$ $c < d$ in the 2hp and 2ph cases, respectively. In the case of products involving 2 species we have:

$$(a_A^\dagger a_i a_I|\hat{H}a_B^\dagger a_j a_J)_0 = \delta_{AB}\delta_{ij}\delta_{IJ}\left[\epsilon_I + \epsilon_i - \epsilon_A\right] \tag{3-31}$$

$$(a_I^\dagger a_a a_A|\hat{H}a_J^\dagger a_b a_B)_0 = \delta_{IJ}\delta_{ab}\delta_{AB}\left[\epsilon_A + \epsilon_a - \epsilon_I\right] \tag{3-32}$$

$$(a_A^\dagger a_i a_I|\hat{H}a_B^\dagger a_j a_J)_1 = -\delta_{ij}\langle IB||AJ\rangle + \delta_{AB}\langle iI|jJ\rangle - \delta_{IJ}\langle iB|jA\rangle \tag{3-33}$$

$$(a_I^\dagger a_a a_A|\hat{H}a_J^\dagger a_b a_B)_1 = \delta_{ab}\langle AJ||IB\rangle - \delta_{IJ}\langle aA|bB\rangle + \delta_{AB}\langle aI|bJ\rangle \tag{3-34}$$

$$(a_a^\dagger a_i a_j|\hat{H}a_A^\dagger a_k a_I)_1 = -\delta_{ik}\langle Aj|Ia\rangle \tag{3-35}$$

$$(a_i^\dagger a_a a_b|\hat{H}a_I^\dagger a_c a_A)_1 = \delta_{ac}\langle iA|bI\rangle \tag{3-36}$$

Finally, for products involving 3 species:

$$(a_A^\dagger a_i a_I | \hat{H} a_\Lambda^\dagger a_j a_\Gamma)_0 = (a_I^\dagger a_a a_A | \hat{H} a_\Gamma^\dagger a_b a_\Lambda)_0 = 0 \tag{3-37}$$

$$(a_A^\dagger a_i a_I | \hat{H} a_\Lambda^\dagger a_j a_\Gamma)_1 = -\delta_{ij}\langle I\Lambda | A\Gamma \rangle \tag{3-38}$$

$$(a_I^\dagger a_a a_A | \hat{H} a_\Gamma^\dagger a_b a_\Lambda)_1 = \delta_{ab}\langle A\Gamma | I\Lambda \rangle \tag{3-39}$$

$$\tag{3-40}$$

3.2.2 Non-diagonal approximations

A way to find the poles arises from Eq.(3-9). Inspecting this equation we can realize that the poles of the one-α-Green function, ω^α, correspond to the eigenvalues of the so-called super–Hamiltonian matrix, $\hat{\mathbf{H}}$:

$$\hat{\mathbf{H}}\mathbf{U} = \boldsymbol{\omega}^\alpha \mathbf{U} \tag{3-41}$$

$$\begin{bmatrix} (\mathbf{a}^\alpha|\hat{H}\mathbf{a}^\alpha) & (\mathbf{a}^\alpha|\hat{H}\mathbf{f}^\alpha) \\ (\mathbf{f}^\alpha|\hat{H}\mathbf{a}^\alpha) & (\mathbf{f}^\alpha|\hat{H}\mathbf{f}^\alpha) \end{bmatrix} \begin{bmatrix} \mathbf{U}_{a,n}^\alpha \\ \mathbf{U}_{f,n}^\alpha \end{bmatrix} = \omega_n^\alpha \begin{bmatrix} \mathbf{U}_{a,n}^\alpha \\ \mathbf{U}_{f,n}^\alpha \end{bmatrix} \tag{3-42}$$

The super-operator matrix evaluate up to second and complete third order are:

$$\begin{bmatrix} (\mathbf{a}^\alpha|\hat{H}\mathbf{a}^\alpha)^{(0)} & (\mathbf{a}^\alpha|\hat{H}\mathbf{f}^\alpha)^{(1)} \\ (\mathbf{f}^\alpha|\hat{H}\mathbf{a}^\alpha)^{(1)} & (\mathbf{f}^\alpha|\hat{H}\mathbf{f}^\alpha)^{(0)} \end{bmatrix} \qquad \begin{bmatrix} (\mathbf{a}^\alpha|\hat{H}\mathbf{a}^\alpha)^{(3)} & (\mathbf{a}^\alpha|\hat{H}\mathbf{f}^\alpha)^{(2)} \\ (\mathbf{f}^\alpha|\hat{H}\mathbf{a}^\alpha)^{(2)} & (\mathbf{f}^\alpha|\hat{H}\mathbf{f}^\alpha)^{(1)} \end{bmatrix} \tag{3-43}$$

For several quantum species, the structure of $\hat{\mathbf{H}}$ become complex as it must include the inner products between different combinations of second quantized operators for several species:

$$\hat{\mathbf{H}} = \begin{bmatrix} (\mathbf{a}^\alpha|\hat{\mathbf{H}}\mathbf{a}^\alpha) & (\mathbf{a}^\alpha|\hat{\mathbf{H}}\mathbf{f_3}^{\alpha\alpha\alpha}) & (\mathbf{a}^\alpha|\hat{\mathbf{H}}\mathbf{f_3}^{\beta\alpha\beta}) & (\mathbf{a}^\alpha|\hat{\mathbf{H}}\mathbf{f_3}^{\gamma\alpha\gamma}) & \cdots \\ (\mathbf{f_3}^{\alpha\alpha\alpha}|\hat{\mathbf{H}}\mathbf{a}^\alpha) & (\mathbf{f_3}^{\alpha\alpha\alpha}|\hat{\mathbf{H}}\mathbf{f_3}^{\alpha\alpha\alpha}) & (\mathbf{f_3}^{\alpha\alpha\alpha}|\hat{\mathbf{H}}\mathbf{f_3}^{\beta\alpha\beta}) & (\mathbf{f_3}^{\alpha\alpha\alpha}|\hat{\mathbf{H}}\mathbf{f_3}^{\gamma\alpha\gamma}) & \cdots \\ (\mathbf{f_3}^{\beta\alpha\beta}|\hat{\mathbf{H}}\mathbf{a}^\alpha) & (\mathbf{f_3}^{\beta\alpha\beta}|\hat{\mathbf{H}}\mathbf{f_3}^{\alpha\alpha\alpha}) & (\mathbf{f_3}^{\beta\alpha\beta}|\hat{\mathbf{H}}\mathbf{f_3}^{\beta\alpha\beta}) & (\mathbf{f_3}^{\beta\alpha\beta}|\hat{\mathbf{H}}\mathbf{f_3}^{\gamma\alpha\gamma}) & \cdots \\ (\mathbf{f_3}^{\gamma\alpha\gamma}|\hat{\mathbf{H}}\mathbf{a}^\alpha) & (\mathbf{f_3}^{\gamma\alpha\gamma}|\hat{\mathbf{H}}\mathbf{f_3}^{\alpha\alpha\alpha}) & (\mathbf{f_3}^{\gamma\alpha\gamma}|\hat{\mathbf{H}}\mathbf{f_3}^{\beta\alpha\beta}) & (\mathbf{f_3}^{\gamma\alpha\gamma}|\hat{\mathbf{H}}\mathbf{f_3}^{\gamma\alpha\gamma}) & \cdots \\ \vdots & \vdots & \vdots & \vdots & \ddots \end{bmatrix} \tag{3-44}$$

where we have considered only the $\mathbf{f_3}^\alpha$ space explicitly. If now we introduce the clasification of operators as h, p, 2hp and 2ph, we arise to a more explicit form of the $\hat{\mathbf{H}}$ matrix:

$$\hat{\mathbf{H}} = \begin{bmatrix} \mathbf{H}_{h,h}^{\alpha,\alpha} & \mathbf{H}_{h,p}^{\alpha,\alpha} & \mathbf{H}_{h,2hp}^{\alpha,\alpha\alpha\alpha} & \mathbf{H}_{h,2ph}^{\alpha,\alpha\alpha\alpha} & \mathbf{H}_{h,phh}^{\alpha,\beta\alpha\beta} & \mathbf{H}_{h,hpp}^{\alpha,\beta\alpha\beta} & \mathbf{H}_{h,phh}^{\alpha,\gamma\alpha\gamma} & \mathbf{H}_{h,hpp}^{\alpha,\gamma\alpha\gamma} & \cdots \\ \mathbf{H}_{p,h}^{\alpha,\alpha} & \mathbf{H}_{p,p}^{\alpha,\alpha} & \mathbf{H}_{p,2hp}^{\alpha,\alpha\alpha\alpha} & \mathbf{H}_{p,2ph}^{\alpha,\alpha\alpha\alpha} & \mathbf{H}_{p,phh}^{\alpha,\beta\alpha\beta} & \mathbf{H}_{p,hpp}^{\alpha,\beta\alpha\beta} & \mathbf{H}_{p,phh}^{\alpha,\gamma\alpha\gamma} & \mathbf{H}_{p,hpp}^{\alpha,\gamma\alpha\gamma} & \cdots \\ \mathbf{H}_{2hp,h}^{\alpha\alpha\alpha,\alpha} & \mathbf{H}_{2hp,p}^{\alpha\alpha\alpha,\alpha} & \mathbf{H}_{2hp,2hp}^{\alpha\alpha\alpha,\alpha\alpha\alpha} & \mathbf{H}_{2hp,2ph}^{\alpha\alpha\alpha,\alpha\alpha\alpha} & \mathbf{H}_{2hp,phh}^{\alpha\alpha\alpha,\beta\alpha\beta} & \mathbf{H}_{2hp,hpp}^{\alpha\alpha\alpha,\beta\alpha\beta} & \mathbf{H}_{2hp,phh}^{\alpha\alpha\alpha,\gamma\alpha\gamma} & \mathbf{H}_{2hp,hpp}^{\alpha\alpha\alpha,\gamma\alpha\gamma} & \cdots \\ \mathbf{H}_{2ph,h}^{\alpha\alpha\alpha,\alpha} & \mathbf{H}_{2ph,p}^{\alpha\alpha\alpha,\alpha} & \mathbf{H}_{2ph,2hp}^{\alpha\alpha\alpha,\alpha\alpha\alpha} & \mathbf{H}_{2ph,2ph}^{\alpha\alpha\alpha,\alpha\alpha\alpha} & \mathbf{H}_{2ph,phh}^{\alpha\alpha\alpha,\beta\alpha\beta} & \mathbf{H}_{2ph,hpp}^{\alpha\alpha\alpha,\beta\alpha\beta} & \mathbf{H}_{2ph,phh}^{\alpha\alpha\alpha,\gamma\alpha\gamma} & \mathbf{H}_{2ph,hpp}^{\alpha\alpha\alpha,\gamma\alpha\gamma} & \cdots \\ \mathbf{H}_{phh,h}^{\beta\alpha\beta,\alpha} & \mathbf{H}_{phh,p}^{\beta\alpha\beta,\alpha} & \mathbf{H}_{phh,2hp}^{\beta\alpha\beta,\alpha\alpha\alpha} & \mathbf{H}_{phh,2ph}^{\beta\alpha\beta,\alpha\alpha\alpha} & \mathbf{H}_{phh,phh}^{\beta\alpha\beta,\beta\alpha\beta} & \mathbf{H}_{phh,hpp}^{\beta\alpha\beta,\beta\alpha\beta} & \mathbf{H}_{phh,phh}^{\beta\alpha\beta,\gamma\alpha\gamma} & \mathbf{H}_{phh,hpp}^{\beta\alpha\beta,\gamma\alpha\gamma} & \cdots \\ \mathbf{H}_{hpp,h}^{\beta\alpha\beta,\alpha} & \mathbf{H}_{hpp,p}^{\beta\alpha\beta,\alpha} & \mathbf{H}_{hpp,2hp}^{\beta\alpha\beta,\alpha\alpha\alpha} & \mathbf{H}_{hpp,2ph}^{\beta\alpha\beta,\alpha\alpha\alpha} & \mathbf{H}_{hpp,phh}^{\beta\alpha\beta,\beta\alpha\beta} & \mathbf{H}_{hpp,hpp}^{\beta\alpha\beta,\beta\alpha\beta} & \mathbf{H}_{hpp,phh}^{\beta\alpha\beta,\gamma\alpha\gamma} & \mathbf{H}_{hpp,hpp}^{\beta\alpha\beta,\gamma\alpha\gamma} & \cdots \\ \mathbf{H}_{phh,h}^{\gamma\alpha\gamma,\alpha} & \mathbf{H}_{phh,p}^{\gamma\alpha\gamma,\alpha} & \mathbf{H}_{phh,2hp}^{\gamma\alpha\gamma,\alpha\alpha\alpha} & \mathbf{H}_{phh,2ph}^{\gamma\alpha\gamma,\alpha\alpha\alpha} & \mathbf{H}_{phh,phh}^{\gamma\alpha\gamma,\beta\alpha\beta} & \mathbf{H}_{phh,hpp}^{\gamma\alpha\gamma,\beta\alpha\beta} & \mathbf{H}_{phh,phh}^{\gamma\alpha\gamma,\gamma\alpha\gamma} & \mathbf{H}_{phh,hpp}^{\gamma\alpha\gamma,\gamma\alpha\gamma} & \cdots \\ \mathbf{H}_{hpp,h}^{\gamma\alpha\gamma,\alpha} & \mathbf{H}_{hpp,p}^{\gamma\alpha\gamma,\alpha} & \mathbf{H}_{hpp,2hp}^{\gamma\alpha\gamma,\alpha\alpha\alpha} & \mathbf{H}_{hpp,2ph}^{\gamma\alpha\gamma,\alpha\alpha\alpha} & \mathbf{H}_{hpp,phh}^{\gamma\alpha\gamma,\beta\alpha\beta} & \mathbf{H}_{hpp,hpp}^{\gamma\alpha\gamma,\beta\alpha\beta} & \mathbf{H}_{hpp,phh}^{\gamma\alpha\gamma,\gamma\alpha\gamma} & \mathbf{H}_{hpp,hpp}^{\gamma\alpha\gamma,\gamma\alpha\gamma} & \cdots \\ \vdots & \vdots & \vdots & \vdots & \vdots & \vdots & \vdots & \vdots & \ddots \end{bmatrix} \tag{3-45}$$

Note that these blocks can be evaluated by using the formulas of subsection 3.2.1. The blocked structure of the $\hat{\mathbf{H}}^\alpha$ allows us to generate different approximations of the self-energy by changing the order of perturbation at which each block is computed. This flexibility in the construction of the super-Hamiltonian matrix has been extensively exploited by Ortiz et al. to reduce the computational cost of electron propagator calculations by discarding the evaluation of blocks with small contribution in the calculation of certain types of ionization processes. The current version of the propagator module in the LOWDIN program does not include non-diagonal methods, although some steps have been taken towards its implementation.

3.2.3 Self-energy approximations

As exposed in the previous section, poles of the Green function can be determined by finding the eigenvalues of super-Hamiltonian matrix. A second option is to solve the non-linear Dyson equation (3-10). With that aim we have to build the self energy matrix, $\mathbf{\Sigma}^\alpha$. Using the MBPT expansion proposed in section 2.4.3 for the APMO wavefunction, the second order (2) and third order (3) APMO self-energies corresponds to:

$$\mathbf{\Sigma}^\alpha_{(\mathbf{2})}(\omega^\alpha) = (\mathbf{a}^\alpha|\hat{H}\mathbf{f}^\alpha_{\mathbf{3}})_1\left[\omega^\alpha\hat{I} - (\mathbf{f}^\alpha_{\mathbf{3}}|\hat{H}\mathbf{f}^\alpha_{\mathbf{3}})_0\right]^{-1}(\mathbf{f}^\alpha_{\mathbf{3}}|\hat{H}\mathbf{a}^\alpha)_1 \tag{3-46}$$

$$\begin{aligned}
\mathbf{\Sigma}^\alpha_{(\mathbf{3})}(\omega^\alpha) =& \mathbf{\Sigma}^\alpha_{(\mathbf{2})}(\omega^\alpha) + \mathbf{\Sigma}^\alpha_{\mathbf{3}}(\omega^\alpha) \\
=& \mathbf{\Sigma}^\alpha_{(\mathbf{2})}(\omega^\alpha) \tag{3-47} \\
& + (\mathbf{a}^\alpha|(\omega^\alpha\hat{I} - \hat{H})\mathbf{a}^\alpha)_3 \\
& + (\mathbf{a}^\alpha|\hat{H}\mathbf{f}^\alpha_{\mathbf{3}})_2\left[\omega^\alpha\hat{I} - (\mathbf{f}^\alpha_{\mathbf{3}}|\hat{H}\mathbf{f}^\alpha_{\mathbf{3}})_0\right]^{-1}(\mathbf{f}^\alpha_{\mathbf{3}}|\hat{H}\mathbf{a}^\alpha)_1 \\
& + (\mathbf{a}^\alpha|\hat{H}\mathbf{f}^\alpha_{\mathbf{3}})_1\left[\omega^\alpha\hat{I} - (\mathbf{f}^\alpha_{\mathbf{3}}|\hat{H}\mathbf{f}^\alpha_{\mathbf{3}})_0\right]^{-1}(\mathbf{f}^\alpha_{\mathbf{3}}|\hat{H}\mathbf{a}^\alpha)_2 \\
& + (\mathbf{a}^\alpha|\hat{H}\mathbf{f}^\alpha_{\mathbf{3}})_1\left[\omega^\alpha\hat{I} - (\mathbf{f}^\alpha_{\mathbf{3}}|\hat{H}\mathbf{f}^\alpha_{\mathbf{3}})_0\right]^{-1}(\mathbf{f}^\alpha_{\mathbf{3}}|\hat{H}\mathbf{f}^\alpha_{\mathbf{3}})_1\left[\omega^\alpha\hat{I} - (\mathbf{f}^\alpha_{\mathbf{3}}|\hat{H}\mathbf{f}^\alpha_{\mathbf{3}})_0\right]^{-1}(\mathbf{f}^\alpha_{\mathbf{3}}|\hat{H}\mathbf{a}^\alpha)_1
\end{aligned}$$

Ortiz proposed a new approximation for the third order self energy [44] by replacing the regular MBPT expansion of the wavefunction (Eq.2-95) by a Coupled Cluster (CC) expansion, in the evaluation of inner products:

$$(Y|Z) = \langle\Psi_0|e^{-\hat{T}}[Y^\dagger, Z]_- \, e^{\hat{T}}|\Psi_0\rangle \tag{3-48}$$

This change produces asymmetric propagator matrix. For instance, if $\hat{T}$ is truncated to $\hat{T}_2$, the evaluation of the inner products proceed by the following rules for each type of expansion:

$$(Y|Z) = \langle\Psi_0|(1 + \hat{T}_2^\dagger)[Y^\dagger, Z]_-(1 + \hat{T}_2)|\Psi_0\rangle \quad \text{(MBPT)} \tag{3-49}$$

$$(Y|Z) = \langle\Psi_0|(1 - \hat{T}_2^\dagger)[Y^\dagger, Z]_-(1 + \hat{T}_2)|\Psi_0\rangle \quad \text{(CC)} \tag{3-50}$$

By using Eq.3-50 to build the third order self-energy, several terms appearing in Eq.3-47 cancel out. The new self-energy matrix in third order is asymmetric and is written as:

$$
\begin{aligned}
\mathbf{\Sigma}^{\alpha}_{(\text{P3})}(\omega^{\alpha}) =& \mathbf{\Sigma}^{\alpha}_{(\mathbf{2})}(\omega^{\alpha}) + \mathbf{\Sigma}^{\alpha}_{\text{P3}}(\omega^{\alpha}) \\
=& \mathbf{\Sigma}^{\alpha}_{(\mathbf{2})}(\omega^{\alpha}) + (\mathbf{a}^{\alpha}|\hat{H}\mathbf{f}^{\alpha}_{\mathbf{3}})_1 \left[\omega^{\alpha}\hat{I} - (\mathbf{f}^{\alpha}_{\mathbf{3}}|\hat{H}\mathbf{f}^{\alpha}_{\mathbf{3}})_0\right]^{-1} (\mathbf{f}^{\alpha}_{\mathbf{3}}|\hat{H}\mathbf{a}^{\alpha})_2 \\
& + (\mathbf{a}^{\alpha}|\hat{H}\mathbf{f}^{\alpha}_{\mathbf{3}})_1 \left[\omega^{\alpha}\hat{I} - (\mathbf{f}^{\alpha}_{\mathbf{3}}|\hat{H}\mathbf{f}^{\alpha}_{\mathbf{3}})_0\right]^{-1} (\mathbf{f}^{\alpha}_{\mathbf{3}}|\hat{H}\mathbf{f}^{\alpha}_{\mathbf{3}})_1 \left[\omega^{\alpha}\hat{I} - (\mathbf{f}^{\alpha}_{\mathbf{3}}|\hat{H}\mathbf{f}^{\alpha}_{\mathbf{3}})_0\right]^{-1} (\mathbf{f}^{\alpha}_{\mathbf{3}}|\hat{H}\mathbf{a}^{\alpha})_1
\end{aligned}
\tag{3-51}
$$

Since this approximation can be seen as a reduced version of Eq.(3-47), it was designated as P3 (partial third order).

3.2.4 Quasiparticle (diagonal) APMO methods

Several studies of the self-energy matrix for several ionization processes, such as valence electron ionization of closed-shell molecules, generally indicate that off-diagonal elements of the self-energy matrix in the canonical basis are small and can be neglected for the calculation of binding energies [6]. This approach, known as the quasiparticle (diagonal) approximation, leads to a simpler form of the Dyson equation:

$$
\omega^{\alpha}_p = \varepsilon^{\alpha}_p + \mathbf{\Sigma}^{\alpha}_{pp}(\omega^{\alpha})
\tag{3-52}
$$

where ε^{α}_p is the pth canonical orbital energy for the species α. The quasiparticle Dyson equation can be interpreted as a corrected Koopmans' theorem, where the relaxation and correlation effects missing in the Koopmans's approximation are introduced through the diagonal self–energy term: $\mathbf{\Sigma}^{\alpha}_{pp}(\omega^{\alpha})$. In APMO theory the term $\mathbf{\Sigma}^{\alpha}_{pp}(\omega^{\alpha})$ comprises interspecies and intraspecies contributions. For instance, the working equation for the quasiparticle second order APMO propagator method (APMO/P2) has the form:

$$
\omega^{\alpha}_p = \varepsilon^{\alpha}_p + \mathbf{\Sigma}^{\alpha\alpha}_{\mathbf{2}\,pp}(\omega^{\alpha}) + \sum_{\beta\neq\alpha}^{N^Q} \mathbf{\Sigma}^{\alpha\beta}_{\mathbf{2}\,pp}(\omega^{\alpha})
\tag{3-53}
$$

Where the terms $\mathbf{\Sigma}^{\alpha\alpha}_{\mathbf{2}\,pp}(\omega^{\alpha})$ and $\mathbf{\Sigma}^{\alpha\beta}_{\mathbf{2}\,pp}(\omega^{\alpha})$ represent the intraspecies and interspecies contributions to $\mathbf{\Sigma}^{\alpha}_{pp}(\omega^{\alpha})$ at second order, which are given by:

$$
\mathbf{\Sigma}^{\alpha\alpha}_{\mathbf{2}\,pp}(\omega^{\alpha}) = \sum_{a,i>j\in\alpha} \frac{|\langle pa||ij\rangle|^2}{\omega_p + \epsilon_a - \epsilon_i - \epsilon_j} + \sum_{i,a>b\in\alpha} \frac{|\langle pi||ab\rangle|^2}{\omega_p + \epsilon_i - \epsilon_a - \epsilon_b}
\tag{3-54}
$$

$$
\mathbf{\Sigma}^{\alpha\beta}_{\mathbf{2}\,pp}(\omega^{\alpha}) = \sum_{i\in\alpha}\sum_{A,I\in\beta} \frac{|\langle pA|iI\rangle|^2}{\omega_p + \epsilon_A - \epsilon_I - \epsilon_i} + \sum_{a\in\alpha}\sum_{A,I\in\beta} \frac{|\langle pI|aA\rangle|^2}{\omega_p + \epsilon_I - \epsilon_A - \epsilon_a}
\tag{3-55}
$$

At third order the self-energy becomes more complex, comprising terms with contributions of up to three different species. The working equation for the quasiparticle third order APMO

propagator method (APMO/P3) and the partial third order APMO propagator method (APMO/PP3) can be written as:

$$\omega_p^\alpha = \varepsilon_p^\alpha + \mathbf{\Sigma_2^{\alpha\alpha}}_{pp}(\omega^\alpha) + \sum_{\beta\neq\alpha}^{N^Q} \mathbf{\Sigma_2^{\alpha\beta}}_{pp}(\omega^\alpha) + \sum_{\beta,\gamma}^{N^Q} \mathbf{\Sigma_3^{\alpha\beta\gamma}}_{pp}(\omega^\alpha) \tag{3-56}$$

$$\omega_p^\alpha = \varepsilon_p^\alpha + \mathbf{\Sigma_2^{\alpha\alpha}}_{pp}(\omega^\alpha) + \sum_{\beta\neq\alpha}^{N^Q} \mathbf{\Sigma_2^{\alpha\beta}}_{pp}(\omega^\alpha) + \sum_{\beta,\gamma}^{N^Q} \mathbf{\Sigma_{P3}^{\alpha\beta\gamma}}_{pp}(\omega^\alpha) \tag{3-57}$$

Where $\mathbf{\Sigma_3^{\alpha\beta\gamma}}_{pp}(\omega^\alpha)$ and $\mathbf{\Sigma_{P3}^{\alpha\beta\gamma}}_{pp}(\omega^\alpha)$ represent the diagonal terms of the matrices defined in equations 3-47 and 3-51, respectively.

Results of third order poles can be improved by estimating higher order results. One approach to do so is the Outer Valence Green Function (OVGF) renormalization technique proposed by Cederbaum []. We have adapted this renormalization procedure to the APMO propagator approach. For the A version of the propagator method, the self-energy takes the form:

$$\omega_p^\alpha = \varepsilon_p^\alpha + \mathbf{\Sigma_2^{\alpha\alpha}}_{pp}(\omega^\alpha) + \sum_{\beta\neq\alpha}^{N^Q} \mathbf{\Sigma_2^{\alpha\beta}}_{pp}(\omega^\alpha) + + \sum_{\beta\neq\gamma\neq\alpha}^{N^Q} \mathbf{\Sigma_3^{\alpha\beta\gamma}}_{pp}(\omega^\alpha) + (1+X_p^\beta)^{-1}\mathbf{\Sigma_3^{\alpha\beta\alpha}}_{pp}(\omega^\alpha)$$
$$+ \sum_{\beta\neq\alpha}^{N^Q} (1+X_p^\beta)^{-1}\left[\mathbf{\Sigma_3^{\alpha\beta\alpha}}_{pp}(\omega^\alpha) + \mathbf{\Sigma_3^{\alpha\beta\beta}}_{pp}(\omega^\alpha) + \mathbf{\Sigma_3^{\alpha\alpha\beta}}_{pp}(\omega^\alpha)\right]$$
$$\tag{3-58}$$

3.2.5 Working equations for diagonal propagator methods

In this section we present the explicit expressions of Eq. (3-52) evaluated at second and third order, within the APMO approach. The second order transition operator method is also introduced.

Second–order quasiparticle self-energy in APMO (APMO/P2)

In a system comprised for N^Q quantum species, the second order self-energy terms for an orbital p of the species α, have the following form:

$$\Sigma_{PP}^{\alpha,\alpha(2)}(\omega_p) = \sum_{a,i>j\in\alpha} \frac{|\langle pa||ij\rangle|^2}{\omega_p + \epsilon_a - \epsilon_i - \epsilon_j} + \sum_{i,a>b\in\alpha} \frac{|\langle pi||ab\rangle|^2}{\omega_p + \epsilon_i - \epsilon_a - \epsilon_b} \tag{3-59}$$

$$\Sigma_{PP}^{\alpha,\beta(2)}(\omega_P) = \sum_{\beta\neq\alpha}^{N^Q}\left[\sum_{i\in\alpha}\sum_{A,I\in\beta} \frac{|\langle pA|iI\rangle|^2}{\omega_p + \epsilon_A - \epsilon_I - \epsilon_i} + \sum_{a\in\alpha}\sum_{A,I\in\beta} \frac{|\langle pI|aA\rangle|^2}{\omega_p + \epsilon_I - \epsilon_A - \epsilon_a}\right] \tag{3-60}$$

Where the convention for virtual orbitals is the same of the table **3-2**. Eq. (3-59) and Eq. (3-60) are the working expressions to calculate corrected binding energies for α species at

second order. The simple form of Eqs. (3-59) and Eq. (3-60) (reminiscent of the APMO/MP2 formulas) is suitable to analyze the nature of the self-energy correction. Pickup and Goscinski [8, 34] proposed a decomposition of the second self-energy for electrons into relaxation and correlation terms that can be used to identify which of these effects predominates in a specific ionization process. This information is useful to design accurate and efficient approximations to the self-energy for higher orders of perturbation theory. Following Pickup and Goscinski, we can factorize the second self-energy expression for the APMO wavefunction. For the intraspecies term we have:

$$
\begin{aligned}
\Sigma_{pp}^{\alpha,\alpha(2)}(\omega_p) =& \text{PRM} + \text{PRX} + \text{ORX} \\
=& \sum_{i,a,b} \frac{|\langle pi|ab\rangle|^2}{\omega_p + \epsilon_i - \epsilon_a - \epsilon_b} + \sum_{i\neq p}\sum_{a,j} \frac{|\langle pa|ij\rangle|^2}{\omega_p + \epsilon_a - \epsilon_i - \epsilon_j} + \sum_{a,i} \frac{|\langle pa|pi\rangle|^2}{\omega_p + \epsilon_a - \epsilon_p - \epsilon_i}
\end{aligned}
$$
(3-61)

where the first term is the lowest order pair α-α correlation term in the system containing N α particles, also known as the pair-removal correlation (PRM), which correspond to excitations of the type $\binom{p\to a}{i\to j}$. The second term is an extra correlation term arising from excitations of the type $\binom{i\to p}{j\to a}$ in the system containing $N-1$ electrons, and it is called pair-relaxation (PRX). Note that this terms appears because in the ionized system, the orbital p becomes a virtual orbital. The third term is the orbital relaxation term (ORX) which correspond to single excitations from the remaining occupied orbitals in the system containing $N-1\alpha$ particles ($i \to a$ with $i \neq a$). Similarly, for the interspecies term:

$$
\begin{aligned}
\Sigma_{pp}^{\alpha,\beta(2)}(\omega_p) =& \text{PRM} + \text{PRX} + \text{ORX} \\
=& \sum_{\beta\neq\alpha}^{NQ}\sum_{a,I,A} \frac{|\langle pI|aA\rangle|^2}{\omega_p + \epsilon_I - \epsilon_a - \epsilon_A} + \sum_{\beta\neq\alpha}^{NQ}\sum_{i\neq p}\sum_{A,I} \frac{|\langle pA|iI\rangle|^2}{\omega_p + \sum_{\beta\neq\alpha}^{NQ}\epsilon_A - \epsilon_i - \epsilon_I} \\
& + \sum_{\beta\neq\alpha}^{NQ}\sum_{A,I} \frac{|\langle pA|pI\rangle|^2}{\omega_p + \epsilon_A - \epsilon_p - \epsilon_I}
\end{aligned}
$$
(3-62)

now, the PRM term corresponds to the α-β correlation correction in the system containing N α particles, corresponding to excitations of the type: $\binom{p\to a}{I\to A}$. The PRX term correspond to α-β correlation correction in the system containing $N-1$ α particles: $\binom{i\to p}{I\to A}$. The interspecies ORX term (ORX) involve single excitations for only β particles: $(I \to A)$, accounting for relaxation of the orbitals belonging to quantum species different from α. Examples of the application of the above decomposition will be presented in the following chapter.

Second–order + Transition Operator quasiparticle self-energy in APMO (APMO/TOP2)

The second order expression for the self-energy can be derived using a grand-canonical reference ensemble, where occupations of orbitals are explicitly considered [45–48]. Doing this

within the APMO approach, the second order self-energy becomes:

$$\Sigma_{PP}^{\alpha,\alpha(2)}(\omega_p) = \sum_{a,i>j\in\alpha} \frac{|\langle pa||ij\rangle|^2 n_i n_j}{\omega_p + \epsilon_a - \epsilon_i - \epsilon_j} + \sum_{i,a>b\in\alpha} \frac{|\langle pi||ab\rangle|^2}{\omega_p + \epsilon_i - \epsilon_a - \epsilon_b}$$

$$+ \sum_{a,i>j\in\alpha} \frac{|\langle pi||pa\rangle|^2 (1-n_p)}{\omega_p + \epsilon_a - \epsilon_p - \epsilon_j} \tag{3-63}$$

$$\Sigma_{PP}^{\alpha,\beta(2)}(\omega_P) = \sum_{\beta\neq\alpha}^{N^Q} \left[\sum_{i\in\alpha}\sum_{A,I\in\beta} \frac{|\langle pA|iI\rangle|^2 n_i n_I}{\omega_p + \epsilon_A - \epsilon_i - \epsilon_I} + \sum_{a\in\alpha}\sum_{A,I\in\beta} \frac{|\langle pI|aA\rangle|^2}{\omega_p + \epsilon_I - \epsilon_A - \epsilon_a} \right]$$

$$+ \sum_{\beta\neq\alpha}^{N^Q}\sum_{i\in\alpha}\sum_{A,I\in\beta} \frac{|\langle pA|pI\rangle|^2 (1-n_p)}{\omega_p + \epsilon_A - \epsilon_p - \epsilon_I} \tag{3-64}$$

where n_p represents the occupation of the orbital p, ranging from zero to unit. Note that Eqs. 3-59 and 3-60 are special cases of 3-63 and 3-64 with $n_p = 1$. The transition operator (TO) method, originally proposed by Slater [49], was generalized by Janak [50] in the framework of density functional theory as the following theorem:

$$E(N^\alpha) - E(N^\alpha - 1) = \int_0^1 \epsilon_i(n_p) dn_p \tag{3-65}$$

where $E(N^\alpha)$ and $E(N^\alpha - 1)$ represent the energy of the system contaning N^α and $N^\alpha - 1$ α particles, respectively, n_p is the occupation number of the orbital p and ϵ_p its orbital energy. The Janak's theorem states that the ionization or attachment process can be seen as a continuous process where the occupation number of an specific orbital changes from 0 to 1 or viceversa. The integral appearing in Eq.(3-65) can be approximated using a simple quadrature:

$$\int_1^0 \epsilon_i(n_i) dn_i \approx \epsilon(1/2)(1-0) = \epsilon(1/2) \tag{3-66}$$

This means that the ionization or affinity energy associated to an orbital p can be approximated as the energy of the half-occupied orbital. Eq(3-63 and 3-64) allow the calculation of the second order corrected binding energy for half-occupied orbital p, using an APMO/HF reference state where the occupation of p has been already set to 1/2. The transition operator + second order propagator method for electrons (TOEP2) has proven to include more relaxation effects in the propagator calculation [48], producing results of superior accuracy than the bare second order approach. The TOEP2 method is specially useful for the calculation of core ionization, with average deviation of less than 1eV.

Third order quasiparticle self-energies in APMO

The explicit formula for the quasiparticle third order terms within the APMO method can be written using the W and U terms, which are defined as:

$$W_{paij} = \langle pa||ij\rangle + \frac{1}{2}\sum_{b,c}\frac{\langle pa||bc\rangle\langle bc||ij\rangle}{\epsilon_i + \epsilon_j - \epsilon_b - \epsilon_c} + (1 - P_{ij})\left[\sum_{b,k}\frac{\langle pk||bi\rangle\langle ba||jk\rangle}{\epsilon_j + \epsilon_k - \epsilon_a - \epsilon_b} + \sum_{\beta\neq\alpha}^{N^Q}\sum_{I,A}\frac{\langle pA|jI\rangle\langle iI|aA\rangle}{\epsilon_i + \epsilon_I - \epsilon_a - \epsilon_A}\right]$$

$$(3\text{-}67)$$

$$W_{piab} = \langle pi||ab\rangle + \frac{1}{2}\sum_{j,k}\frac{\langle pi||jk\rangle\langle jk||ab\rangle}{\epsilon_j + \epsilon_k - \epsilon_a - \epsilon_b} + (1 - P_{ab})\left[\sum_{j,c}\frac{\langle pc||ja\rangle\langle ji||bc\rangle}{\epsilon_i + \epsilon_j - \epsilon_b - \epsilon_c} + \sum_{\beta\neq\alpha}^{N^Q}\sum_{I,A}\frac{\langle pA|bI\rangle\langle iI|aA\rangle}{\epsilon_i + \epsilon_I - \epsilon_a - \epsilon_A}\right]$$

$$(3\text{-}68)$$

$$U_{paij}(\omega_p) = -\frac{1}{2}\sum_{k,l}\frac{\langle pa||kl\rangle\langle kl||ij\rangle}{\omega_p + \epsilon_a - \epsilon_k - \epsilon_l} - (1 - P_{ij})\left[\sum_{b,k}\frac{\langle pb||jk\rangle\langle ak||bi\rangle}{\omega_p + \epsilon_b - \epsilon_j - \epsilon_k} + \sum_{\beta\neq\alpha}^{N^Q}\sum_{I,A}\frac{\langle pA|jI\rangle\langle iI|aA\rangle}{\omega_p + \epsilon_A - \epsilon_j - \epsilon_I}\right]$$

$$(3\text{-}69)$$

$$U_{piab}(\omega_p) = \frac{1}{2}\sum_{c,d}\frac{\langle pi||cd\rangle\langle cd||ab\rangle}{\omega_p + \epsilon_i + \epsilon_c - \epsilon_d} + (1 - P_{ab})\left[\sum_{j,c}\frac{\langle pj||bc\rangle\langle ic||ja\rangle}{\omega_p + \epsilon_j + \epsilon_b - \epsilon_c} + \sum_{\beta\neq\alpha}^{N^Q}\sum_{I,A}\frac{\langle pI|bA\rangle\langle iI|aA\rangle}{\omega_p + \epsilon_I - \epsilon_b - \epsilon_A}\right]$$

$$(3\text{-}70)$$

$$W_{pAiI} = \langle pA|iI\rangle + \sum_{a,B}\frac{\langle pA|aB\rangle\langle iI|aB\rangle}{\epsilon_i + \epsilon_I - \epsilon_a - \epsilon_B} - \sum_{a,J}\frac{\langle pI|aJ\rangle\langle iJ|aA\rangle}{\epsilon_i + \epsilon_J - \epsilon_a - \epsilon_A} - \sum_{a,j}\frac{\langle pj||ai\rangle\langle jI|aA\rangle}{\epsilon_j + \epsilon_I - \epsilon_a - \epsilon_A}$$

$$(3\text{-}71)$$

$$+ \sum_{J,B}\frac{\langle pJ|iB\rangle\langle AB||IJ\rangle}{\epsilon_I + \epsilon_J - \epsilon_A - \epsilon_B}$$

$$W_{pIaA} = \langle pI|aA\rangle + \sum_{i,J}\frac{\langle pI|iJ\rangle\langle iJ|aA\rangle}{\epsilon_i + \epsilon_J - \epsilon_a - \epsilon_A} - \sum_{i,B}\frac{\langle pA|iB\rangle\langle iJ|aB\rangle}{\epsilon_i + \epsilon_J - \epsilon_a - \epsilon_B} - \sum_{i,b}\frac{\langle pi||ba\rangle\langle iI||bA\rangle}{\epsilon_i + \epsilon_I - \epsilon_b - \epsilon_A}$$

$$(3\text{-}72)$$

$$+ \sum_{J,B}\frac{\langle JI||BA\rangle\langle pJ||aB\rangle}{\epsilon_I + \epsilon_J - \epsilon_A - \epsilon_B}$$

$$U_{pAiI}(\omega_p) = -\sum_{j,J}\frac{\langle pJ|jA\rangle\langle iI|jJ\rangle}{\omega_p + \epsilon_A - \epsilon_j - \epsilon_J} + \sum_{J,B}\frac{\langle pJ|iB\rangle\langle IJ||BA\rangle}{\omega_p + \epsilon_B - \epsilon_i - \epsilon_J} + \sum_{j,B}\frac{\langle pI|jB\rangle\langle iA|jB\rangle}{\omega_p + \epsilon_B - \epsilon_j - \epsilon_I} \quad (3\text{-}73)$$

$$- \sum_{a,j}\frac{\langle iI|aA\rangle\langle pa||ij\rangle}{\omega_p + \epsilon_a - \epsilon_i - \epsilon_j} - \sum_{\gamma\neq\beta,\gamma\neq\alpha}^{N^Q}\sum_{\Lambda,\Gamma}\frac{\langle I\Lambda|A\Gamma\rangle\langle p\Lambda|i\Gamma\rangle}{\omega_p + \epsilon_\Gamma - \epsilon_i - \epsilon_\Lambda}$$

$$U_{pIaA}(\omega_p) = \sum_{b,B} \frac{\langle pI|bB\rangle\langle aA|bB\rangle}{\omega_p + \epsilon_I - \epsilon_b - \epsilon_B} - \sum_{J,B} \frac{\langle pJ|aB\rangle\langle IJ||BA\rangle}{\omega_p + \epsilon_J - \epsilon_a - \epsilon_B} - \sum_{b,J} \frac{\langle pJ|bA\rangle\langle aI|bJ\rangle}{\omega_p + \epsilon_J - \epsilon_b - \epsilon_A} \quad (3\text{-}74)$$

$$+ \sum_{i,b} \frac{\langle iI|aA\rangle\langle pi||ab\rangle}{\omega_p + \epsilon_i - \epsilon_a - \epsilon_b} + \sum_{\gamma\neq\beta,\gamma\neq\alpha}^{N^Q} \sum_{\Lambda,\Gamma} \frac{\langle I\Lambda|A\Gamma\rangle\langle p\Lambda|a\Gamma\rangle}{\omega_p + \epsilon_\Lambda - \epsilon_a - \epsilon_\Gamma}$$

Using the previous definitions we can express the quasiparticle P3-APMO self-energy as:

$$\Sigma_{PP}^{\alpha(P3)}(\omega_p) = \frac{1}{2} \sum_{a,i,j} \frac{\langle pa||ij\rangle(W_{paij} + U_{paij}(\omega_p))}{\omega_p + \epsilon_a - \epsilon_i - \epsilon_j} + \frac{1}{2} \sum_{i,a,b} \frac{\langle pi||ab\rangle(W_{piab} + U_{piab}(\omega_p))}{\omega_p + \epsilon_i - \epsilon_a - \epsilon_b} \quad (3\text{-}75)$$

$$+ \sum_{\beta\neq\alpha}^{N^Q} \left[\sum_{i,A,I} \frac{\langle pA|iI\rangle(W_{pAiI} + U_{pAiI}(\omega_p))}{\omega_p + \epsilon_A - \epsilon_I - \epsilon_i} + \sum_{a,A,I} \frac{\langle pI|aA\rangle(W_{pIaA} + U_{pIaA}(\omega_p))}{\omega_p + \epsilon_I - \epsilon_A - \epsilon_a} \right]$$

and the Complete-P3 (CP3) APMO self-energy as:

$$\Sigma_{PP}^{\alpha(CP3)}(\omega_p) = \sum_{rs} \langle pr||qs\rangle\rho_{rs}^{(2)} + \sum_{\beta\neq\alpha}^{N^Q} \sum_{P,Q} (pq|PQ)\rho_{PQ}^{(2)}$$

$$+ \sum_{a,i,j} \frac{\langle pa||ij\rangle(W_{paij} + \frac{U_{paij}(\omega_p)}{2})}{\omega_p + \epsilon_a - \epsilon_i - \epsilon_j} + \sum_{i,a,b} \frac{\langle pi||ab\rangle(W_{piab} + \frac{U_{piab}(\omega_p)}{2})}{\omega_p + \epsilon_i - \epsilon_a - \epsilon_b} \quad (3\text{-}76)$$

$$+ \sum_{\beta\neq\alpha}^{N^Q} \left[\sum_{i,A,I} \frac{\langle pA|iI\rangle(W_{pAiI} + U_{pAiI}(\omega_p))}{\omega_p + \epsilon_A - \epsilon_I - \epsilon_i} + \sum_{a,A,I} \frac{\langle pI|aA\rangle(W_{pIaA} + U_{pIaA}(\omega_p))}{\omega_p + \epsilon_I - \epsilon_A - \epsilon_a} \right]$$

where the elements of the second order densities $\rho_{rs}^{(2)}$ for a species α are given by equations 3-18 and 3-19.

3.3 Working equations written for all the diagonal methods

4 Implementation in LOWDIN program

4.1 The LOWDIN program

LOWDIN [51] is a computational program that implements the Any Particle Molecular Orbital (APMO) method. The current version of the code encompasses Hartree-Fock, second-order Møller-Plesset, configuration interaction, density functional apart from propagator theories. LOWDIN has been fully coded in the FORTRAN 2003 standard, with some C/C++ bindings to external libraries. Although FORTRAN 2003 is not a full Object Oriented Programming (OOP) language, most OOP capabilities can be easily emulated, such as class definitions, some polymorphism and inheritance [52]. Figure **4-1** shows an schematic representation of LOWDIN structure, which is based on a *CORE* program with small programs around it. These programs are completely encapsulated and independent from one another.

The basic structure of LOWDIN is the CORE program, that implements a set of tools to load the input file, generate the molecular system and run all the requested tasks. This program also include the *INTEGRALS* and *SCF* programs. The INTEGRALS program evaluates the one- and two-particle integrals for the Gaussian Type Orbitals (GTOs) basis set functions. One-particle integrals such as overlap, kinetic and nuclear attraction energy have been implemented for Gaussian basis functions of any angular momentum following Obara-Saika [53] and Head-Gordon-Pople [54] recursive schemes.

Two-particle interaction integrals of the type $(pq|r_{12}{}^{-1}|rs)$ are calculated either with propietary routines or with LIBINT library [55]. Integrals of the type $(pq|e^{-\gamma r_{12}^2}|rs)$ are calculated with the LIBINT library. Integrals can be stored on either memory or disk. Integrals stored on disk are collected in stacks containing a maximum of 30.000 of them. Several stacks are calculated simultaneously to exploit the computational power of the machine. Different schemes have been implemented to exploit the permutational symmetry of the integrals.

The Self Consistent Field (SCF) program has been designed to minimize the energy of a molecular systems composed of multiple quantum species for the Hartree-Fock APMO scheme. In a multi-species calculation, LOWDIN creates Fock-like operators for every quantum species, and this matrices are interated until convergence. Convergence acceleration methods such as DIIS [56], level shifting [57] and optimal damping [58] have been implemented and are fully operational for any type of quantum species.

Figure **4-1**: Structure of LOWDIN program.
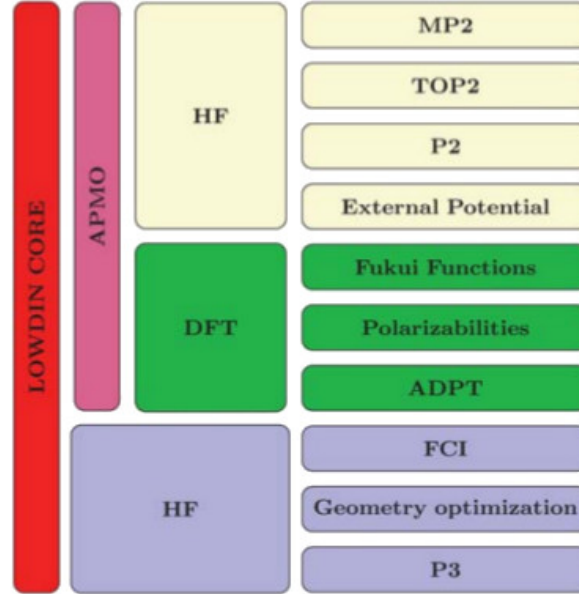
4.2 Implementation of diagonal propagator approaches

The APMO propagator theory developed on section 3 was implemented in a new module fully coded in the FORTRAN 2003 language standard [59] following the object-oriented programming philosophy of LOWDIN program. The following subsections describe details on the solution of the Dyson equation, the structure of the created propagator module and other modifications done to LOWDIN program.

4.2.1 Solving the Dyson Equation

The diagonal Dyson equation has the form shown in Eq.(3-52):

$$\omega_p^\alpha = \varepsilon_p^\alpha + \Sigma_{pp}^\alpha(\omega_p^\alpha) \tag{4-1}$$

Since the self-energy depends on ω, Eq.(3-52) is non-linear. Finding the solution of Eq.(3-52) is equivalent to finding the zeros of the function $f(\omega^\alpha)$ defined as:

$$f(\omega_p^\alpha) = \omega_p^\alpha - \varepsilon_p^\alpha - \Sigma_{pp}^\alpha(\omega_p^\alpha) \tag{4-2}$$

This task can be accomplished by using the Newton-Raphson method:

$$\omega_{p,n+1}^\alpha = \omega_{p,n}^\alpha - \frac{f(\omega_{p,n}^\alpha)}{f'(\omega_{p,n}^\alpha)} \tag{4-3}$$

Where a the value of ω^α is determined iteratively. As exposed in section 3.2.5, up to third order the self-energy includes three kind of terms, classified according to its dependence on

ω^α: 1) Independent terms 2) Terms depending once in ω_p^α and 3) terms depending twice in ω_p^α. This means that up to third order, the self energy can be schematically represented as:

$$\Sigma_{pp}^\alpha(\omega_p^\alpha) = C + \sum_{A,B} \frac{A}{\omega_p^\alpha + B} + \sum_{D,E,F} \frac{D}{(\omega_p^\alpha + E)(\omega_p^\alpha + F)} \tag{4-4}$$

where C is the sum of all the terms independent from ω^α, A and E represent the numerators of formulas 3-59 and 3-60 or 3-63 and 3-64, and D, E and F the corresponding denominators. Numerators are products of Coulomb and exchange integrals in the molecular orbital basis (MO integrals) and denominators are sums of Hartree-Fock orbital energies. Using the expression 4-4, $f(\omega_n^\alpha)$ and its derivative with respect to ω_n^α, can be expressed as:

$$f(\omega_p^\alpha) = \omega_p^\alpha - \varepsilon_p^\alpha - C - \sum_{A,B} \frac{A}{\omega_p^\alpha + B} - \sum_{D,E,F} \frac{D}{(\omega_p^\alpha + E)(\omega_p^\alpha + F)} \tag{4-5}$$

$$f'(\omega_p^\alpha) = 1 + \sum_{A,B} \frac{A}{(\omega_p^\alpha + B)^2} + \sum_{D,E,F} \frac{D * (2\omega_p^\alpha + E + F)}{(\omega_p^\alpha + E)^2(\omega_p^\alpha + F)^2} \tag{4-6}$$

Eqs. 4-3, 4-5 and 4-6 are the formulas implemented in LOWDIN program to solve the diagonal Dyson equation.

4.2.2 The PROPAGATOR program in LOWDIN

The propagator program included in LOWDIN calculates corrected binding energies for any type of particle species following the algorithm shown in Figure **4-2** and briefly described below:

1. An APMO/HF calculation is performed. This calculation produces the interaction integrals in the atomic basis (AO integrals) and the eigenvectors (molecular coefficient: MC) and eigenvalues of the Hartree-Fock matrix.

2. Get the required interaction integrals in the molecular basis (MO integrals) by transforming the AO integrals. This step is the blottleneck of the calculation.

3. Store the numerators and denominators of the self-energy.

4. Compute ω_p^α using the Newton-Raphson method (Eq.4-3) and Eqs.4-5 and 4-6. Iterations stop when the difference in the value of ω_p^α between two consecutive iterations is less than 0.0001 a.u.

The four index integrals transformation is performed by using one of the two modules available in LOWDIN to perform this task.

Figure **4-2**: Scheme of the operation of the propagator module implemented in LOWDIN
program
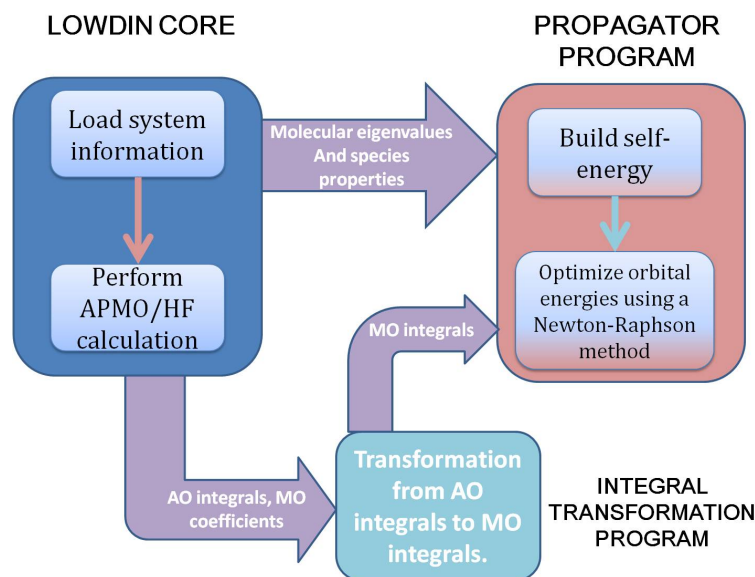
4.2.3 Other modifications to the LOWDIN code

The following list shows the modifications and other implementations that have been done
in LOWDIN program as part of this thesis:

1. **Implementation of the module `integralTransform2` for the four-index inte-gral transformation**: the previous version of LOWDIN had only one module for integral transformation, based on a modified version of the program of Yamamoto et al[60], called `integralTransform`. Although efficient, this module performs the transformation of all the integrals (most of them not required for APMO/P2 calculations) and uses N^4 memory, with N the number of basis set functions. This fact limited the applicability of the propagator method to small systems. To overcome this limitation, a second integral transformation module, called `integralTransform2`, was fully coded in LOWDIN following a matrix multiplication scheme [61]. The `integralTransform2` module, although much less efficient than the `integralTransform`, has the advantage of using only N^2 memory, expanding the applicability of propagator calculations in LOWDIN program to larger systems.

2. **Implementation of the rotational and translational free schemes proposed by Nakai (Section 2.4.4)**. This task was accomplished by modifying the modules that performs the kinetic and overlap integrals calculation in LOWDIN.

3. **Modification of the SCF program to assure convergence of TOP2 calculations**. Using fractional occupations for an orbital can cause orbital rotations that

Table **4-1**: Control variables for propagator calculations in the LOWDIN program

Option	Variable type	Description	Default value
`IonizeMO`	INTEGER	Specifies the number of the orbital to be calculated	All the orbitals are calculated.
`ionizeSpecie`	CHARACTER	Specifies only one species for which the propagator calculation will be run.	All the species are calculated
`ptTransitionOperator`	LOGICAL	When .TRUE. activates the TOP2 method. Options `IonizeMO`, `ionizeSpecie` and `MOfractionOccupation` are mandatory.	FALSE
`MOfractionOccupation`	REAL	Specifies fractional occupation of the orbital of interest for the TOP2 method. Values between 0 and 1.	0.5 (Recommended)

prevent SCF to converge. The SCF module of LOWDIN was modified to avoid orbital rotations and assure convergence of TOP2 calculations.

4.3 Running propagator calculations in LOWDIN

The version 2.0 of LOWDIN program includes second and complete third order diagonal propagator methods as well as the diagonal second order plus transition operator approach (APMO/TOP2). Implementation of non-diagonal methods is in progress but it will not be discussed in this work.

To perform a propagator calculations using LOWDIN, the order of perturbational series must be specified in the `TASKS` block using the keyword `propagatorTheoryCorrection`, as illustrated in Fig.(**4-3**). The options to control propagator calculations, described in table **4-1**, must be specified in the `OPTIONS` block.

```
SYSTEM_DESCRIPTION='Water molecule'

GEOMETRY
e-(O)    6-31G   0.0000 0.0000 0.1173   multiplicity=1
e-(H) 6-31G   0.0000 0.7572 -0.4692
e-(H) 6-31G   0.0000 -0.7572 -0.4692
O_16  Nakai-TRF-7SPD   0.0000 0.0000 0.1173
H-a_1 Nakai-TRF-7SPD   0.0000 0.7572 -0.4692
H-b_1 Nakai-TRF-7SPD   0.0000 -0.7572 -0.4692
END GEOMETRY

TASKS
        method = "RHF"
        propagatorTheoryCorrection=2
END TASKS

CONTROL
! removeRotationalContamination=T
! removeTranslationalContamination=T
END CONTROL
```

Figure **4-3**: Example of input file for APMO/P2 calculations in LOWDIN

4.3.1 Input file examples

Ionization energies for a water molecule using APMO/P2

Figure **4-3** shows the input file to perform a second order propagator calculations of the water molecule. In this example nuclei and electron are treated as quantum particles. Note that the GEOMETRY block includes the information of the particles, electronic multiplicity, and the name and positions of the basis sets to be employed. The TASK block specifies a restricted Hartree-Fock (RHF) calculation followed by the propagator calculation at second order (`propagatorTheoryCorrection=2`). For third order calculations 2 is replaced by 3. The CONTROL block also includes the options to remove the rotational and translational contaminations (Section 2.4.4). These options are recommended for calculations where all nuclei are treated quantum mechanically, although in the present example, they appear commented (using the symbol !).

The results of the propagator calculation appears at the end of the the output file as a table, as shown in figure **4-4**. The KT and EP2 columns display the Koopmans (Hartree-Fock) and propagator corrected binding energies in eV, respectively. The P.S. column displays the value of the pole strength. Columns `Sigma a-a` and `Sigma a-a` display the values of Σ_{pp}^{α} and Σ_{pp}^{β}, as defined in Eq.(**??**). Note that the default calculation applies propagator theory to all the

```
POST HARTREE-FOCK CALCULATION
PROPAGATOR THEORY:
  ===============================


PROPAGATOR FORMALISM FOR SEVERAL FERMIONIC SPECIES
ORDER OF CORRECTION =      2
  SPECIE:           e-
   -----------------------------------------------------------------------------
    Orbital       KT (eV)        Sigma a-a       Sigma a-b        EPT (eV)       P.S
   -----------------------------------------------------------------------------
        1        553.8569        -19.7701        -0.1119         533.9750      0.7631
        2         35.8160         -2.5987        -0.4668          32.7505      0.3661
        3         18.4704         -1.2463        -0.4830          16.7411      0.6922
        4         14.7729         -2.3422        -0.2690          12.1616      0.8494
        5         13.3647         -2.9090        -0.2761          10.1797      0.8562
   -----------------------------------------------------------------------------
  SPECIE:        O_16
   -----------------------------------------------------------------------------
    Orbital       KT (eV)        Sigma a-a       Sigma a-b        EPT (eV)       P.S
   -----------------------------------------------------------------------------
        1       4836.1165          0.0000        -24.5030       4811.6135      0.7585
   -----------------------------------------------------------------------------
  SPECIE:        H-a_1
   -----------------------------------------------------------------------------
    Orbital       KT (eV)        Sigma a-a       Sigma a-b        EPT (eV)       P.S
   -----------------------------------------------------------------------------
        1         24.6233          0.0000         -7.6088          17.0145      0.8775
   -----------------------------------------------------------------------------
  SPECIE:        H-b_1
   -----------------------------------------------------------------------------
    Orbital       KT (eV)        Sigma a-a       Sigma a-b        EPT (eV)       P.S
   -----------------------------------------------------------------------------
        1         24.6233          0.0000         -7.6088          17.0145      0.8775
   -----------------------------------------------------------------------------
```

Figure **4-4**: Results of APMO/P2 calculations using LOWDIN

species and all the occupied orbitals of the system. If the user wants to run calculations for the orbitals of only one species, the option `ionizeSpecie` needs to be specified. In addition, if the user is only interested on just one orbital, the option `ptJustOneOrbital` must be turn on and the number of the orbital must be specified using the option `IonizeMO`, in addition to the species name. For instance, to modify the example presented on figure **4-3** in order to calculate only the corrected binding energy for the electronic HOMO (5th orbital) of the water molecule the following options must be added to the CONTROL block:

```
CONTROL
    ...
    IonizeMO=5
    ionizeSpecie="e-"
    ptJustOneOrbital=T
    ...
END CONTROL
```

Ionization energies for a water molecule using APMO/TOP2

Transition operator calculations are only available at second order. In a single calculation, only one orbital of one specific species can have a fractional occupation. The default and recommended occupation is 1/2. The variable `ptTransitionOperator` must be turn on, and the fractional occupation must be specified using `MOfractionOccupation` along with the number of the orbital of interest and the species it belongs. If the calculation is for electrons, the UHF reference state must be employed. Fig. (**4-5**) illustrate how to use these options. The output file for the APMO/TOP2 calculation is shown in Fig.(**4-6**)

```
SYSTEM_DESCRIPTION='Water molecule'

GEOMETRY
e-(O)    6-31G        0.0000         0.0000  0.1173    multiplicity=1
e-(H)    6-31G        0.0000         0.7572 -0.4692
e-(H)    6-31G        0.0000        -0.7572 -0.4692
O_16     Nakai-TRF-7SPD   0.0000     0.0000  0.1173
H-a_1    Nakai-TRF-7SPD   0.0000     0.7572 -0.4692
H-b_1    Nakai-TRF-7SPD   0.0000    -0.7572 -0.4692
END GEOMETRY


TASKS
        method = "UHF"
        propagatorTheoryCorrection=2
END TASKS


CONTROL
        ionizeSpecie="e-ALPHA"
        IonizeMO=5
        MOfractionOccupation=0.5
        ptTransitionOperator=T
END CONTROL
```

Figure **4-5**: Example of input file for APMO/TOP2 calculations in LOWDIN

```
POST HARTREE-FOCK CALCULATION
PROPAGATOR THEORY:
==============================
PROPAGATOR FORMALISM FOR SEVERAL FERMIONIC SPECIES
ORDER OF CORRECTION =     2  + TRANSITION OPERATOR
 SPECIE:    e-ALPHA

 --------------------------------------------------------------------------------
   Orbital       KT (eV)       Sigma a-a       Sigma a-b       EPT (eV)      P.S
 --------------------------------------------------------------------------------
      5          12.1432        0.8333         -0.4043         12.5722      0.3398
 --------------------------------------------------------------------------------
```

Figure **4-6**: Results of APMO/TOP2 calculations using LOWDIN

5 Applications of APMO propagator theory

In this chapter we present the numerical assessment of the propagator methods previously proposed. The first three sections present calculation for atoms and molecules where nuclei and electrons are treated quantum mecanically. We assess the performance of the propagator second order propagator approximations proposed in sections 3.2.5 - 3.2.5 to predict electron and proton binding energies [35, 62]. We also analyze the impact of removing the translational and rotational contaminations by comparing with regular electronic structure calculations (in the case of electrons) and experimental results. A phenomenological characterization of the proton and electron ionization proccesses is proposed in terms of a decomposition of the self-energy term into its relaxation and correlation contributions.

5.1 Calculation of electron binding energies

The propagator approximations implemented in LOWDIN program can be employed to perform regular electron propagator calculations based on the BOA approximation. Nevertheless, LOWDIN program can also performed non-BOA calculations where nuclei and electron are simultaneusly treated quantum mechanically. In this section we present electron propagator calculations considering nuclei as quantum particles and analyze the effect of this treatment on the description of the ionization process and the quality of the predicted electron ionization energies.

5.1.1 Atoms

In table **5-1** we contrast the experimental valence ionization energies for the atoms of the first three periods of the periodic table with those calculated with regular electronic structure theory and the APMO approach. APMO results were obtained employing the mass of the most abundant isotope for each element. The translational contribution to the total energy was removed. We observe that including NQE in the calculation of ionization energies for atoms only has a minor effect on the average deviations of less than 0.025 eV.

Table **5-1**: Calculated valence ionization energies (in eV) for atoms. Electronic cc-pVTZ [63] and nuclear 7s7p [24] basis sets were used.

	Ionization	EP2	APMO/EP2	TOEP2	APMO/TOEP2	Exp.[a]
H[b]		13.6086	13.5965	13.6086	13.5896	13.5984
He	$^1S \to\, ^2S$	24.5513	24.5405	24.2985	24.2882	24.5874
Li	$^2S \to\, ^1S$	5.3670	5.3430	5.3678	5.3672	5.3917
Be	$^1S \to\, ^2S$	8.9241	8.4646	8.9297	9.2575	9.3226
B	$^2P \to\, ^1S$	8.6653	8.6679	8.3441	8.3459	8.2980
C	$^3P \to\, ^2P$	11.9391	11.9408	11.3069	11.3083	11.2603
N	$^4P \to\, ^3P$	14.4296	14.4308	14.4975	14.4988	14.5341
O	$^3P \to\, ^4P$	12.9746	12.9746	13.0900	13.0896	13.6181
F	$^2P \to\, ^3P$	16.3797	16.3795	16.9077	16.9089	17.4228
Ne	$^1S \to\, ^2P$	20.1000	20.1013	21.1073	21.1078	21.5645
Na	$^2S \to\, ^1S$	4.9840	4.9837	4.9841	4.9838	5.1391
Mg	$^1S \to\, ^2S$	7.3547	7.3543	7.3571	7.3568	7.6462
Al	$^2P \to\, ^1S$	5.9178	5.9181	5.8736	5.8740	5.9858
Si	$^3P \to\, ^2P$	8.1110	8.1114	8.0542	8.0549	8.1517
P	$^4P \to\, ^3P$	10.4901	10.4907	10.4670	10.4678	10.4867
S	$^3P \to\, ^4P$	10.0281	10.0297	10.0181	10.0187	10.3600
Cl	$^2P \to\, ^3P$	12.5953	12.5961	12.6902	12.6909	12.9676
Ar	$^1S \to\, ^2P$	15.3891	15.3899	15.6029	15.6034	15.7596
Δ		0.3558	0.3831	0.2108	0.1934	

[a] See Refs.[64] for experimental values. [b] Aug-cc-pVQZ basis set.

Δ: Absolute average deviation from experimental values (in eV).

Figure **5-1**: Isotope effects calculated by APMO/EP2 methods in the ionization potential of hydrogen atom isotopologues. Electronic aug-cc-pVQZ [63] and nuclear 17s [24] basis sets were used.
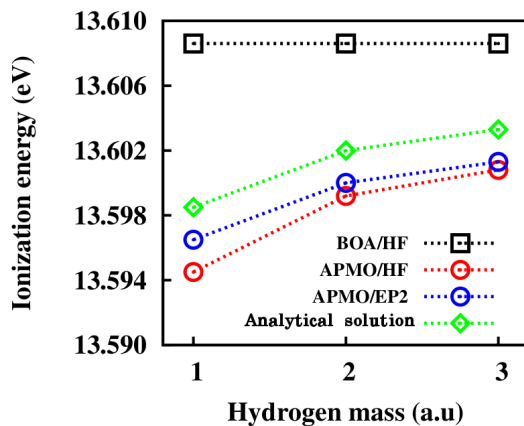
5.1.2 Molecules

Now we turn our attention to molecules. In this case we need to take into account the following considerations:

1. A rigorous treatment of the nuclear-electron wavefunction should consider all nuclei as quantum particles. In that case translational and rotational motions are included in the total wavefunction. However, as exposed in section 2.4.4, GTOs cannot properly describe translational and rotational wavefunctions. To deal with this problem, the translational and rotational contaminations are removed and then an analysis of the impact of this correction is required.

2. In regular propagator calculations for molecules, ionization energies are associated to vertical values, with nuclear positions remaining fixed between the original and the ionized state at any order of perturbation. In the APMO approximation this is not neccesarily true, given that the self-energy terms include a contribution from nuclear relaxation. As a result, the expected properties of nuclear wavefunctions, such as expected positions, will change between the original and the ionized state. In terms of regular electronic structure theory this process can be interpreted as partially adiabatic. In APMO theory a vertical ionization can be obtained imposing a nuclear frozen approximation, where nuclear wave functions remain fixed between the original and the ionized state. At zero order in the APMO theory, propagator calculations for electrons predict vertical ionization energies because nuclear and electronic wavefunctions remain frozen during the ionization proccess (Koopmans approximation). In the case of higher order calculations an analysis of the impact of nuclear-electron relaxation is still needed to determine the nature of the ionization process.

3. The simultaneous calculation of nuclear and electron wavefunctions in the APMO method leads to the inclusion of NQEs. The impact on this effect on the study of the electron

      ionization process has to be determined.

In the following subsections we address each of the above points.

Effect of removing translational and rotational motions

Tables **5-2** and **5-3** show a comparison of valence electron binding energies calculated for a set of small molecules employing APMO-P2 and TOP2 methods and regular electronic structure calculations using EP2 and TOEP2 methods. The performance of the APMO approach is similar to that of the regular electronic structure calculations. Differences between the TRC, TF and TRF treatments are within 0.1 eV for the P2 method and 0.05 eV for the TOEP2 calculation. We also observe that in the case of the TOEP2 calculation, results considering quantum nuclei are slightly better than those of regular electronic structure calculation.

A closer inspection to the results of tables **5-2** and **5-3** allow us to conclude that in most of the cases differences between the regular propagator calculations and the APMO treatment considering quantum nuclei are small, specially for the case of APMO-TRF calculations. However for molecules such as methane and silane, differences are much larger. We will come back to this topic shortly in the section about the impact of NQE on the electron ionization.

Now we analyze results for inner ionizations, where it is expected that nuclei have a larger impact because of the larger interaction between nuclei and inner electrons. In this case we only compared the results of APMO-TOEP2 calculations; it has been shown that this method is the most accurate propagator method currently available to calculate inner ionization energies, where electron relaxation makes up the main contribution to the self-energy term.

In first place we observe than inner ionization energies calculated with APMO methods are smaller that those of regular structure calculations. We understood this result as an effect of the nuclear delocalization that reduces the magnitude of the electron-nuclear attraction in comparison with the BOA approximation, where nuclei are simply point charges. However, this effect seems to have a negative effect on the quality of the prediction, as demonstrated by the magnitude of the deviations respect to experimental values of the APMO-TOP2, which are much larger than the regular TOEP2 calculation. Even the TRF treatment that has a a better performance than TF and TRC, fails on achieving the same accuracy of the regular BOA treatment. Average deviations of APMO-TOP2 are at least four times larger than those of regular TOEP2. These results allow us to conclude that the APMO-TOEP2 treatment underestimates the electron-nuclear interaction term, in other words, that more nuclear-electron correlation needs to be included to achieved a better performance.

Now we analyze isotope effects. Figure **5-2** shows the results of the isotope shift between the electron ionization energy of H_2 and D_2 molecules. In this case it is clear that the TRF calculation produces better estimations of isotope effects that its TRC and TF counterparts.

Table **5-2**: Comparison between APMO -TRF -TF -TRC and regular BOA-EP2 calculations of valence and inner valence ionization energies for a set of small molecules. Values in eV.

Molecule	Orbital	Koopmans result				APMO-P2 and EP2				Expt.
		TRC	TF	TRF	BOA	TRC	TF	TRF	BOA	
LiH	1σ	8.037	8.053	8.120	8.172	7.966	7.969	7.940	7.943	7.90
BH3	1e	13.242	13.243	13.317	13.564	12.776	12.778	12.851	13.250	12.30
CH4	1t2	14.443	14.440	14.503	14.838	13.497	13.499	13.573	14.104	13.60
SiH4	1t2	12.923	12.923	12.965	11.936	12.492	12.490	12.518	12.680	12.30
F2	1π	18.169	18.147	18.114	18.093	14.276	14.256	14.227	14.209	15.83
	$1\sigma_g$	20.462	20.447	20.433	20.410	20.466	20.456	20.449	20.432	21.10
HNC	1π	13.263	13.277	13.295	13.370	11.937	11.947	11.966	12.055	12.55
HCN	1π	13.470	13.457	13.446	13.469	13.513	13.501	13.492	13.665	13.61
HF	1π	17.469	17.435	17.490	17.528	14.441	14.417	14.548	14.706	16.19
NH3	$3a_1$	11.458	11.453	11.488	11.612	9.671	9.680	9.749	10.179	10.80
	2a1	25.202	25.264	25.323	25.677	23.975	22.931	22.998	23.410	23.10
H2O	1b1	13.651	13.631	13.668	13.748	11.213	11.205	11.307	11.506	12.78
	1a1	15.486	15.487	15.603	15.740	13.388	13.404	13.554	13.821	14.74
HCl	1π	12.915	12.900	12.927	12.947	12.228	12.216	12.303	12.399	12.70
H_2S	$2b_1$	10.420	10.408	10.424	10.462	9.896	9.888	9.970	10.161	10.50
Average Deviation		0.82	0.82	0.86	0.94	0.77	0.72	0.68	0.66	

TRC: Translation Rotational Contaminated.

TF: Translation Free.

TRF: Translationa Rotational Free.

Table **5-3**: Comparison between APMO-TRF -TF -TRC and regular BOA-TOEP2 calculations of valence and inner valence ionization energies for a set of small molecules. Values in eV.

Molecule	Orbital	Koopmans result				APMO-TOP2 and TOEP2				
		TRC	TF	TRF	BOA	TRC	TF	TRF	BOA	Expt.
LiH	1σ	6.725	6.738	6.802	6.838	7.568	7.562	7.466	7.522	7.90
BH3	1e	11.738	11.755	11.967	12.397	12.233	12.235	12.457	13.163	12.30
CH4	1t2	12.384	12.396	12.467	13.224	12.897	12.901	14.031	14.312	13.60
SiH4	1t2	11.380	11.382	11.434	11.936	11.886	11.885	12.433	12.680	12.30
F2	1π	16.195	16.174	16.143	16.123	14.966	14.946	14.916	14.898	15.83
	$1\sigma_g$	18.320	18.308	18.296	18.279	20.971	20.963	20.956	20.941	21.10
HNC	1π	10.649	10.662	10.686	10.785	11.910	11.923	11.945	12.025	12.55
HCN	1π	11.875	11.863	11.854	12.205	13.997	13.983	13.974	13.536	13.54
HF	1π	13.929	13.902	14.033	14.124	15.725	15.690	15.646	15.693	16.19
NH3	$3a_1$	8.921	8.912	8.954	9.216	10.666	10.644	10.645	10.667	10.80
	2a1	23.301	23.366	23.419	24.128	23.344	23.494	23.529	23.957	23.10
H2O	1b1	10.572	10.556	10.631	10.763	12.415	12.391	12.409	12.313	12.78
	1a1	12.376	12.385	12.644	13.040	14.204	14.218	14.390	14.512	14.74
HCl	1π	11.421	11.407	11.451	11.478	12.628	12.610	12.649	12.588	12.70
Average Deviation		1.48	1.49	1.42	1.27	0.39	0.40	0.37	0.45	

TRC: Translation Rotational Contaminated.

TF: Translation Free.

TRF: Translationa Rotational Free.

Table **5-4**: Comparison between APMO-TRF -TF -TRC and regular BOA TOEP2 calculations for 1s orbitals. Values in eV.

Molecule	Atom	TOM values				APMO-TOP2 and TOEP2				Expt.
		TRC	TF	TRF	BOA	TRC	TF	TRF	BOA	
HF	F	686.10	691.32	692.31	693.09	686.37	691.09	691.67	694.45	694.18
H2O	O	533.09	536.91	537.68	539.16	533.40	537.20	537.98	539.81	539.86
H2CO	O	532.40	534.20	535.90	538.20	532.95	534.69	536.10	538.83	539.48
	C	290.33	291.11	291.69	294.10	290.55	291.26	291.99	294.20	294.47
CO	O	535.89	537.84	539.86	541.54	536.29	537.63	540.58	542.20	542.39
	C	293.60	294.43	295.88	297.05	294.05	294.88	296.32	297.48	296.13
HCN	C	289.55	290.43	291.06	293.13	289.88	290.71	291.21	293.60	293.50
	N	401.65	403.04	404.46	406.27	402.23	403.56	404.94	406.89	406.36
N2	N	414.91	416.14	417.74	419.12	405.54	406.77	408.35	409.73	409.83
F2	F	702.57	690.66	706.86	708.83	688.86	691.32	694.02	695.83	696.69
Average Deviation		5.47	3.98	3.60	2.75	5.32	3.42	2.05	0.48	

TRC: Translation Rotational Contaminated.

TF: Translation Free.

TRF: Translationa Rotational Free.
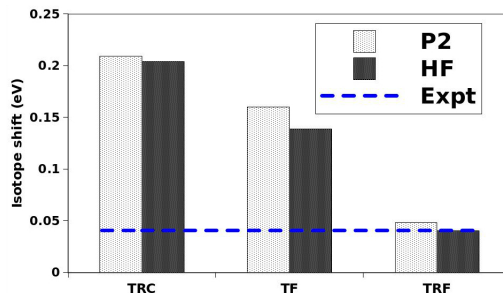
Figure **5-2**: Isotope shift of the electron ionization energy between H_2 and D_2, as calculated with APMO-HF and APMO-P2 approximations.

Nature of the electron ionization process: adiabatic or vertical ionization?

To gain better insights into the effects of nuclear-electron terms we compared the calculated ionization energies for a set of small molecules with and without considering nuclei as quantum particles. In Table **5-5** we separated the terms contributing to the corrected ionization energy in Eq. (3-10) and present the Koopmans' energies, ε_p^{e-}, and the self-energy terms, $\Sigma_{pp}^{e-,e-(2)}$ and $\Sigma_{pp}^{e-,p+(2)}$, obtained from EP2, TOEP2, APMO/EP2 and APMO/TOEP2 propagator calculations for a set of small molecules. A detailed analysis of the regular and APMO energy terms reveals: First, that in all cases the zero order energy term, ε_p^{α}, presents the largest energy variations (around 0.22 eV and 0.20 eV for EP2 and TOEP2 methods, respectively). It is also observed that zero order values for APMO methods are always smaller that those obtained considering hydrogen nuclei as fixed particles. Since zero order values correspond to Koopmans approximation, it is not expected that the observed effect is due to nuclear relaxation. Nevertheless, the lowering in zero order values can be understood as a consequence of describing nuclei as quantum particles and not as point charges. In this regard, Gonzalez et al. [32] demonstrated that by treating nuclei as charge densities there is a lowering of the nuclear-electron attraction energy and consequently a reduction of electron eigenvalues.

We also observe that differences of the $\Sigma_{pp}^{e-,e-(2)}$ energies in regular and APMO methods are considerably smaller than those of the ε_p^{e-} terms. A comparison of $\Sigma_{pp}^{e-,e-(2)}$ in regular and APMO methods reveals that it is almost the same, with small average variations of 0.0066 eV and 0.0241 eV for EP2 and TOEP2 methods, respectively. The third decomposition term, $\Sigma_{pp}^{e-,p+(2)}$, contains both, nuclear-electron relaxation and correlation terms. This term, only appearing in APMO calculations, contributes little to the total ionization energy, with and average of 0.0171 and 0.0184 eV for APMO/EP2 and APMO/TOEP2 methods, respectively. These results are at least one order of magnitude smaller than average differences between vertical and adiabatic ionization energies [65], suggesting a small contribution from nuclear-relaxation terms.

Table **5-5**: Contributions to regular and APMO second order (EP2) and second order plus transition operator (TOEP2) calculated valence ionization energies (in eV) for the set of small molecules. Electronic cc-pVTZ [63] and nuclear 7s7p [24] basis sets were used. Electrons and hydrogenic nuclei were treated quantum mechanically in APMO calculations.

Molecule	Orbital (p)	EP2 only electrons [a]			APMO/EP2 [a]		
		ε_p^{e-}	$\Sigma_{pp}^{e-,e-(2)}$	$\Sigma_{pp}^{e-,p+(2)}$	ε_p^{e-}	$\Sigma_{pp}^{e-,e-(2)}$	$\Sigma_{pp}^{e-,p+(2)}$
LiH	1σ	6.8683	0.7098	0.0000	6.7688	0.6937	0.0518
BH$_3$	$1e$	12.3965	0.7661	0.0000	11.8568	0.7806	0.0814
NH$_3$	$3a_1$	9.2158	1.4508	0.0000	8.9155	1.4568	0.0112
CH$_4$	$1t_2$	14.8387	-0.7339	0.0000	14.4193	-0.7220	0.0564
SiH$_4$	$1t_2$	13.2412	-0.4085	0.0000	12.8997	-0.3935	0.0759
H$_2$O	$1b_1$	10.7630	1.5528	0.0000	10.5055	1.5572	0.0014
HF	1π	14.1239	1.5691	0.0000	13.8492	1.5725	0.0008
H$_2$S	$2b_1$	9.1727	1.1131	0.0000	9.0836	1.1150	0.0005
HCl	1π	11.4779	1.1099	0.0000	11.3928	1.1094	0.0003
$|\Delta|^b$		0.2298	0.0066	0.0171			
		TOEP2 only electrons [a]			APMO/TOEP2 [a]		
LiH	1σ	8.2006	-0.2034	0.0000	8.0661	-0.1765	0.0687
BH$_3$	$1e$	13.5639	-0.3138	0.0000	13.2001	-0.3059	0.0762
NH$_3$	$3a_1$	11.6128	-1.4338	0.0000	11.4330	-1.4761	0.0054
CH$_4$	$1t_2$	13.2239	1.0883	0.0000	12.4633	1.1197	0.0802
SiH$_4$	$1t_2$	11.9363	0.7433	0.0000	11.4389	0.7663	0.0758
H$_2$O	$1b_1$	13.7510	-2.2419	0.0000	13.5972	-2.2857	-0.0053
HF	1π	17.5288	-2.8211	0.0000	17.4020	-2.8406	-0.0043
H$_2$S	$2b_1$	10.4619	-0.3010	0.0000	10.3988	-0.3282	-0.0010
HCl	1π	12.9461	-0.5474	0.0000	12.8887	-0.5633	-0.0008
$|\Delta|^b$		0.1969	0.0239	0.0245			

[a] See Ref.[66] for geometry details. [b] $|\Delta|$: Average absolute difference between regular and APMO methods.

Table **5-6**: Decomposition analysis for $\Sigma_{pp}^{e-,p+(2)}$ (in eV) for the set of small molecules [a]. Electronic cc-pVTZ [63] and nuclear 7s7p [24] basis sets were used. Electrons and hydrogenic nuclei were treated quantum mechanically in APMO calculations.

Molecule	Orbital	APMO/EP2 $\Sigma_{pp}^{e-,p+(2)}$			
		PRM	PRX	ORX	ERX
LiH	1σ	0.0695	0.0000	-0.0008	0.0000
BH$_3$	$1e$	0.0810	-0.0014	-0.0034	0.0000
NH$_3$	$3a_1$	0.0139	-0.0031	-0.0053	0.0000
CH$_4$	$1t_2$	0.0649	-0.0029	-0.0056	0.0000
SiH$_4$	$1t_2$	0.0795	-0.0013	-0.0022	0.0000
H$_2$O	$1b_1$	0.0040	-0.0029	-0.0064	0.0000
HF	1π	0.0022	-0.0016	-0.0049	0.0000
H$_2$S	$2b_1$	0.0017	-0.0013	-0.0014	0.0000
HCl	1π	0.0010	-0.0008	-0.0011	0.0000
		APMO/TOEP2 $\Sigma_{pp}^{e-,p+(2)}$			
LiH	1σ	0.0518	0.0000	-0.0003	0.0003
BH$_3$	$1e$	0.0828	-0.0014	-0.0015	0.0015
NH$_3$	$3a_1$	0.0142	-0.0030	-0.0022	0.0022
CH$_4$	$1t_2$	0.0831	-0.0029	-0.0027	0.0027
SiH$_4$	$1t_2$	0.0768	-0.0010	-0.0012	0.0012
H$_2$O	$1b_1$	0.0046	-0.0030	-0.0028	0.0027
HF	1π	0.0026	-0.0017	-0.0020	0.0020
H$_2$S	$2b_1$	0.0019	-0.0013	-0.0007	0.0006
HCl	1π	0.0011	-0.0008	-0.0005	0.0005

[a] See Ref.[66] for geometry details.

To explicitly quantify the nuclear-relaxation contribution, we have further decomposed $\Sigma_{pp}^{e-,p+(2)}$ into four terms, following a procedure analogous to that proposed by Pickup and Goscinski [8, 34]:

$$\Sigma_{pp}^{e-,p+(2)}(\omega_p^{e-}) =$$

$$\lambda^{e-}\lambda^{p+}\sum_{\substack{a^{e-}\\ a^{p+}}}\sum_{i^{p+}}\frac{|\langle p^{e-}i^{p+}|a^{e-}a^{p+}\rangle|^2}{\omega_p^{e-}+\epsilon_i^{p+}-\epsilon_a^{e-}-\epsilon_a^{p+}} + \lambda^{e-}\lambda^{p+}\sum_{i^{e-}\neq p^{e-}}\sum_{\substack{i^{p+}\\ a^{p+}}}\frac{|\langle p^{e-}a^{p+}|i^{e-}i^{p+}\rangle|^2 n_i^{e-}n_i^{p+}}{\omega_p^{e-}+\epsilon_a^{p+}-\epsilon_i^{e-}-\epsilon_i^{p+}}$$

$$+\,\lambda^{e-}\lambda^{p+}\sum_{\substack{i^{p+}\\ a^{p+}}}\frac{|\langle p^{e-}a^{p+}|p^{e-}i^{p+}\rangle|^2 n_i^{e-}n_i^{p+}}{\omega_p^{e-}+\epsilon_a^{p+}-\epsilon_i^{e-}-\epsilon_i^{p+}} + \lambda^{e-}\lambda^{p+}\sum_{\substack{i^{p+}\\ a^{p+}}}\frac{|\langle p^{e-}i^{p+}|p^{e-}a^{p+}\rangle|^2 (1-n_p^{e-})}{\omega_p^{e-}+\epsilon_i^{p+}-\epsilon_a^{e-}-\epsilon_a^{p+}} \qquad (5\text{-}1)$$

In the above equation, the first term is the lowest order pair proton-electron correlation term in the system containing N electrons; it is also known as the pair-removal correlation (PRM). The second term is an extra correlation arising from excitations of the type $\binom{i^{e-}\to p^{e-}}{i^{p+}\to a^{p+}}$ in the system containing $N-1$ electrons, and it is called pair-relaxation (PRX). The third term is the orbital relaxation term (ORX) which correspond to single excitations of the type $i^{e-}\to p^{e-}$. The fourth term is analogous to the third one, but it only appears when the transition operator method is employed. We call this term extra relaxation (ERX). We highlight here that the first and second terms contribute to proton-electron correlation, while the third and fourth terms contribute to proton-electron relaxation.

Table **5-6** reports the decomposition of $\Sigma_{pp}^{e-,p+(2)}$ into the contribution terms mentioned above. A detailed examination of these contributions reveals that: first, in those cases where $\Sigma_{pp}^{e-,p+(2)}$ has a significant value (more than 0.01 eV), most of the contribution comes from the pair removal term (PRM), which is a correlation term. Second, contributions from PRX, ORX and ERX (in the case of APMO/TOEP2) are always smaller than 0.01 eV. Third, the two relaxation terms, ORX and ERX, practically cancel out in APMO/TOEP2 calculations.

We observe that the contribution to total electron ionization energies of nuclear-electron relaxations terms is small (less than 0.01 eV) in the case of EP2 calculations and negligible for TOEP2. We also find that the largest effects on ionization energies come from zero order values. These observations clearly indicate that the electron ionization proccess described by propagator approaches based on APMO wavefunctions does not involve significant changes in nuclear wavefunctions; in other words, they correspond to electron ionizations with large Franck-Condon factors, which are nearly vertical.

Impact of NQE on electron ionization energies

Now we analyze the impact of NQE on the accuracy of calculated ionization energies. Results of tables **5-2** and **5-3** reveals that as observed for zero order values, ionization energies calculated with APMO propagator methods are smaller than those calculated with regular methods. As previously discussed, this is a consequence of reduction in nuclear-electron attraction when considering nuclei as quantum particles. As we will explain shortly, it can be also a consequence of including vibronic coupling.

We point out that for some molecules, such as CH_4 and SiH_4, regular propagator methods predict ionization energies that are much higher than the corresponding experimental values, as shown
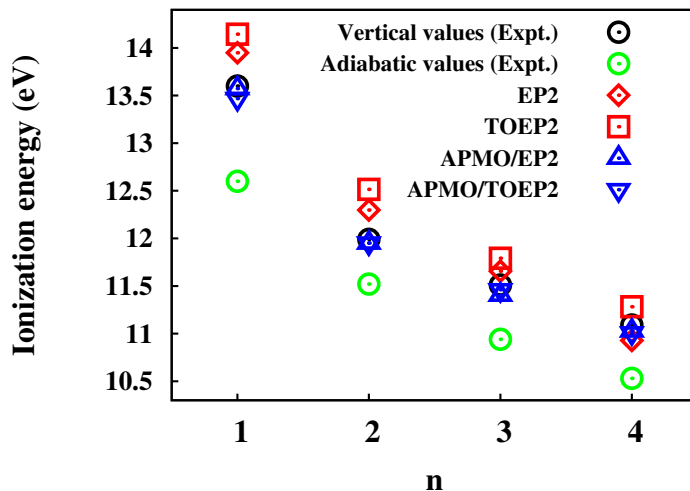
Figure **5-3**: Calculated ionization energies for n-alkanes (**n**=1-4). Electronic 6-31++G(d,p) and nuclear DZSPDN [26] basis set were used.

in tables **5-2** and **5-3**. BOA/TOEP2 predictions for CH_4 and SiH_4 are 0.5 and 0.3 eV larger, in average, than the first experimental vertical ionization energy, respectively. In the case of these two molecules, the ionized state experience a Jahn-Teller effect, leading to three possible symmetries in the ionized state. For the CH_4, for example, photoelectron spectra present three bands located at 13.6, 14.4 and 15.0 eV. Consequently, a regular electron propagator calculations, where nuclei are treated as classical particles in fixed positions, cannot properly predict the lowest ionization energy due to the lack of vibronic coupling, as demonstrated by Velasco et al. [67, 68].

However, propagator methods based on APMO wavefunctions predict ionization energies for CH_4 and SiH_4 that are closer to the first experimental ionization energy (13.6 eV), as evidenced in tables **5-2** and **5-3**. These results suggest that part of the vibronic coupling can be included considering hydrogen nuclei as quantum particles. We point out that by describing a hydrogen nuclei as charge distributions instead of point charges, fluctuations in the potential due to nuclear motion can be partially accounted for.

Inspired by methane results, we decided to investigate if hydrogen NQE are also observed in other alkanes. In figure **5-3** we plot the calculated ionization potentials at the regular and APMO methods for the first four n-alkanes. These results are contrasted with vertical and adiabatic experimental values. We observe that ionization energies calculated with APMO methods are again in better agreement with vertical ionization energies. We also find that the inclusion of hydrogen NQE with APMO approaches leads to remarkable improvements of the calculated vertical ionization energies. For instance, average deviations from experimental vertical values decrease from 0.39 eV to 0.06 eV with TOEP2 and APMO/TOEP2 approaches, respectively.

To gain a better insight into the origin of the improvement of the ionization energies of n-alkanes with the inclusion of NQE, we have performed the energy decomposition scheme of Eq. (3-10). Table **5-7** presents the Koopmans energies, ε_p^{e-}, the self-energy terms, $\Sigma_{pp}^{e-,e-(2)}$ and $\Sigma_{pp}^{e-,p+(2)}$, obtained from APMO/TOEP2 propagator calculations. We observe in all the systems conside-

red that zero order energy terms, ε_p^e, present the largest energy variations when TOEP2 and APMO/TOEP2 are compared, as previously shown. On the other hand, APMO/TOEP2 intraspecies terms, $\Sigma_{pp}^{e-,e-(2)}$, are very similar in magnitude while contribution from the interspecies term, $\Sigma_{pp}^{e-,p+(2)}$ are small. Although hydrogen NQE are mainly due to differences introduced at zero order, it is important to point out that propagator corrections,$\Sigma_{pp}^{e-,e-(2)}$ and $\Sigma_{pp}^{e-,p+(2)}$, are necessary to gain experimental acurracy. The results presented in this section reveal that the explicit description of the nuclear degrees of freedom may have a significant impact on the description of the electron ionization process.

Table **5-7**: Contributions to the APMO/TOEP2 corrected valence ionization energies (in eV) for n-alkanes (n=1-4). Electronic 6-31++G(d,p) and nuclear DZSPDN [26] basis sets were used. Electrons and hydrogenic nuclei were treated quantum mechanically.

Molecule	Orbital (p)	Only electrons [a]			APMO method [a]		
		ε_p^{e-}	$\Sigma_{pp}^{e-,e-(2)}$	$\Sigma_{pp}^{e-,p+(2)}$	ε_p^{e-}	$\Sigma_{pp}^{e-,e-(2)}$	$\Sigma_{pp}^{e-,p+(2)}$
CH_4	5	13.2802	0.8638	0.0000	12.4933	0.9000	0.0701
C_2H_6	9	12.1736	0.3425	0.0000	11.6141	0.2624	0.0752
C_3H_8	13	11.2983	0.4932	0.0000	10.9798	0.4491	0.0316
C_4H_{10}	17	10.8783	0.4038	0.0000	10.6017	0.3770	0.0288

[a] See Ref.[66] for geometry details.

5.2 Calculation of proton binding energies

The proton binding energy (PBE) can be defined as the energy change associated to the reaction $AH \longrightarrow A^- + H^+$, in other words, corresponds to the energy required to release a proton from a molecule, an extremely important value that defines the acid behaviour. Given that in an APMO calculation, protons, as other nuclei, can be treated quantum mecanically, the APMO-propagator allows the definition of a one proton Green function and the corresponding calculation of proton binding energies.

In Subsection 5.2.1, we compare experimental and theoretical APMO/HF and APMO/PP2 values of PBEs. APMO/HF and APMO/PP2 calculations were performed at the experimental geometries [66] with the aug-cc-pVTZ[63] electronic and 7s7p[24] nuclear basis sets using the LOWDIN program.

5.2.1 Influence of removing translational and rotational motions in PBEs calculation

We calculated the PBEs for a set of small A-X (X = H, D) molecules at the APMO/HF and APMO/P2 levels of theory and compared them with experimental values determined via Threshold Ion-Pair Production Spectroscopy (TIPPS) [69–74]. As in the case of electron ionization energies, we run calculations for the TRC, TF and TRF APMO wavefunctions.

Results summarized in Table **5-8** reveal that: 1) propagator corrections are very large. For instance,

Figure **5-4**: Isotope shift on proton binding energies calculated with APMO Koopmans and propagator approximations. Values in eV.
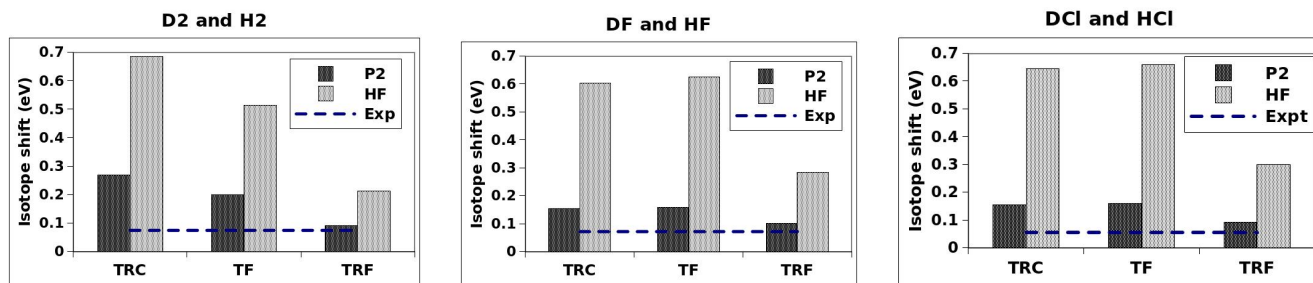
we observe average deviations from experimental results around 9 and 0.2 eV at the APMO/HF and APMO/P2 levels respectively. 2) predicted PBEs increases in the order TRC<TF<TRF. At the Koopmans level TRF predictions are worse than those of TF or TRC treatments, and slightly worse also in the case of P2 calculations. However, differences between TRF, TRC and TF propagator results are much smaller than those at Koopmans' level.

The increase of PBE for the TF and TRF treatments can be explained as a result of the localization experienced by the nuclear wavefunction when these corrections are included [75]. A more localized nuclear wavefunction interacts stronger with the electrons leading to larger values of PBEs. However, given that differences between TRF, TF and TRC treatments are small at the APMO/P2 level (0.01 and 0.02 eV) we conclude that the remotion of translational and rotational motions are not crucial to determine absolute values of PBEs.

Table **5-8**: Proton binding energies calculated using APMO Koopmans and propagator approximations. Values in eV.

Molecule	Koopmans result			Propagator P2			Expt.
	TRC	TF	TRF	TRC	TF	TRF	
HF	22.9513	23.0197	24.1554	16.0525	16.0699	16.2889	16.063
DF	23.555	23.6446	24.4389	16.2066	16.2281	16.3909	16.1347
HCl	23.2625	23.3038	24.5459	14.0099	14.0205	14.2751	14.4178
DCl	23.9078	23.9628	24.8449	14.1651	14.1788	14.3671	14.4729
HCN	23.8106	23.8581	24.0368	15.0779	15.0898	15.1335	15.1563
H_2S	25.2611	25.3020	26.1179	15.5365	15.5477	15.7392	15.1828
Average Deviation	8.55	8.61	9.45	0.21	0.20	0.22	

Instead, the inclusion of TRF corrections could become important to properly described isotope effects. Experimental data presented in Table **5-8** reveal that deuterated molecules present larger PBEs than their protonated counterparts. Figure **5-4** compares the magnitudes of the isotopic shifts on PBEs for H_2, HF and HCl molecules as calculated by APMO/HF and APMO/P2 approaches. As observed in the case of electron binding energies, the APMO approaches suceed on predicting the right trend of isotope effects, however only the TRF treatment provides results of the same magnitude of the experimental values, even when absolute values of PBEs predicted with the TRF

treatment are not better than those obtained with its TRC and TF counterparts.

In addition to the previous discussion, we anticipate that for calculations of PBEs in large systems, the effect of considering all nuclei as quantum particles could be neglect. Consequently, in the rest of this section, calculations where run treating hydrogen nuclei quantum mechanically and heavier nuclei as point charges. In the rest of this section we will see how this approach is enough to provide excellent predictions of proton binding energies and related properties.

5.2.2 Nature of the proton ionization process

To reveal the nature of the propagator correction for protons, we decomposed the self-energy term (Eq. (**??**)) into pair-removal correlation (PRM), pair-relaxation (PRX) and orbital relaxation (ORX), by following the procedure proposed by Pickup and Goscinski [8, 34]. For the inter-particle term we have:

$$
\begin{aligned}
\Sigma_{pp}^{p+,e-(2)}(\omega_P) =& \text{PRM} + \text{PRX} + \text{ORX} \\
=& \sum_A \sum_{i,a} \frac{|\langle Pi|Aa\rangle|^2}{\omega_P + \epsilon_i - \epsilon_A - \epsilon_a} + \sum_{I \neq P} \sum_{a,i} \frac{|\langle Pa|Ii\rangle|^2}{\omega_P + \epsilon_a - \epsilon_I - \epsilon_i} \\
& + \sum_{a,i} \frac{|\langle Pa|Pi\rangle|^2}{\omega_P + \epsilon_a - \epsilon_P - \epsilon_i}
\end{aligned}
\tag{5-2}
$$

The PRM and PRX terms are related to proton-electron correlation, while the ORX term is related to electron relaxation after proton release. For all the A-X systems considered in Table **5-9**, the PRX term becomes zero because there is only one occupied proton orbital and the intraspecies terms are zero because there is only one hydrogen nucleus present in each molecule.

For each of the molecular systems presented in Table **5-9** the magnitude of the ORX term is at least 50 times that of the PRM term. These results allow us to conclude that properly accounting for the relaxation of the electronic density is crucial for determining accurate PBEs. APMO/HF approach does not offer a quantitive description of the proton removal because Koopmans's approximation lacks relaxation effects. On the other hand, the APMO/PP2 approach recovers enough relaxation to provide an improved estimation of PBEs. This analysis show that the proton ionization process keep some characteristics of the ionization of internal electrons, where is well known that relaxation effects are predominant. Table **5-9** also includes PBEs calculated by the ΔSCF procedure [76] to estimate the relaxation effects at the APMO/HF level (RXL). Comparison of the ORX and RXL terms reveals that their magnitudes are similar, suggesting that most of the relaxation effects come from relaxation at the APMO/HF level [6, 8].

5.3 Application of PBEs calculation

In subsection 5.3.1, we report calculated PBEs for a set of organic molecules and compare them with reported PAs. The PA of molecule A was calculated by optimizing the molecular structure with an extra hydrogen atom, HA$^+$, employing the VWN [78] functional and the 6-311++G(2d,2p) [79–82] electronic basis set and the GEN-A2* [83, 84] auxiliary basis set. Optimizations were performed

Table **5-9**:   Comparison between experimental and predicted PBEs calculated with APMO/HF and APMO/PP2 methods and decomposition analysis for $\Sigma_{PP}^{\alpha,\beta(2)}(\omega_P^\alpha)$ (in eV) for a set of small molecules. Electronic aug-cc-pVTZ [63] and protonic 7s7p [24] basis sets were used.

Molecule	Exp[a]	KT [c]	ΔSCF Value	ΔSCF RXL	PP2[b]	$\Sigma_{PP}^{p^+,e^-(2)}$ PRM	$\Sigma_{PP}^{p^+,e^-(2)}$ ORX	$\Sigma_{PP}^{p^+,e^-(2)}$ Total
DF	16.1347	23.3426	15.8203	-7.5223	15.8705	0.1004	-7.5725	-7.4721
HF	16.0630	22.7339	15.5148	-7.2191	15.6708	0.1529	-7.2161	-7.0632
HCN	15.1563	23.6996	14.2678	-9.4318	14.8340	0.1566	-9.0222	-8.8656
DCl	14.4729	23.8216	13.7753	-10.0463	13.9819	0.0950	-9.9347	-9.8397
HCl	14.4178	23.1572	13.4825	-9.6747	13.7764	0.1488	-9.5295	-9.3808
$|\mathbf{\Delta}|$[d]		8.1020	0.6768		0.4222			

[a] Determined by TIPPS technique[73, 74, 77].   [b] APMO/PP2 calculations.

[c] Koopmans (APMO/HF) values. [d]$|\mathbf{\Delta}|$: Average deviation from experiment

using the deMon2k[85] software package. APMO/PP2 calculations were performed with the 6-311G [79, 80] electronic and DZSPDN[26] nuclear basis sets using the LOWDIN program. The lowest PBE value for each molecule was reported and compared with the experimental PA.

In subsection 5.3.2, we study the solvation of a proton in water. Structures of the type $(H_2O)_nH^+$, with $n = 1 - 7$ were modeled. A stochastic algorithm was employed to explore the potential energy surface of these clusters and generate several cluster candidate structures. Candidate structures underwent further optimization with the PW91 [86] density functional employing the 6-31++G** [87, 88] orbital basis set and the GEN-A2* [83, 84] auxiliary basis set, using the deMon2k[85] software.

In subsection 5.3.3, we estimate the proton hydration free energy. Total energies and PBEs of $(H_2O)_nH^+$ were calculated with APMO/HF and APMO/PP2 methods, respectively, employing 6-311G [79, 80] electronic and DZSPDN nuclear basis set [26], using the LOWDIN program [51]. After choosing the lowest PBE for each structure, the solvation energy of the proton was calculated as a Boltzmann average of all isomeric structures [89, 90].

5.3.1 Prediction of proton affinities

The proton affinity (PA) of a species A is an intrinsic acidity measure. It is defined as the negative of the enthalpy change of the gas-phase reaction [91]:

$$A + H^+ \rightarrow AH^+ \quad PA(A) = -\Delta H = -\Delta E(T) + RT, \qquad (5-3)$$
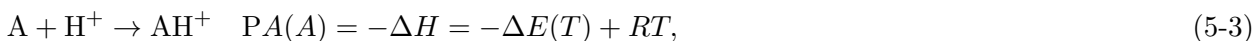
here R is the universal gas constant, T is the absolute temperature and ΔE is the energy difference between the AH^+ and the molecule A. In the case of a nonlinear polyatomic molecules, ΔE can be approximated in terms of translational, rotational, vibrational and electronic thermodinamical

contributions:

$$\Delta E(T) = \Delta E_{rot}(T) + \Delta E_{trans}(T) + \Delta E_{vib}(T) + \Delta E_{ele}. \tag{5-4}$$

In an ideal gas approximation, $\Delta E_{trans}(T) = -\frac{3}{2}RT$. Values of $\Delta E_{rot}(T)$ becomes negligible as shown in [92] given that $\Delta E_{rot,AH^+}(T) \approx \Delta E_{rot,A}(T)$ and $\Delta E_{rot,H^+}(T) = 0$. After these considerations, the PA expression becomes:

$$PA = -\Delta E_{ele} - \Delta E_{vib} + \frac{5}{2}RT. \tag{5-5}$$

In APMO proton propagator calculations, PBEs account for changes due to proton release. In our calculations electrons and hydrogen nuclei are treated quantum mechanically, consequently, PBEs include ΔE_{ele} and part of ΔE_{vib}[93] (relaxation of quantum hydrogen atoms). The contributions to $\Delta E_{vib}(T)$ associated to the motion of classical nuclei is assumed to be close to zero, i.e., $\Delta E_{vib,A}(T) \approx \Delta E_{vib,HA^+}(T)$. Proton affinities for standard conditions of temperature and pressure (298.15 K and 1 bar) are approximated as:

$$PA \approx PBE(AH^+) \ + \ 0.064 \ eV \tag{5-6}$$

where $PBE(AH^+)$ is the proton binding energy of the species AH^+.

Table **5-10**: Comparison between experimental and predicted proton affinities (in eV) using APMO/HF and APMO/PP2 methods (Eq.5-6) for a set of organic and inorganic molecules. Electronic 6-311G and protonic DZSPDN basis sets were employed [a].

Molecule	Proton affinity		
	Exp[b]	KT[c]	P2[d]
Amines			
NH_3	8.85	16.68	8.79
CH_3NH_2	9.32	17.54	9.31
$CH_3CH_2NH_2$	9.45	17.83	9.48
$CH_3CH_2CH_2NH_2$	9.51	17.89	9.51
$(CH_3)_2NH$	9.63	18.21	9.64
$(CH_3)_3N$	9.84	18.68	9.82
$|\mathbf{\Delta}|$[e]		8.37	0.02
Aromatic			
$C_6H_5NH_2$	9.15	17.78	9.31
$C_6H_5COO^-$	14.75	22.97	15.07
$C_6H_5O^-$	15.24	23.70	15.53
$|\mathbf{\Delta}|$[e]		8.44	0.26
Inorganic			
HS^-	15.31	24.24	14.82
CN^-	15.31	23.60	14.80
NO_2^-	14.75	22.72	14.77
$|\mathbf{\Delta}|$[e]		8.40	0.34

Carboxylic Acids			
HCOO$^-$	14.97	22.66	14.86
CH$_3$COO$^-$	15.11	23.04	15.22
CH$_3$CH$_2$COO$^-$	15.07	23.04	15.17
CH$_3$(CH$_2$)$_2$COO$^-$	15.03	23.09	15.23
CH$_3$(CH$_2$)$_3$COO$^-$	15.01	23.09	15.24
CH$_2$FCOO$^-$	14.71	22.41	14.65
CHF$_2$COO$^-$	14.32	21.92	14.19
CF$_3$COO$^-$	13.99	21.54	13.85
ClCH$_2$COO$^-$	14.58	22.43	14.63
Cl(CH$_2$)$_2$COO$^-$	14.78	22.53	14.68
CH$_3$COCOO$^-$	14.46	22.40	14.60
$|\mathbf{\Delta}|^e$		7.83	0.12
$|\mathbf{\Delta}|^e$ Total		8.12	0.14

^{a} Geometries optimized at VWN/6-311++G(2d,2p) level.

 Regular electronic structure calculation.

^{b}References [94–98]

^{c} APMO/HF proton affinities

^{d} APMO/PP2 proton affinities

$^e|\mathbf{\Delta}|$: Average absolute difference.

In Table **5-10** we contrast the calculated PAs using APMO methods (employing Eq. (5-6)) and experimental values[94–98] for a set of inorganic and organic molecules. The reported PAs are associated to the proton with the lowest PBE, highlighted with green circles in Figures **5-5**, **5-6**, **5-7**, and **5-8**. We observe in Table **5-10** that the total average deviation from experiment for APMO/PP2 is 0.14 eV (3.23 kcal/mol), which is one order of magnitude smaller than the average deviation with the APMO/HF method. Table **5-10** also shows partial average deviations calculated for molecules with the same functional group. We observe that predictions with the APMO/PP2 method for amines and carboxylic acids are in excellent agreement with experiment, with average deviations of 0.02 (0.46) and 0.12 (2.77) eV (kcal/mol). Figures **5-5** and **5-6** compare observed experimental trends for PAs associated to the homologous series of amines and carboxylic acids with those calculated with APMO methods. We observe that both APMO/HF and APMO/PP2 reproduce the decreasing trend in the acidity of the ammonium ions (associated to to the increasing trend in basicity of amines) and the decreasing trend in the acidity of carboxylic acids. However, only APMO/PP2 produces quantitatively accurate results.

For aromatic and inorganic molecules we observe larger deviations. This can be attributed to large nuclear relaxation effects that are not completely recovered at the APMO/PP2 level. Therefore, higher order proton propagators are required for more accurate calculations of the PAs of these systems.
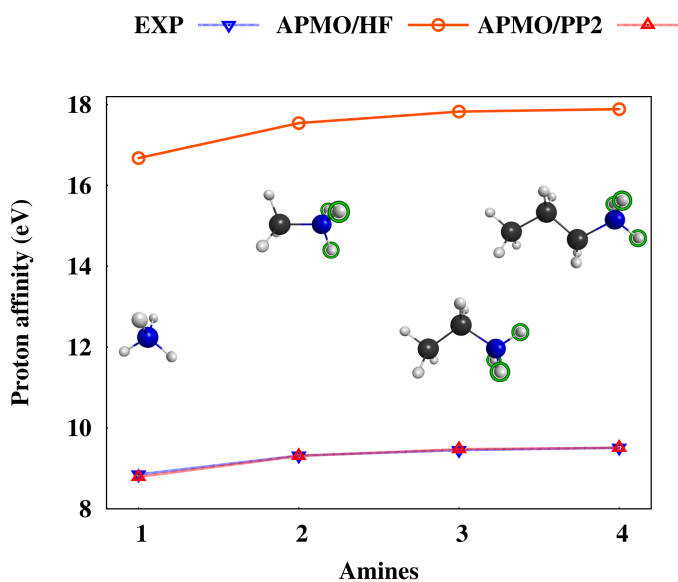
Figure **5-5**: Proton affinities for primary amines (in kcal/mol), calculated at APMO/HF and APMO/PP2 levels. Electronic 6-311G and protonic DZSPDN basis sets were used.
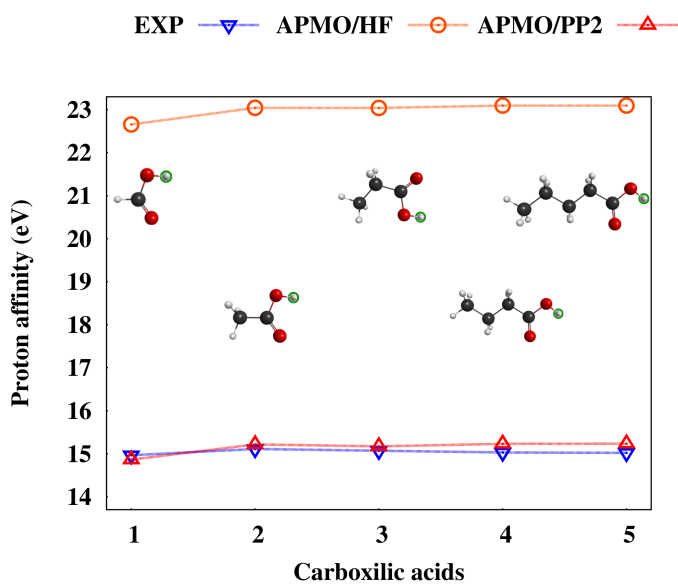
Figure **5-6**: Proton affinities for terminal carboxylic acids (in kcal/mol), calculated at APMO/HF and APMO/PP2 level. Electronic 6-311G and protonic DZSPDN basis sets were used.
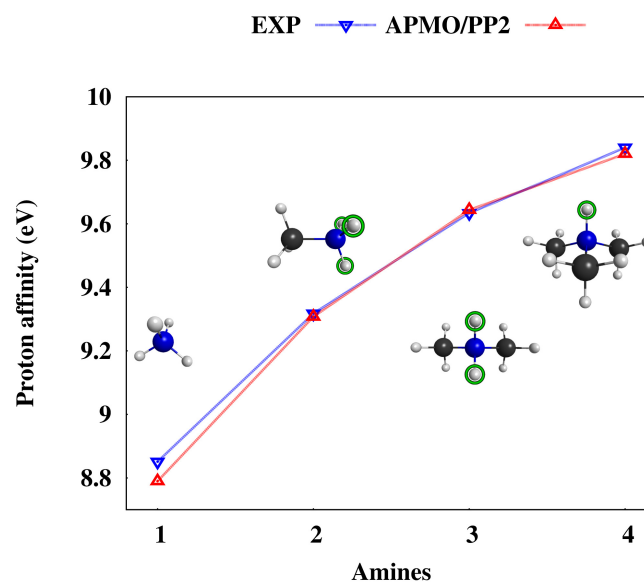
Figure **5-7**: Proton affinities for substituted amines (in kcal/mol), calculated at APMO/PP2 level. Electronic 6-311G and protonic DZSPDN basis sets were used.
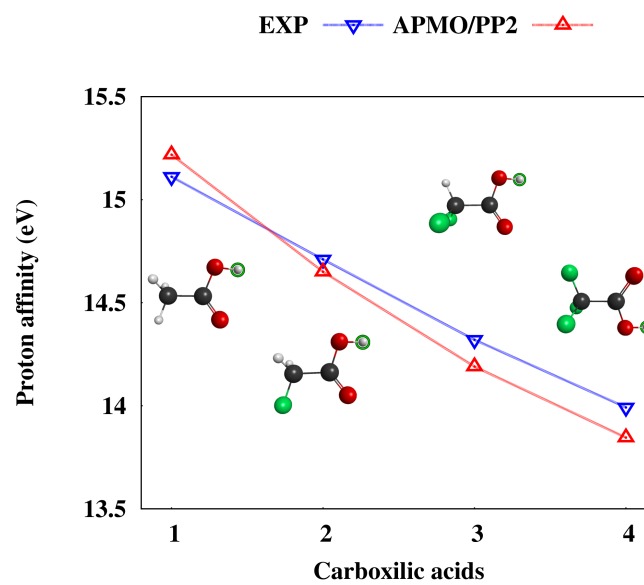
Figure **5-8**: Proton affinities for substituted cloro-acetic acids (in kcal/mol), calculated at APMO/PP2 level. Electronic 6-311G and protonic DZSPDN basis sets were used.

Despite the observed limitations, APMO/PP2 calculations are capable of providing reliable predictions of PAs, reproducing chemical trends in acidity. For instance, in Figures **5-7** and **5-8** we present calculated PAs for series of substituted organic compounds. We observe in Figure **5-7** how APMO/PP2 calculations properly predict differences in acidity between primary, secondary and ternary amine ions. Inductive effects in acetic acid are also well described, as shown in Figure **5-8**.

5.3.2 Analysis of protonated water structure employing PBEs

A PBE, when defined as a measure of the energy required to extract a selected proton from a molecule, can be employed to analyze the propensity of a proton to be released. This feature is exploited here to study of proton hydration.

To that aim, we calculated total energies and PBEs for a set of protonated water clusters, $(H_2O)_nH^+$, employing the APMO/HF and APMO/PP2 approaches. Geometries for clusters containing $n = 2 - 7$ water molecules were generated by employing a stochastic search algorithm. A total of 10, 20, 11, 26, 16 and 18 structures were generated for $n = 2 - 7$, respectively. Additional geometries, reported by Hodges et al[99] were also considered in this analysis.

Of all possible geometries generated for each n, we analyzed only those presenting the Lowest Total Energy (LTE) and the Lowest Proton Binding Energy (LPBE). LTE structures are of special importance because they are expected to resemble the most stable geometrical configuration of a hydrated proton in solution whereas LPBE structures are related to geometrical configurations where protons can be more easily donated. The geometries of LTE and LPBE are shown in Table **5-11**.

We observe that the LTE and LPBE structures for $n = 1$ are the same. Structures for $n = 2, 3$ are very similar, presenting only small variations in dihedral angles between water molecules. For $n = 4$ the LTE structure is the $H_9O_4^+$ eigencation, where the H_3O^+ cation is linked to three water molecules through single hydrogen bonds. This structure has been already identified as the most likely solvation structure for the hydrated proton [100]. In constrast, the LPBE structure presents a four–member ring comprising an H_3O^+ cation and three water molecules, one of them linked to the other two through a two–donor one acceptor hydrogen bond. Similar ring configurations have been observed in pure water clusters [101–103].

At this stage large differences in the distribution of PBEs are observed. As shown in **5-12**, for structures with $n = 4$, differences in PBEs between all the protons of the LTE structures do not exceed 1.2 kcal/mol . These results indicate that in the case of the $H_9O_4^+$ eigencation, protons are already equivalent. This effect can be associated to "proton resonances" observed in molecular dynamics simulations [100]. In contrast, differences in the PBEs for the LPBE structures reach up to 16.4 kcal/mol and protons are consequently not equivalent. Protons associated to the double acceptor water molecule present the smallest PBEs for $n \geq 4$, as shown in Table **5-11**. This finding indicates that proton detachment on the LPBE structure produces a hydroxyl anion, that eventually leads to a ring structure where a H_3O^+ and OH^- coexist.

For $n > 4$, LTE structures present a $H_9O_4^+$ eigencation surrounded by water molecules forming single hydrogen bonds. For $n = 7$, protons in the water molecules attached to the $H_9O_4^+$ cation have the smallest PBEs and are expected to be more reactive. For $n > 4$, LPBE structures maintain the features of the LPBE with $n = 4$, exhibiting ring structures composed by a H_3O^+ cation and

water molecules. As for $n = 4$, the ring comprises a double hydrogen-bond acceptor water molecule that has the protons with the smallest PBE.

Table **5-12** also shows differences in total energies (DTE) and differences in lowest PBEs (DPBE) between LTE and LPBE structures, revealing that DTE are always smaller than DPBE for $n > 2$. This fact suggests that although LTE and LPBE structures have similar total energies and can coexist in gas phase and even in liquid water, the LPBE configurations are considerably more reactive towards proton transfer than LTE structures.

In summary, the study of PBEs and total energies of protonated water clusters allows us to conclude that protons with the largest susceptibility to be released, present in LPBE structures, are not those belonging to H_3O^+ but those in double hydrogen-bond acceptor water molecules. We also point out that even when LTE and LPBE structures have similar total energies, they have different reactivities towards proton donation.

5.3.3 Estimation of proton hydration free energy

The proton hydration free energy, $\Delta G_{hyd}(H^+)$ is required for calculating acidity constants in water. [104–108]. Regular approaches for estimating $\Delta G_{hyd}(H^+)$ usually involve taking the limit of the difference between free energies of neutral and protonated n-water clusters as n increases[92, 108, 109].

Alternatively, we propose to utilize our propagator approach to estimate proton hydration energies by considering the PBEs calculated for the set of protonated water clusters of the previous section. The proton hydration process can be associated to the following reaction:

$$H^+_{(gas)} \rightarrow H^+_{(aq)} \tag{5-7}$$

As a first step, this process can be approximated by the reaction:

$$H^+_{(gas)} + (H_2O)_n \rightarrow H(H_2O)^+_n \tag{5-8}$$

Enthalpies of Eq. (5-8) are calculated using Eq. (5-3) and Eq. (5-6). The entropy change is obtained using the equation:

$$\Delta S = S_{H(H_2O)^+_n} - S_{(H_2O)_n} - S_{H^+_{(gas)}}, \tag{5-9}$$

where ΔS includes the entropy contribution of the free proton, $S(H^+)$, and the difference in entropy of the structures, $S_{H(H_2O)^+_n} - S_{(H_2O)_n}$. Calculation of the proton entropy change using the Sakur-Tetrode equation[92, 104, 110] yields the entropy factor, $TS_{H^+_{(gas)}} = 7.76$ kcal/mol at standard conditions of temperature and pressure (STD). Assuming that $S_{H(H_2O)^+_n} - S_{(H_2O)_n}$ is negligible, the change in entropy and the change in free energy can be approximated as:
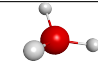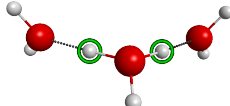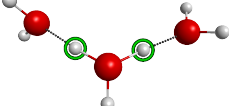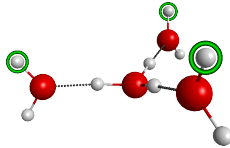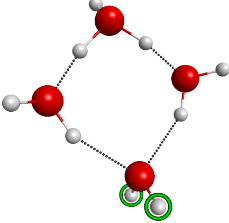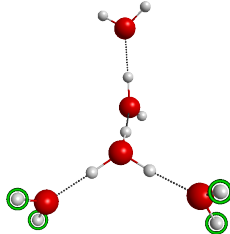
$$T\Delta S = -7.76 \text{kcal/mol} \tag{5-10}$$
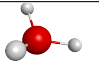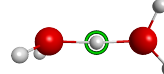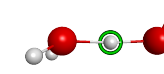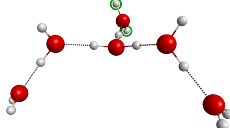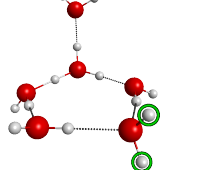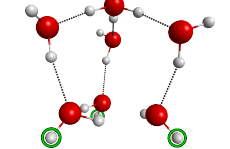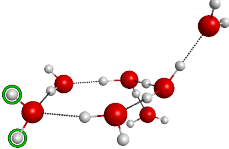
$$\Delta G = \Delta H - T\Delta S \tag{5-11}$$

$$\Delta G \approx \text{PBE} - \frac{5}{2}RT - (-7.76 \text{kcal/mol}) \tag{5-12}$$

$$\Delta G \approx \text{PBE} + 6.28 \text{kcal/mol} \tag{5-13}$$

Table **5-11**: Protonated water clusters with the Lowest Total Energy (LTE) and the Lowest
Proton Binding Energy (LPBE) for $n = 1 - 7$. Protons with the lowest PBEs
are highlighted with green circles.

n^{a}	LTE^{b}	LPBE^{c}
1		
2		
3		
4		
5		
6		
7		

^{a} Number of water molecules

^{b} Structure with the lowest total energy

^{c} Structure with the lowest proton binding energy

Table **5-12**: Lowest and highest proton binding energies (PBEs) calculated for protonated water clusters with the Lowest Total Energy (LTE) and the Lowest Proton Binding Energy (LPBE) for $n = 1 - 7$. Differences in total energies and lowest PBEs between LTE and LPBE structures are also included. The APMO/PP2 method, with electronic 6-311G and protonic DZSPDN basis sets, was used. All values in kcal/mol.

n^a	LTE^b		LPBE^c		DTE^d	DPBE^e
	LPBE^f	HPBE^g	LPBE^f	HPBE^g		
1	156.1	156.1	156.1	156.1	0.00	0.00
2	205.4	220.2	204.8	219.8	0.30	0.68
3	246.0	256.9	242.9	256.0	0.67	3.02
4	274.4	275.6	252.3	268.7	4.53	22.06
5	284.2	300.5	262.1	289.9	2.96	22.10
6	289.9	318.6	261.6	312.0	5.49	28.30
7	280.1	298.0	267.6	324.1	8.91	12.46

^{a} Number of water molecules.

^{b} Structure with the Lowest total energy.

^{c} Structure with the Lowest proton binding energy.

^{d} Difference in total energy between LTE and LPBE structures.

^{e} Difference in lowest PBE between LTE and LPBE structures.

^{f} Lowest proton binding energy in the structure.

^{g} Highest proton binding energy in the structure.

Table **5-13**: Thermodynamic properties: ΔE, ΔH, $T\Delta S$ and ΔG (in kcal/mol) calculated for protonated water clusters $n = 1 - 7$ employing the APMO/PP2 method. Electronic 6-311G and protonic DZSPDN basis sets were used.

n^a	N^b	PBE^c	ΔE	ΔH	$T\Delta S$	ΔG
1	1	156.1	-157.0	-157.6	-7.76	-149.8
2	10	205.0	-205.9	-206.5	-7.76	-198.7
3	20	243.9	-244.8	-245.4	-7.76	-237.6
4	11	256.7	-257.6	-258.2	-7.76	-250.4
5	26	258.9	-259.8	-260.4	-7.76	-252.6
6	18	266.7	-267.6	-268.2	-7.76	-260.4
7	20	276.5	-277.4	-278.0	-7.76	-270.2

[a] Number of water molecules in cluster.

[b] Number of structures found.

[c] APMO/PP2 results

Average ΔEs were calculated using Boltzmann factors that are based on the total energies of the cation and neutral clusters. The Boltzmann-weighted average energy of the cationic cluster is subtracted from its neutral counterpart to produce PBEs for a given n.

Thermodynamic properties calculated at the APMO/PP2 level using the previous equations are presented in Table **5-13**. Values of ΔG as a function of n are shown in Figure **5-9**; results at APMO/HF level were also included for comparison.

An analysis of our results reveals that trends in ΔG calculated at APMO/HF and APMO/PP2 level are similar, decreasing as n increases and presenting a smooth slope for $n > 3$. However, only the APMO/PP2 approach reproduces quantitatively proton hydration free energies, as evidenced by values of ΔG for $n = 6 - 7$ (-260.4 kcal/mol and -270.2 kcal/mol, respectively). These estimations are in excellent agreement with experimental and calculated proton hydration energies quoted in literature [92, 107–109, 111, 112].

We suggest that a faster convergence on ΔG with respect to n could be achieved by including long–range solvent effects, as shown by other authors [92, 108, 109]. Nevertheless, the results presented here demonstrate that the proton propagator is a promising tool for predicting acid/base properties such as the proton hydration free energy.
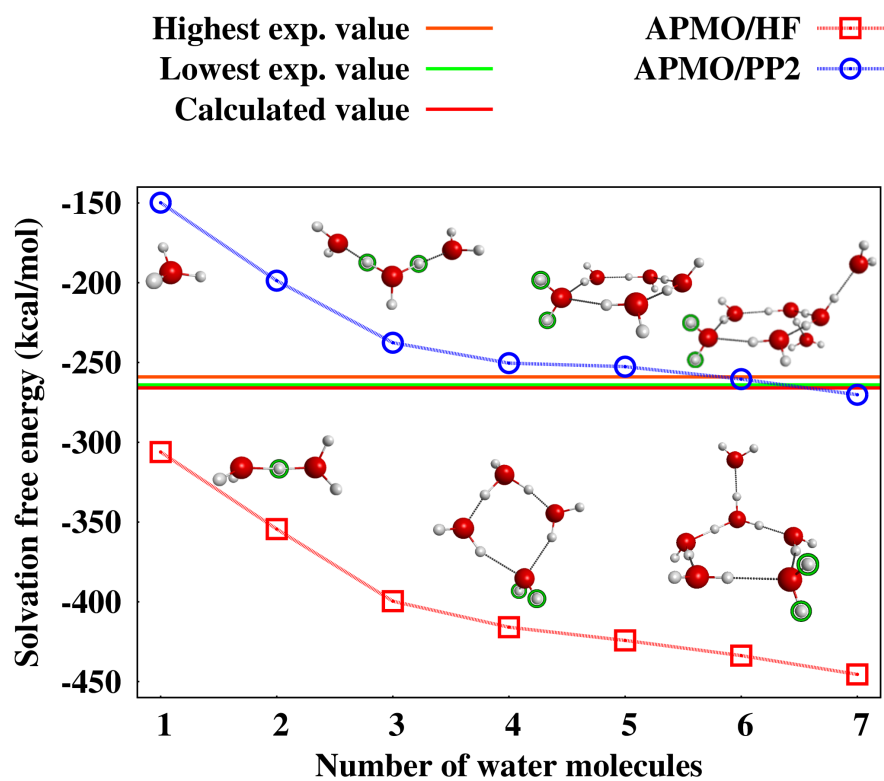
Figure **5-9**: Proton solvation energy free energies (in kcal/mol) calculated for protonated water clusters, ΔG, as a function of n, employing the APMO/PP2 method. Electronic 6-311G and protonic DZSPDN basis sets were used. Values quoted in literature [92, 108, 109, 111, 112] are included for comparison.

6 Conclusions and perspectives

In this work we presented an extension of the propagator theory for the APMO approach. We derived expressions for the second order APMO/PT using the APMO/HF wavefunction as reference state and implemented these equations in the LOWDIN program. We performed sample calculations with the APMO/PT method on a set of atoms and small molecules to determine its accuracy and performance.

As a first application of our method we studied NQE and isotope effects on molecular electronic ionization calculations. In this case, we determined the importance of substracting the translational and rotational contamination. Our results allowed us to conclude that the properly study of electron ionization energies within the APMO framework requires the inclusion of higher orders of nuclear electron correlations, specially to calculate inner ionization energies. We also found that calculation of electron ionization energies using APMO/PT could give insights into the Jahn-Teller effects on photoelectron spectra experienced by some systems such as methane. Despite of the limitation of second order approximations, it was also shown that the APMO/P2 method suceeds on describing isotope effects on electron ionization energies, especially when the rotational and translational contaminations are removed.

As a second applications we utilized the APMO/PT method to calculate PBEs and PAs for a set of inorganic and organic molecules. Our results revealed that the APMO/P2 approximation suffices to quantitatively reproduce experimental trends in PBE with an average deviation of less than 0.22 eV, with small influence of TRF and TF corrections. We also estimated proton affinities with an average deviation of 0.14 eV and the proton hydration free energy using APMO/P2 with a resulting value of -270.2 kcal/mol, in agreement with results reported in literature. The results presented so far allow us to conclude that the proton propagator is a promising tool for calculating and understanding acid/base chemistry, with the PBE as a reactivity index that gives information of the relative acidity of protons in a molecule.

We believe that the proposed methodology opens up a wide range of applications in molecular ionization studies of systems containing electrons, nuclei and other exotic particles such as muons and positrons. We are currently exploring the application of our approach to study positron binding energies and extending our method to renormalized non-diagonal versions of second and third order with the aim of achieving higher accuracy in our calculations. Future work also will be devoted to estimation of pK_a values by combining our method with implicit solvent models and calculation of PAs for large systems using a divide and conquer approach [113].

Bibliography

[1] T. Daniel Crawford, Steven S. Wesolowski, Edward F. Valeev, Rollin A. King, Matthew L. Leininger, and Henry F. Schaefer III. *The Past, Present, and Future of Quantum Chemistry*, pages 219–246. Wiley-VCH Verlag GmbH, 2007.

[2] Richard A Friesner. Ab initio quantum chemistry: methodology and applications. *PNAS*, 102(19):6648–6653, 2005.

[3] Christopher J Barden, Henry F Schaefer, et al. Quantum chemistry in the 21 st century. *Pure Appl. Chem.*, 72(8):1405–1423, 2000.

[4] Peter Politzer and Fakher Abu-Awwad. A comparative analysis of hartree-fock and kohn-sham orbital energies. *Theor. Chem. Acc.*, 99(2):83–87, 1998.

[5] Sebastien Hamel, Patrick Duffy, Mark E Casida, and Dennis R Salahub. Kohn–sham orbitals and orbital energies: fictitious constructs but good approximations all the same. *J. Electron Spectrosc. Relat. Phenom.*, 123(2):345–363, 2002.

[6] J. Linderberg and Y. Öhrn. *Propagators in Quantum Chemistry, 2nd ed.* Wiley-Interscience, Hoboken, NJ, 2004.

[7] P. Jørgensen and J. Simons. *Second Quantization-Based Methods in Quantum Chemistry, 1st ed.* Academic, New York, NY, 1981.

[8] B.T. Pickup and O. Goscinski. Direct calculation of ionization energies. *Mol. Phys.*, 26(4): 1013–1035, 1973. doi: 10.1080/00268977300102261.

[9] L. S. Cederbaum. One–body Green's function for atoms and molecules: theory and application. *J. Phys. B.*, 8:290–303, 1975.

[10] L. S. Cederbaum and W. Domcke. *Theoretical Aspects of Ionization Potentials and Photo-electron Spectroscopy: A Green's Function Approach*, pages 205–344. John Wiley & Sons, Inc., 1977. ISBN 9780470142554. doi: 10.1002/9780470142554.ch4.

[11] Michael F. Herman, Karl F. Freed, and D. L. Yeager. *Analysis and Evaluation of Ionization Potentials, Electron Affinities, and Excitation Energies by the Equations of Motion?Green's Function Method*, pages 1–69. John Wiley & Sons, Inc., 2007. ISBN 9780470142684. doi: 10.1002/9780470142684.ch1.

[12] Michael F. Herman, Karl F. Freed, and D. L. Yeager. *Analysis and Evaluation of Ionization Potentials, Electron Affinities, and Excitation Energies by the Equations of Motion–Green's Function Method*, pages 1–69. Advances in Chemical Physics, 1981.

[13] W. von Niessen, J. Schirmer, and L.S. Cederbaum. Computational methods for the one-particle green's function. *Computer Physics Reports*, 1(2):57 – 125, 1984. doi: 10.1016/0167-7977(84)90002-9.

[14] M. Ohno, V. G. Zakrzewski, J. V. Ortiz, and W. von Niessen. Theoretical study of the valence ionization energies and electron affinities of linear c[sub 2n + 1] (n = 1–6) clusters. *J. Chem. Phys.*, 106(8):3258–3269, 1997. doi: 10.1063/1.473064.

[15] J. Schirmer, L. S. Cederbaum, and O. Walter. New approach to the one–particle Green's function for finite Fermi systems. *Phys. Rev. A*, 28:1237, 1983.

[16] V. G. Zakrzewski, O. Dolgounitcheva, and J. V. Ortiz. Ionization energies of anthracene, phenanthrene, and naphthacene. *J. Chem. Phys.*, 105(19):8748–8753, 1996. doi: 10.1063/1.472654. URL http://link.aip.org/link/?JCP/105/8748/1.

[17] JV Ortiz. Toward an exact one-electron picture of chemical bonding. *Adv. Quantum Chem.*, 35:33–52, 1999.

[18] J.V. Ortiz. Electron propagator theory: an approach to prediction and interpretation in quantum chemistry. *WIREs Comput. Mol. Sci.*, 3:123–142, 2012.

[19] YC Jean, PE Mallon, and DM Schrader. *Principles and applications of positron & positronium chemistry*. World Scientific Singapore, 2003.

[20] David C Walker. *Muon and muonium chemistry*. Cambridge University Press, 1983.

[21] S.A. González, N.F. Aguirre, and A. Reyes. Theoretical investigation of isotope effects: The any-particle molecular orbital code. *Int. J. Quantum Chem.*, 108(10):1742–1749, 2008.

[22] M. Tachikawa, K. Mori, H. Nakai, and K. Iguchi. An extension of ab initio molecular orbital theory to nuclear motion. *Chem. Phys. Lett.*, 290(4-6):437–442, 1998.

[23] S.P. Webb, T. Iordanov, and S. Hammes-Schiffer. Multiconfigurational nuclear-electronic orbital approach: Incorporation of nuclear quantum effects in electronic structure calculations. *J. Chem. Phys.*, 117:4106, 2002.

[24] H. Nakai. Simultaneous determination of nuclear and electronic wave functions without Born–Oppenheimer approximation: Ab initio NO+ MO/HF theory. *Int. J. Quantum Chem.*, 86(6):511–517, 2002.

[25] H. Nakai and K. Sodeyama. Many-body effects in nonadiabatic molecular theory for simultaneous determination of nuclear and electronic wave functions: Ab initio NOMO-MBPT and CC methods. *J. Chem. Phys.*, 118:1119, 2003.

[26] A. Reyes, M.V. Pak, and S. Hammes-Schiffer. Investigation of isotope effects with the nuclear-electronic orbital approach. *J. Chem. Phys.*, 123:064104, 2005.

[27] H. Nakai. Nuclear orbital plus molecular orbital theory: Simultaneous determination of nuclear and electronic wave functions without Born–Oppenheimer approximation. *Int. J. Quantum Chem.*, 107(14):2849–2869, 2007.

[28] H. Nakai, Y. Ikabata, Y. Tsukamoto, Y. Imamura, K. Miyamoto, and M. Hoshino. Isotope effect in dihydrogen-bonded systems: application of the analytical energy gradient method in the nuclear orbital plus molecular orbital theory. *Mol. Phys.*, 105(19):2649–2657, 2007. ISSN 0026-8976.

[29] P.E. Adamson, X.F. Duan, L.W. Burggraf, M.V. Pak, C. Swalina, and S. Hammes-Schiffer. Modeling positrons in molecular electronic structure calculations with the nuclear-electronic orbital method. *J. Phys. Chem. A*, 112(6):1346–1351, 2008.

[30] T. Ishimoto, M. Tachikawa, and U. Nagashima. Review of multicomponent molecular orbital method for direct treatment of nuclear quantum effect. *Int. J. Quantum Chem.*, 109(12): 2677–2694, 2009. ISSN 1097-461X.

[31] T. Udagawa and M. Tachikawa. *Multi-Component Molecular Orbital Theory*. Nova Science Publishers, New York, 2009.

[32] S.A. González and A. Reyes. Nuclear quantum effects on the He2H+ complex with the nuclear molecular orbital approach. *Int. J. Quantum Chem.*, 110(3):689–696, 2010.

[33] Félix Moncada, Daniel Cruz, and Andrés Reyes. Muonic alchemy: Transmuting elements with the inclusion of negative muons. *Chem. Phys. Lett.*, 539:209–213, 2012.

[34] Attila Szabo and Neil S. Ostlund. *Modern Quantum Chemistry: Introduction to Advanced Electronic Structure Theory*. Dover Publications, New York, 1996.

[35] J. Romero, E. Posada, R. Flores-Moreno, and A. Reyes. A generalized any particle propagator theory: Assessment of nuclear quantum effects on electron propagator calculations. *J. Chem. Phys.*, 137(7):074105, 2012.

[36] M. Müller and L. S. Cederbaum. Many-body theory of composite electronic-positronic systems. *Phys. Rev. A*, 42:170–183, 1990.

[37] M. Hoshino and H. Nakai. Elimination of translational and rotational motions in nuclear orbital plus molecular orbital theory: Application of Møller-Pleßet perturbation theory. *J. Chem. Phys.*, 124:194110, 2006.

[38] C. Møller and M. S. Plesset. *Phys. Rev.*, 46:618–622, 1934.

[39] Per-Olov Löwdin. Studies in perturbation theory. ix. connection between various approaches in the recent development—evaluation of upper bounds to energy eigenvalues in schr[o-umlaut]dinger's perturbation theory. *J. Math. Phys*, 6(8):1341–1353, 1965. doi: 10.1063/1.1704781.

[40] Hiromi Nakai, Minoru Hoshino, Kaito Miyamoto, and Shiaki Hyodo. Elimination of translational and rotational motions in nuclear orbital plus molecular orbital theory. *J. Chem. Phys.*, 122(16):164101–164101, 2005.

[41] Kaito Miyamoto, Minoru Hoshino, and Hiromi Nakai. Elimination of translational and rotational motions in nuclear orbital plus molecular orbital theory: Contribution of the first-order rovibration coupling. *J. Chem. Theory Comput.*, 2(6):1544–1550, 2006.

[42] Per-Olov Löwdin. Studies in perturbation theory. x. lower bounds to energy eigenvalues in perturbation-theory ground state. *Phys. Rev.*, 139:A357–A372, Jul 1965. doi: 10.1103/PhysRev.139.A357.

[43] L. S. Cederbaum and W. Domcke. Theoretical aspects of ionization potentials and photoelectron spectroscopy: a manyâˆ'body approach. *Adv. Chem. Phys.*, 36:205, 1977.

[44] J. V. Ortiz. Partial third-order quasiparticle theory: Comparisons for closed-shell ionization energies and an application to the borazine photoelectron spectrum. *J. Chem. Phys.*, 104 (19):7599–7605, 1996. doi: 10.1063/1.471468.

[45] Henry A Kurtz and Yngve Öhrn. On the calculation of electron binding energies. *J. Chem. Phys.*, 69:1162, 1978.

[46] George D. Purvis and Yngve Ohrn. The transition state, the electron propagator, and the equation of of motion method. *J. Chem. Phys.*, 65(3):917–922, 1976. doi: 10.1063/1.433160.

[47] J.V. Ortiz, R. Basu, and Y. Öhrn. Electron-propagator calculations with a transition-operator reference. *Chem. Phys. Lett.*, 103(1):29 – 34, 1983. ISSN 0009-2614. doi: 10.1016/0009-2614(83)87067-5.

[48] Roberto Flores-Moreno, V. G. Zakrzewski, and J. V. Ortiz. Assessment of transition operator reference states in electron propagator calculations. *J. Chem. Phys.*, 127(13):134106, 2007. doi: 10.1063/1.2784638.

[49] John C Slater and Keith H Johnson. Self-consistent-field xα cluster method for polyatomic molecules and solids. *Phys. Rev. B*, 5(3):844, 1972.

[50] JF Janak. Proof that de/dn= ε in density-functional theory. *Phys. Rev. B*, 18:7165–7168, 1978.

[51] R. Flores-Moreno, E. Posada, F. Moncada, J. Romero, J. Charry, M. Díaz-Tinoco, S. Gonzalez, N. Aguirre, and A. Reyes. Lowdin: The any particle molecular orbital code. *Int. J. Quantum Chem.*, DOI:10.1002/qua.24500, 2013.

[52] ISO/IEC 1539-1:2010. *Information technology – Programming languages – Fortran – Part 1: Base language.* International Organization for Standardization (ISO), 2009.

[53] Shigeru Obara and A Saika. Efficient recursive computation of molecular integrals over cartesian gaussian functions. *J. Chem. Phys.*, 84:3963, 1986.

[54] M. Head-Gordon and J. A. Pople. A method for two?electron gaussian integral and integral derivative evaluation using recurrence relations. *J. Chem. Phys.*, 89:5777, 1988.

[55] J. T. Fermann and E. F. Valeev. Libint: Machine-generated library for efficient evaluation of molecular integrals over gaussians, 2003. URL `http://sourceforge.net/p/libint`.

[56] P Pulay. Convergence acceleration of iterative sequences. the case of scf iteration. *J. Comput. Chem.*, 3:556–560, 1982.

[57] V. R. Saunders and I. H. Hillier. A level?shifting method for converging closed shell hartree?fock wave functions. *Int. J. Quantum Chem.*, 7(4):699–705, 1973. doi: 10.1002/qua.560070407.

[58] Eric Cancès and Claude Le Bris. Can we outperform the diis approach for electronic structure calculations? *Int. J. Quantum Chem.*, 79(2):82–90, 2000. doi: 10.1002/1097-461X(2000)79:2⟨82::AID-QUA3⟩3.0.CO;2-I.

[59] Fortran: Information technology – programming languages – fortran – part 1: Base language (international organization for standarization (iso), 2009).

[60] Shigeyoshi Yamamoto and Umpei Nagashima. Four-index integral transformation exploiting symmetry. *Comput. Phys. Commun.*, 166(1):58 – 65, 2005. doi: 10.1016/j.cpc.2004.01.008.

[61] Charles W Bauschlicher Jr. An efficient two-electron integral transformation for vector-concurrent computer architectures. *Theoretica Chimica Acta*, 76(3):187–193, 1989.

[62] M. Díaz-Tinoco, J. Romero, J. V. Ortiz, A. Reyes, and R. Flores-Moreno. A generalized any-particle propagator theory: Prediction of proton affinities and acidity properties with the proton propagator. *J. Chem. Phys.*, 138:194108, 2013.

[63] T.H. Dunning Jr. Gaussian basis sets for use in correlated molecular calculations. i. the atoms boron through neon and hydrogen. *J. Chem. Phys.*, 90:1007, 1989.

[64] S. G. Lias, J. E. Bartmess, J. F. Liebman, J. L. Holmes, R. D. Levin, and W. G. Mallard. Nist: "ion energetics data" in **nist chemistry webbook, nist standard reference database number 69**, eds. p.j. linstrom and w.g. mallard, national institute of standards and technology, gaithersburg md, 20899, http://webbook.nist.gov, (retrieved november 24, 2011).

[65] E. G. Lewars. *Computational Chemistry: Introduction to the Theory and Applications of Molecular and Quantum Mechanics.* Springer-Verlag, Peterborough, Ontario, 2011.

[66] Nist computational chemistry comparison and benchmark database, nist standard reference database number 101, release 15b, august 2011, edited by r. d. johnson, iii, see http://cccbdb.nist.gov.sci-hub.org/ (retrieved november 24, 2011).

[67] A. M. Velasco, J. Pitarch-Ruiz, Alfredo M. J. Sanchez de Meras, J. Sanchez-Marin, and I. Martin. Lower rydberg series of methane: A combined coupled cluster linear response and molecular quantum defect orbital calculation. *J. Chem. Phys.*, 124(12):124313, 2006. doi: 10.1063/1.2179069. URL `http://link.aip.org/link/?JCP/124/124313/1`.

[68] A. M. Velasco, C. Lavin, A. M. J. Sanchez de Meras, and J. Sanchez Marin. The electronic spectrum of sih[sub 4]: Jahn-teller rydberg series. *J. Chem. Phys.*, 135(21):214304, 2011. doi: 10.1063/1.3664629. URL `http://link.aip.org/link/?JCP/135/214304/1`.

[69] J. D. D. Martin. PhD thesis, University of Waterloo, 1998.

[70] JDD Martin and JW Hepburn. Determination of bond dissociation energies by threshold ion-pair production spectroscopy: An improved d (hcl). *J. Chem. Phys.*, 109:8139, 1998.

[71] R.C. Shiell, X. Hu, Q.J. Hu, and J.W. Hepburn. Threshold ion-pair production spectroscopy (tipps) of h2 and d2. *Faraday Discuss.*, 115(0):331–343, 2000.

[72] RC Shiell, XK Hu, QJ Hu, and JW Hepburn. A determination of the bond dissociation energy (d 0 (h-sh)): Threshold ion-pair production spectroscopy (tipps) of a triatomic molecule. *J. Phys. Chem. A*, 104(19):4339–4342, 2000.

[73] QJ Hu, TC Melville, and JW Hepburn. Threshold ion-pair production spectroscopy of hcl/dcl: Born–oppenheimer breakdown in hcl and dcl and dynamics of photoion-pair formation. *J. Chem. Phys.*, 119:8938, 2003.

[74] QJ Hu, Q. Zhang, and JW Hepburn. Threshold ion-pair production spectroscopy of hcn. *J. Chem. Phys.*, 124:074310, 2006.

[75] H. Nishizawa, Y. Imamura, Y. Ikabata, and H. Nakai. Development of the explicitly correlated gaussian-nuclear orbital plus molecular orbital theory: Incorporation of electron-electron correlation. *Chem. Phys. Lett.*, 533:100–105, 2012.

[76] Paul S Bagus. Self-consistent-field wave functions for hole states of some ne-like and ar-like ions. *Phys. Rev.*, 139(3A):A619, 1965.

[77] QJ Hu and JW Hepburn. Energetics and dynamics of threshold photoion-pair formation in hf/ df. *J. Chem. Phys.*, 124:074311, 2006.

[78] S.H. Vosko, L. Wilk, and M. Nusair. Accurate spin-dependent electron liquid correlation energies for local spin density calculations: a critical analysis. *Can, J. Phys*, 58(8):1200–1211, 1980.

[79] AD McLean and GS Chandler. Contracted gaussian basis sets for molecular calculations. i. second row atoms, z= 11–18. *J. Chem. Phys.*, 72(10):5639–5648, 1980.

[80] K. Raghavachari, J.S. Binkley, R. Seeger, and J.A. Pople. Self-consistent molecular orbital methods. 20. a basis set for correlated wave functions. *J. Chem. Phys.*, 72:650–654, 1980.

[81] T. Clark, J. Chandrasekhar, G.W. Spitznagel, and P.V.R. Schleyer. Efficient diffuse function-augmented basis sets for anion calculations. iii. the 3-21+ g basis set for first-row elements, li–f. *J. Comput. Chem.*, 4(3):294–301, 2004.

[82] M.J. Frisch, J.A. Pople, and J.S. Binkley. Self-consistent molecular orbital methods 25. supplementary functions for gaussian basis sets. *J. Chem. Phys.*, 80:3265, 1984.

[83] J. Andzelm, E. Radzio, and DR Salahub. Compact basis sets for lcao-lsd calculations. part i: Method and bases for sc to zn. *J. Comput. Chem.*, 6(6):520–532, 1985.

[84] J. Andzelm, N. Russo, and D.R. Salahub. Ground and excited states of group iva diatomics from local-spin-density calculations: Model potentials for si, ge, and sn. *J. Chem. Phys.*, 87(11):6562–6572, 1987.

[85] AM Köster, P. Calaminici, ME Casida, R. Flores-Moreno, G. Geudtner, A. Goursot, T. Heine, A. Ipatov, F. Janetzko, and J Martín del Campo. demon2k, release 2.4.2, cinvestav, mexico-city, mexico, 2006. URL `URL:http://www.demon-software.com`.

[86] J.P. Perdew, P. Ziesche, and H. Eschrig. *Electronic structure of solids*. Akademie-Verlag, Berlin, 1991.

[87] R. Ditchfield, WJ Hehre, and J.A. Pople. Self-consistent molecular-orbital methods. ix. an extended gaussian-type basis for molecular-orbital studies of organic molecules. *J, Chem. Phys*, 54:724, 1971.

[88] W.J. Hehre, R. Ditchfield, and J.A. Pople. Self–consistent molecular orbital methods. xii. further extensions of gaussian–type basis sets for use in molecular orbital studies of organic molecules. *J. Chem. Phys.*, 56:2257, 1972.

[89] M.N. Saha. On a physical theory of stellar spectra. *Proc. R. Soc. A*, 99(697):135–153, 1921.

[90] Megh Nad Saha. Liii. ionization in the solar chromosphere. *Philos. Mag. 6*, 40(238):472–488, 1920. doi: 10.1080/14786441008636148.

[91] A.D. McNaught and A. Wilkinson. *Compendium of chemical terminology*, volume 1669. Blackwell Science Oxford, UK, 1997.

[92] GJ Tawa, IA Topol, SK Burt, RA Caldwell, and AA Rashin. Calculation of the aqueous solvation free energy of the proton. *J. Chem. Phys.*, 109:4852, 1998.

[93] A.D. Bochevarov, E.F. Valeev, and C.D. Sherrill. The electron and nuclear orbitals model: current challenges and future prospects. *Mol. Phys.*, 102(1):111–123, 2004.

[94] William L. Jolly. *Modern Inorganic Chemistry*. McGraw-Hill, New York, 2nd edition edition, 1991.

[95] E.P.L. Hunter and S.G. Lias. Evaluated gas phase basicities and proton affinities of molecules: An update. *J. Phys. Chem. Ref. Data*, 27:413, 1998.

[96] JB Cumming and P. Kebarle. Summary of gas phase acidity measurements involving acids ah. entropy changes in proton transfer reactions involving negative ions. bond dissociation energies d (ah) and electron affinities ea (a). *Can, J. Chem*, 56(1):1–9, 1978.

[97] S.T. Graul, M.E. Schnute, and R.R. Squires. Gas-phase acidities of carboxylic acids and alcohols from collision-induced dissociation of dimer cluster ions. *Int. J. Mass Spectrom. Ion Processes*, 96(2):181–198, 1990.

[98] K.M. Ervin, J. Ho, and W.C. Lineberger. Ultraviolet photoelectron spectrum of nitrite anion. *J. Phys. Chem*, 92(19):5405–5412, 1988.

[99] M.P. Hodges and A.J. Stone. Modeling small hydronium–water clusters. *J. Chem. Phys.*, 110:6766, 1999.

[100] C. Knight and G.A. Voth. The curious case of the hydrated proton. *Acc. Chem. Res*, 45(1):101–109, 2011.

[101] J.F. Pérez, CZ Hadad, and A. Restrepo. Structural studies of the water tetramer. *Int. J. Quant. Chem.*, 108(10):1653–1659, 2008.

[102] G. Hincapié, N. Acelas, M. Castaño, J. David, and A. Restrepo. Structural studies of the water hexamer. *J. Phys. Chem. A*, 114(29):7809–7814, 2010.

[103] F. Ramírez, CZ Hadad, D. Guerra, J. David, and A. Restrepo. Structural studies of the water pentamer. *Chem. Phys. Lett.*, 507(4):229–233, 2011.

[104] K.S. Alongi and G.C. Shields. Theoretical calculations of acid dissociation constants: a review article. *Annual Reports in Computational Chemistry*, 6:113–138, 2010.

[105] M.D. Liptak and G.C. Shields. Experimentation with different thermodynamic cycles used for pka calculations on carboxylic acids using complete basis set and gaussian-n models combined with cpcm continuum solvation methods. *Int. J. Quantum Chem.*, 85(6):727–741, 2001.

[106] M.D. Liptak, K.C. Gross, P.G. Seybold, S. Feldgus, and G.C. Shields. Absolute p k a determinations for substituted phenols. *J. Am. Chem. Soc.*, 124(22):6421–6427, 2002.

[107] C.P. Kelly, C.J. Cramer, and D.G. Truhlar. Adding explicit solvent molecules to continuum solvent calculations for the calculation of aqueous acid dissociation constants. *J, Phys. Chem. A*, 110(7):2493–2499, 2006.

[108] C.P. Kelly, C.J. Cramer, and D.G. Truhlar. Aqueous solvation free energies of ions and ion-water clusters based on an accurate value for the absolute aqueous solvation free energy of the proton. *J. Phys. Chem. B*, 110(32):16066–16081, 2006.

[109] M.D. Tissandier, K.A. Cowen, W.Y. Feng, E. Gundlach, M.H. Cohen, A.D. Earhart, J.V. Coe, and T.R. Tuttle Jr. The proton's absolute aqueous enthalpy and gibbs free energy of solvation from cluster-ion solvation data. *J. Phys. Chem. A*, 102(40):7787–7794, 1998.

[110] D.M. McQuarrie. *Statistical Mechanics.* Harper and Row, New York, 1970.

[111] A.M. Rebollar-Zepeda, T. Campos-Hernández, M.T. Ramírez-Silva, A. Rojas-Hernández, and A. Galano. Searching for computational strategies to accurately predict p k as of large phenolic derivatives. *J. Chem. Theory. Comput*, 7(8):2528–2538, 2011.

[112] J. Ho and M.L. Coote. p k a calculation of some biologically important carbon acids-an assessment of contemporary theoretical procedures. *J. Chem. Theory. Comput*, 5(2):295–306, 2009.

[113] Masato Kobayashi and Hiromi Nakai. Divide-and-conquer approaches to quantum chemistry: Theory and implementation. In *Linear-Scaling Techniques in Computational Chemistry and Physics*, pages 97–127. Springer, 2011.